INELASTIC COLUMNS SUBJECTED TO PULSE LOADING

CARL F. DEFIBAUGH

INELASTIC COLUMNS SUBJECTED TO PULSE LOADING

* * * * *

Carl F. Defibaugh, Jr.

INELASTIC COLUMNS SUBJECTED TO PULSE LOADING

by

Carl F. Defibaugh, Jr.

Lieutenant, United States Navy

Submitted in partial fulfillment of
the requirements for the degree of

MASTER OF SCIENCE
IN
MECHANICAL ENGINEERING

United States Naval Postgraduate School
Monterey, California

1 9 6 3

INELASTIC COLUMNS SUBJECTED TO PULSE LOADING

by

Carl F. Defibaugh, Jr.

This work is accepted as fulfilling
the thesis requirements for the degree of
MASTER OF SCIENCE
IN
MECHANICAL ENGINEERING
from the
United States Naval Postgraduate School

ABSTRACT

This paper reports an investigation of the dynamic behavior of a pin-ended inelastic column subjected to a half-sine displacement pulse at one end applied with small eccentricity. The rates of end displacement are such that the effects of axial inertia are considered negligible. The column is replaced by a lumped parameter mathematical model and the equations for the model are solved by a high speed digital computer. The stress-strain relation during loading is assumed to be of the Ramberg-Osgood type. Unloading occurs along a line with slope equal to that of the tangent at the origin. Slenderness ratios of 50, 70, and 100 and two different values of eccentricity are considered in the investigation. The maximum load supported by the column and the residual lateral deflection at the center of the column are found as functions of the displacement pulse height and of the displacement pulse duration.

It is shown that an inelastic column, like the elastic column, can support dynamic loads considerably in excess of the static load capacity. It is also shown that within the range of pulse durations studied, the smallest residual deflections generally accompany the largest maximum loads.

ACKNOWLEDGEMENT

The author expresses his appreciation to Professor R. E. Newton, Chairman of the Mechanical Engineering Department of the U. S. Naval Postgraduate School for the constant guidance and encouragement given by him throughout the course of this investigation. The helpful suggestions received from Professor J. E. Brock are also appreciated. The author is indebted to the personnel of the Computer Service Center at the U. S. Naval Postgraduate School for their assistance with programming problems and for their instruction in equipment operational procedures.

TABLE OF CONTENTS

Section	Title	Page
1.	Introduction	1
2.	Development of the Equations for the Mathematical Model	5
3.	The Numerical Solution	21
4.	Results and Discussion	
	a. Character of the response	31
	b. Range of variables	32
	c. Maximum force	33
	d. Slow loading	36
	e. Residual lateral deflection	42
5.	Conclusions	47
6.	Bibliography	48

Appendices

Appendix I	Example of Graphical Output for Program COL 1	I-1
Appendix II	Theoretical and Computer Solution Graphical Comparisons of Maximum Loads for the Static Case	II-1
Appendix III	Column Model Dynamic Response Curves	III-1
Appendix IV	Computer Programs and Notation	
	a. General	IV-1
	b. Notation for Program COL 1	IV-2
	c. Operating instructions for Program COL 1	IV-2
	d. Notation for Program COL 2	IV-11
	e. Operating instructions for Program COL 2	IV-12
Appendix V	Maximum Force, Residual Deflection and Maximum Stress Data	V-1
Appendix VI	Evaluation of the Approximations and of the Accuracy of the Numerical Scheme	VI-1

LIST OF ILLUSTRATIONS

Figure		Page
1.	Geometry of the Mathematical Column Model	6
2.	Stress Behavior in the Column Model Springs	6
3.	Free Body Diagram of Half the Column Model	8
4.	Elastic Column in Free Vibration	12
5.	Elastic Column Model in Free Vibration	12
6.	Dimensionless Ramberg-Osgood Compressive Stress-Strain Curve for the Column Material	18
7.	Simplified Block Diagram of Computer Program COL 2	22
8.	Simplified Block Diagram of Computer Program for Subroutine STRESS	25
9.	Stress-Strain Considerations in Computer Program for Subroutine STRESS	25
10.	Values of P_m/P_E vs. β for an Eccentricity Ratio of 0.05	34
11.	Values of P_m/P_E vs. β for an Eccentricity Ratio of 0.01	35
12.	Values of Residual Deflection vs. β for Column Slenderness Ratio of 100	43
13.	Values of Residual Deflection vs. β for Column Slenderness Ratio of 70	44
14.	Values of Residual Deflection vs. β for Column Slenderness Ratio of 50	45

Table

1.	Computer and Theoretical Static Load Comparison for Ramp Loading of Column Model	40

TABLE OF SYMBOLS

Symbol	Description	Dimensions
A	area of the column cross section	L^2
A_1	half the area of the column cross section ($=A/2$)	L^2
E	Young's Modulus for the column material	FL^{-2}
E_R	reduced modulus ($= \frac{2EE_T}{E+E_T}$)	FL^{-2}
E_T	tangent modulus (local slope of the stress-strain curve, $= \frac{d\sigma}{d\epsilon}$)	FL^{-2}
e	eccentricity of load application	L
F_1, F_2	x-direction forces developed by loaded springs in mathematical model	F
I	moment of inertia of the column cross section area ($= \rho^2 A$)	L^4
K	stiffness of the springs in mathematical model ($=A_1E_T/\ell$, see page 7)	FL^{-1}
L	overall length of column	L
ℓ	initial undeflected length of the springs in mathematical model ($=\frac{32}{\pi^4}L$)	L
m	mass of mathematical model	$FL^{-1}T^2$

Symbol	Description	Dimensions
n	shape parameter of Ramberg-Osgood stress-strain curve	-
P	x-direction force on the ends of mathematical model	F
P_E	Euler load ($= \pi^2 \frac{EA}{(L/\rho)^2}$ for column; $= \frac{\pi^4}{8} \frac{EA}{(L/\rho)^2}$ for mathematical model, see page 15)	F
P_m	maximum force developed in mathematical model	F
P_R	reduced modulus load ($= \pi^2 \frac{E_R A}{(L/\rho)^2}$ for column; $= \frac{\pi^4}{8} \frac{E_R A}{(L/\rho)^2}$ for mathematical model, see pages 15 and 38)	F
P_T	tangent modulus load ($= \pi^2 \frac{E_T A}{(L/\rho)^2}$ for column; $= \frac{\pi^4}{8} \frac{E_T A}{(L/\rho)^2}$ for mathematical model, see pages 15 and 37)	F
Q	lateral force on the ends of the mathematical model	F
S_1, S_2	dimensionless stresses in springs of mathematical model ($= \sigma_1/E, \sigma_2/E$)	-
S_y	dimensionless yield stress of column material ($= \sigma_y/E$)	-

Symbol	Description	Dimensions
T	dimensionless time ($=\omega_n t$)	-
T_f	dimensionless ram pulse duration ($=2\pi/\beta$)	-
t	real time	T
V	dimensionless lateral deflection at mid-length in mathematical model ($= \frac{y}{e}$)	-
$\dot{V}$	dimensionless lateral velocity at mid-length in mathematical model ($= \frac{d(y/e)}{dT}$)	-
$\ddot{V}$	dimensionless lateral acceleration at mid-length in mathematical model ($= \frac{d^2(y/e)}{dT^2}$)	-
X	ram displacement pulse height	L
χ	dimensionless ram displacement ($=\alpha \sin \frac{1}{2}\beta T$)	-
x	displacement of loaded end of mathematical model	L
x_E	end displacement at Euler load ($= \pi^2 \rho^2/L$ for column; $4\rho^2/L$ for mathematical model see page 15)	L
y	lateral deflection at midlength in mathematical model	L
y_m	maximum lateral deflection at midlength in mathematical model	L

Symbol	Description	Dimensions
y_r	residual lateral deflection at midlength in mathematical model	L
$\frac{dy}{dt}$	lateral velocity at midlength in mathematical model	LT^{-1}
$\frac{d^2y}{dt^2}$	lateral acceleration at midlength in mathematical model	LT^{-2}
α	dimensionless pulse height of ram displacement (= $\frac{X}{X_g}$)	-
β	dimensionless ratio of the natural period of first mode lateral vibration of column to the duration of the half-sine ram displacement pulse (= $\frac{\tau_n}{\tau_f}$)	-
δ_1, δ_2	x-direction deflections of springs in mathematical model	L
δ_m	average x-direction deflection of springs in mathematical model (= $\frac{\delta_1 + \delta_2}{2}$)	L
ϵ_1, ϵ_2	strains of springs in mathematical model (= $\frac{\delta_1}{\ell}, \frac{\delta_2}{\ell}$)	-
θ	angle in radians between rigid rods and the x-direction in mathematical model	-

Symbol	Description	Dimensions
μ	mass per unit length of the column	$FL^{-2}T^{2}$
σ_1, σ_2	stresses in springs of mathematical model ($= \frac{F_1}{A_1}, \frac{F_2}{A_1}$; positive, if compressive)	FL^{-2}
σ_y	yield stress of column material	FL^{-2}
ρ	radius of gyration of the column cross sectional area ($= \sqrt{I/A}$)	L
τ_f	duration of the half-sine ram displacement pulse	T
τ_n	natural period of first mode lateral vibration of column	T
ω_n	circular frequency of first mode lateral vibration of column	T^{-1}
ΔT	dimensionless time increment used in numerical solution ($= \frac{2\pi}{\tau_n} \Delta t$)	-

1. INTRODUCTION

In the study of structures the column ranks as one of the more provoking elements as judged from the amount of literature published on its behavior. The development of elastic column theory is comparatively advanced and dates back to 1757 when Euler published his analysis of the strength of columns. In more recent years inelastic column theory has been developed to the point where a satisfactory explanation has been obtained for the phenomenon. Shanley /1/* has been credited with revising and reinterpreting inelastic column theory from previously accepted erroneous conjectures. Utilizing studies of a highly idealized column he concluded that the tangent modulus load is the maximum load at which an initially straight, centrally loaded column will remain straight; loading beyond this load causes bending which produces permanent deformation.

The dynamic behavior of structures has become an increasingly important engineering consideration in recent years and, with the aid of more sophisticated devices for the problem solution, many more phenomena can be included in an analysis than could previously be reasonably considered. The behavior of dynamically loaded elastic columns has received considerable attention and a number of investigations have resulted.

Hoff and associates /2,3/ considered the case of an elastic column of uniform cross section, initially curved in the

* Numbers in / / refer to entries in the bibliography

shape of a half-sine wave, subjected to constant velocity loading such as that encountered in compression tests in commercial testing machines. It was shown that the maximum loads supported by the column are greater than the Euler load when the loading is rapid, the column is slender and the initial deflections are small. Sevin /4/ confirmed the previous results while including the effects of axial inertia which were not considered by Hoff. He inferred that, for an elastic column, axial inertia effects are of negligible importance with regard to the gross behavior of conventional structural columns, regardless of the initial deflected shape, end constraint, or type of axial loading.

Taylor /5/ investigated the case of an eccentrically loaded elastic column subjected to a half-sine force pulse and he included the effects of axial inertia. Using a limiting value of extreme fiber strain as the failure criterion he determined the column failure load quantitatively. He demonstrated that elastic columns will support loads much greater than the Euler load when subjected to rapid loading and that axial inertia effects become significant with this type of loading as the rapidity of loading is increased.

Gerard and Becker /6/ studied column behavior under conditions of impact, by utilizing the properties of a propagated elastic compressive stress wave produced on failure of a tension specimen. They concluded that a column can momentarily support a dynamic compressive stress of any

magnitude and that buckling may be confined to a length less than the entire length of the column.

The inelastic column was investigated by Chawla /7/ in essentially the same manner as Hoff (with an initial curvature or effective eccentricity) and he found that for relatively slow rates of end displacement the maximum column load was less than the tangent modulus load. Brooks and Wilder /8/ studied the effects of dynamic loading on an idealized H-section inelastic column with an initial lateral deflection using a constant velocity end displacement. From their results they concluded that the static maximum load may be employed as a conservative estimate of the maximum load of a column regardless of the rate of end displacement.

Investigations of the dynamic behavior of inelastic columns are limited in number and the problem of determining the behavior of inelastic columns subjected to pulse loading appears to have been neglected. Whereas constant velocity loading leads to the ultimate failure of the column, pulse loading may not necessarily result in failure. Pulse loading allows the column to recover from a deflected position with an amount of residual deflection while retaining a capacity to sustain subsequent load. The problem considered in this investigation is that of determining the dynamic behavior of a pin-ended inelastic column subjected to a half-sine displacement pulse at one end applied with small eccentricity. The problem involves the prediction

of the maximum force developed in the column for a specified pulse height and duration of loading. The problem also includes the prediction of the residual lateral deflection resulting from the pulse loading. The effects of pulse height and duration are investigated for two values of eccentricity and three column slenderness ratios.

2. DEVELOPMENT OF THE EQUATIONS FOR THE MATHEMATICAL MODEL

The column considered in the investigation is initially straight, pin-ended, and of constant cross-section. The effects of axial inertia and shear strains are neglected, but non-linear axial strain components due to bending at the center portion of the column length are considered. The effect of a non-linear stress-strain curve on loading and departure from this curve on unloading is also included.

The loading on the column is produced by axial displacement of the pin at one end. The loaded end is free to rotate about the pin, which is eccentrically placed. The other end is constrained by a fixed pin of equal eccentricity. The end displacement is imposed by a moving ram executing a half-sine displacement pulse. The ram can exert only compressive force on the column (see Fig . 1).

The problem is developed and solved, not in terms of the real column, but in terms of the lumped parameter mathematical model shown in Fig. 1. The equations for the model are then solved in a high speed digital computer. The force-deflection characteristic of the springs is derived from the material stress-strain diagram. The assumed behavior is indicated in Fig. 2 where the solid curve OABD represents the variation of compressive stress σ under montonically increasing compressive strain ϵ . If, upon reaching point B, the strain-

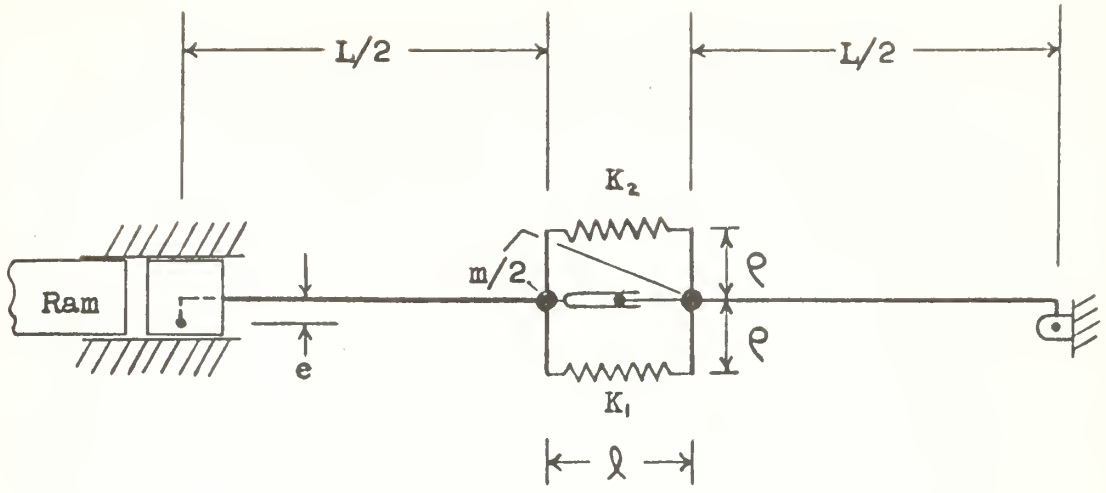

Fig. 1. Geometry of the Mathematical Column Model.

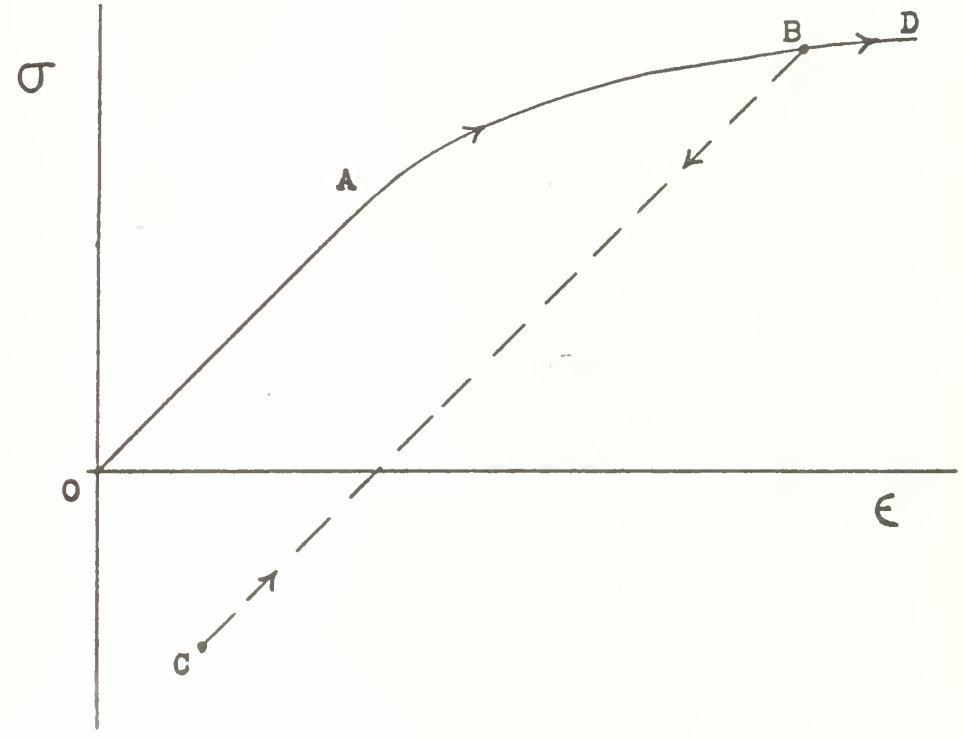

Fig. 2. Stress Behavior in the Column Model Springs.

ing is reversed, the path will be along BC whose slope is that of the tangent to the solid curve at C. A second reversal will cause the compressive stress to increase again following CB. After again reaching the curve at B, the path will be along the solid curve toward D. Additional strain reversals would result in additional "detours" parallel to BC. In the study the stress-strain relationship after departure from the compressive stress-strain curve is considered linear into the tensile stress region. The maximum tensile stresses in the column model are limited to values near the nominal yield stress of the material. It is presumed that any tensile stress in the column model springs is insufficient to cause plastic straining.

This behavior is incorporated in the springs by taking the stiffness of each as $K=A_1 E_T/\ell$, where A_1 is half the column cross-sectional area, E_T is the tangent modulus, and ℓ is the unstrained length of a spring. Again referring to Fig. 2, at any point on the solid curve E_T is the slope of the curve. For points below the curve $E_T=E$ (Young's Modulus).

This model having only two degrees of freedom was chosen for the investigation in order to limit the computer solution time to reasonable values, but yet to retain the effects of inelastic column behavior. It is felt that this model is a good compromise in that it approaches the deflected shape of the inelastic column and also retains the effects of lateral inertia and of the longitudinal strains on each side

of the column due to both the axial load and bending.

From the free body diagram of half the column model shown in Fig. 3, using d'Alembert's principle, the following equations may be written:

$$P = F_1 + F_2 \tag{1}$$

$$Q = \frac{m}{2}\frac{d^2y}{dt^2} \tag{2}$$

$$P\left(e\cos\theta + \frac{L}{2}\sin\theta\right) - Q\left(\frac{L}{2}\cos\theta - e\sin\theta\right) = (F_1 - F_2)\rho\cos\theta$$

Dividing the latter by $\cos\theta$ and substituting for Q from equation (2)

$$P\left(e + \frac{L}{2}\tan\theta\right) - \frac{m}{2}\frac{d^2y}{dt^2}\left(\frac{L}{2} - e\tan\theta\right) = (F_1 - F_2)\rho \tag{3}$$

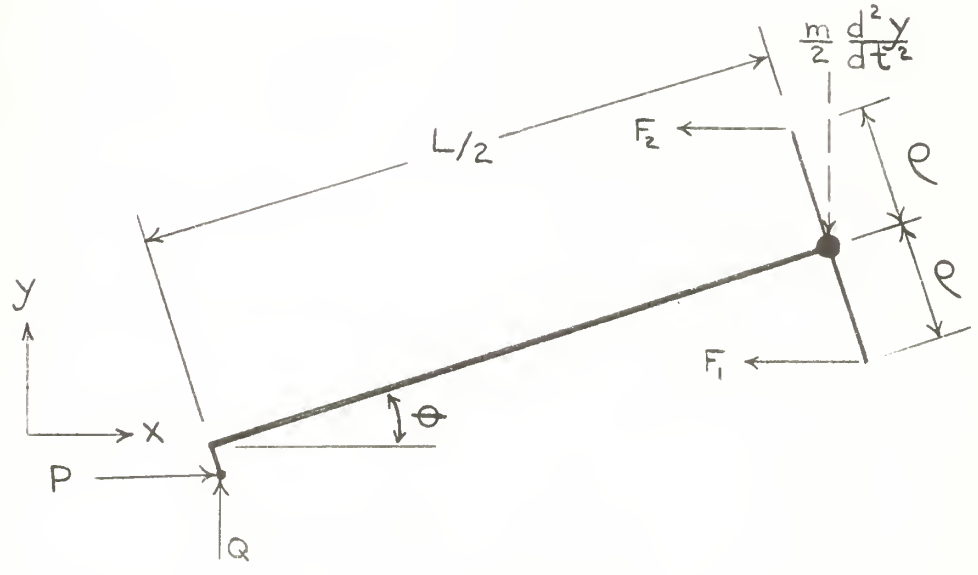

Fig. 3. Free Body Diagram of Half the Column Model.

From kinematic considerations of the column model in a deflected position the following equations may be written:

$$\delta_1 = \delta_m + 2\rho \sin\theta \tag{4}$$

$$\delta_2 = \delta_m - 2\rho \sin\theta \tag{5}$$

where δ_1 and δ_2 are the axial shortening of Spring 1 and Spring 2 respectively and δ_m is the average axial shortening at the center of the model. Further

$$x = \delta_m + 2 \cdot \frac{L}{2}(1-\cos\theta) + 2e\sin\theta \tag{6}$$

$$y = \frac{L}{2}\sin\theta - e(1-\cos\theta) \tag{7}$$

where x is the end displacement at the loaded end of the model and y is the lateral deflection at midlength in the model.

The following approximations are consequences of assuming that θ is small and e/L is small:

$$\frac{L}{2} >> e\tan\theta$$

$$\frac{L}{2}\sin\theta >> e(1-\cos\theta)$$

$$\tan\theta \approx \sin\theta \approx \theta$$

$$1-\cos\theta \approx \frac{1}{2}\theta^2$$

An evaluation of the errors resulting from these approxima-

tions is given in App. VI.

Equation (7) now becomes:

$$y = \frac{L}{2}\theta \tag{8}$$

Now, substituting the approximations, together with equation (8), into equations (3) through (6) and rearranging, results in

$$\frac{d^2y}{dt^2} = \frac{4P}{mL}(e+y) - (F_1 - F_2)\frac{4\rho}{mL} \tag{9}$$

$$\delta_1 = \delta_m + \frac{4\rho}{L}y$$

$$\delta_2 = \delta_m - \frac{4\rho}{L}y$$

$$x = \delta_m + \frac{2}{L}y^2 + \frac{4e}{L}y$$

Solving for δ_m and substituting in the above expressions for δ_1 and δ_2 gives

$$\delta_1 = x - \frac{2}{L}y^2 - \frac{4e}{L}y + \frac{4\rho}{L}y \tag{10}$$

$$\delta_2 = x - \frac{2}{L}y^2 - \frac{4e}{L}y - \frac{4\rho}{L}y \tag{11}$$

Since the model has but two degrees of freedom, only a limited correspondence may be established between column and model parameters. Energy considerations are used for this purpose.

To determine this correspondence both the column and the model are considered for the elastic case. Figure 4 indicates an elastic column in a deflected position during free vibration. It has an assumed half-sine deflected shape and the motion is considered sinusoidal with time.

The maximum potential energy is found from the elastic strain energy due to bending and is

$$\text{Potential Energy} = \frac{EI}{2} \int_0^L \left(\frac{d^2y}{dx^2}\right)^2 dx$$

where $\frac{d^2y}{dx^2}$ is the curvature of the axis of the column and I is the moment of inertia of the column cross-sectional area. I is equal to $\rho^2 A$, where A is the column cross-sectional area. This can be shown to be

$$\text{Potential Energy} = \frac{\pi^4 E I y_m^2}{4 L^3} \qquad \text{(column)}$$

The maximum kinetic energy of the column, neglecting axial inertia effects, is

$$\text{Kinetic Energy} = \tfrac{1}{2} \mu \omega_n^2 \int_0^L y^2 dx$$

which can be shown to be

$$\text{Kinetic Energy} = \tfrac{1}{4} \mu \omega_n^2 y_m^2 L \qquad \text{(column)}$$

where μ is the mass per unit length, ω_n is the circular frequency of first mode lateral vibration of the column and L is the column length. Setting the maximum potential energy equal to the maximum kinetic energy and solving for the circular

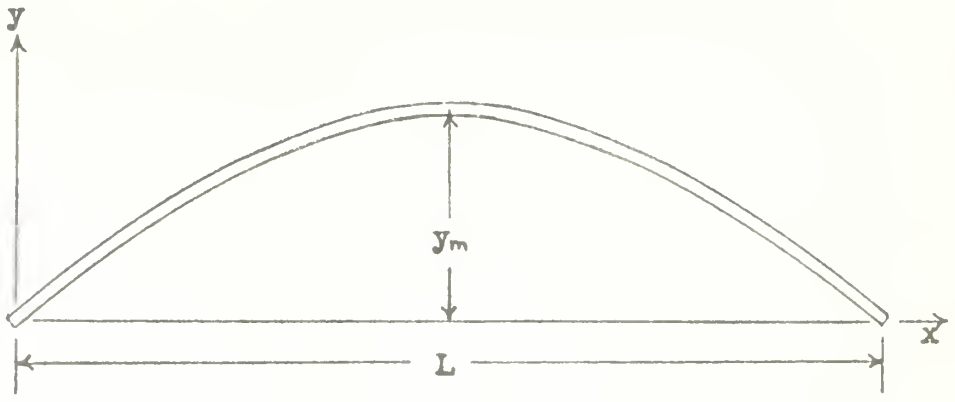

$$y = y_m \sin \frac{\pi x}{L}$$

Fig. 4. Elastic Column in Free Vibration.

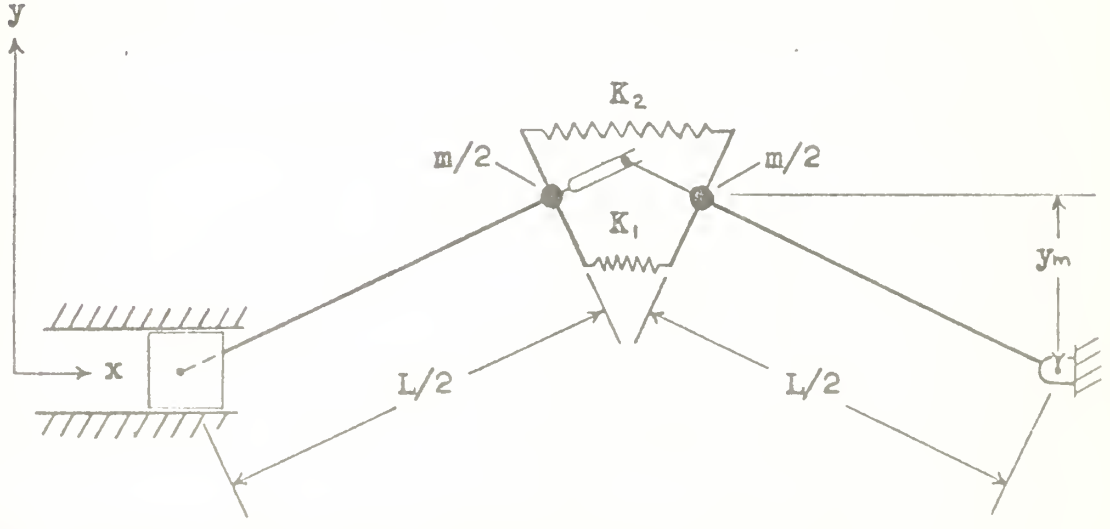

Fig. 5. Elastic Column Model in Free Vibration.

frequency of first mode lateral vibration of the column results in

$$\omega_n = \pi^2 \sqrt{\frac{EI}{ML^4}} \qquad \text{(column)}$$

Figure 5 shows the model with non-eccentric pin connections in a deflected position. The stiffness of each spring is $\frac{A_1 E}{\ell}$ and the motion of the mass is again considered sinusoidal with time. The maximum potential energy as found from the elastic strain energy in the springs is

$$\text{Potential Energy} = \tfrac{1}{2} \frac{A_1 E}{\ell} (\delta_1^2 + \delta_2^2)$$

Considering the model to be in free vibration without axial load the average spring deflection is zero or $\delta_1 = -\delta_2$. Under these conditions it can be shown from equations (10) and (11) that

$$\delta_1^2 = \delta_2^2 = \frac{16\rho^2}{L^2} y^2$$

and the model maximum potential energy becomes

$$\text{Potential Energy} = \frac{16\rho^2 A_1 E}{\ell L^2} y_m^2 \qquad \text{(model)}$$

The maximum kinetic energy of the model neglecting axial inertia effects is

$$\text{Kinetic Energy} = \tfrac{1}{2} m \omega_n^2 y_m^2 \qquad \text{(model)}$$

Now, setting the maximum potential energy equal to the maximum kinetic energy and solving for the circular frequency

of first mode lateral vibration of the model results in

$$\omega_n = \sqrt{\frac{32\rho^2 A_1 E}{m \ell L^2}} \qquad \text{(model)}$$

To determine the undeflected length ℓ of the model springs the potential energies of the column and model are equated. Taking the center deflections y_m of column and model to be equal, ℓ is found to be

$$\ell = \frac{32}{\pi^4} L \qquad (12)$$

To determine the relation between column and model masses the kinetic energies of the column and model are equated. Again taking the center deflections y_m to be equal, m is found to be

$$m = \frac{\mu L}{2} \qquad (13)$$

With the two previous correspondences it can be shown that the circular frequencies of the column and the model are the same.

Now, considering the differential equation of motion (as previously derived for the model) for the elastic case, together with the results of the elastic energy development, Euler load and end displacement correspondences between the column and model are determined. These will be used later in the analysis to define non-dimensional load and displacement parameters. If the acceleration and the eccentricity of the

column model are both zero, equation (9) becomes

$$Py = (F_1 - F_2)\rho \tag{14}$$

Equation (14) applies to static buckling of an elastic column with zero eccentricity. Now, for the elastic case

$$F_1 = \frac{A_1 E}{\ell}\delta_1 \qquad \text{and} \qquad F_2 = \frac{A_1 E}{\ell}\delta_2$$

or

$$F_1 - F_2 = \frac{A_1 E}{\ell}(\delta_1 - \delta_2) = \frac{\pi^4}{32}\frac{A_1 E}{L}(\delta_1 - \delta_2)$$

From equations (10) and (11)

$$\delta_1 - \delta_2 = \frac{8\rho}{L}y$$

Thus

$$F_1 - F_2 = \frac{\pi^4}{4}\frac{\rho A_1 E}{L^2}y$$

Substituting this into equation (14), the Euler load P_E of the column model is found to be

$$P_E = \frac{\pi^4}{4}\frac{A_1 E}{(L/\rho)^2}$$

where L/ρ is the slenderness ratio of the column. In terms of the total cross-sectional area the equation becomes

$$P_E = \frac{\pi^4}{8}\frac{AE}{(L/\rho)^2} \tag{15}$$

The Euler load, in terms of the Euler displacement, is

$$P_E = 2K x_E$$

and, substituting for K and P_E, the Euler displacement becomes

$$x_E = \frac{4\rho^2}{L} \tag{16}$$

With these results determined from elastic behavior of the column and model, the equations for the strains and for dynamic equilibrium of the inelastic column model are developed in a convenient non-dimensional parametric form. From equation (10) the strain in Spring 1 is

$$\epsilon_1 = \frac{\delta_1}{\ell} = \frac{\pi^4}{32} \frac{\delta_1}{L}$$

or

$$\epsilon_1 = \frac{\pi^4}{32} \left[\frac{x}{L} - \frac{2}{L^2} y^2 - \frac{4e}{L^2} y + \frac{4\rho}{L^2} y \right]$$

Defining a non-dimensional lateral deflection as V= y/e and making the substitution y=Ve, together with the substitution for the Euler displacement from equation (16), the strain may be expressed as

$$\epsilon_1 = \frac{\pi^4}{8(L/\rho)^2} \left[\frac{x}{x_E} - \frac{1}{2}\left(\frac{e}{\rho}\right)^2 V^2 - \left(\frac{e}{\rho}\right)^2 V + \frac{e}{\rho} V \right] \qquad (17)$$

Applying this same reasoning for the strain in Spring 2 results in

$$\epsilon_2 = \frac{\pi^4}{8(L/\rho)^2} \left[\frac{x}{x_E} - \frac{1}{2}\left(\frac{e}{\rho}\right)^2 V^2 - \left(\frac{e}{\rho}\right)^2 V - \frac{e}{\rho} V \right] \qquad (18)$$

From these equations for the strains at the center portion of the column model it can be recognized that the first terms are the dimensionless end displacements, the second terms are the corrections to this end displacement due to the angular rotation of the rigid rods, the third terms are the corrections due to the change of the effective eccentricity with lateral deflection, and the fourth terms result

from bending.

The relation between the strains and stresses during initial loading of the column model is given by the Ramberg-Osgood /9/ equation:

$$\epsilon = \frac{\sigma}{E} + \frac{3}{7}\left(\frac{E}{\sigma_y}\right)^{n-1}\left(\frac{\sigma}{E}\right)^n$$

where ϵ is the compressive strain, σ is the compressive stress, σ_y is the yield stress of the material and n is the shape parameter of the stress-strain curve. By defining a non-dimensional stress S as $\frac{\sigma}{E}$ the previous equation may be written as

$$\epsilon = S + \frac{3}{7}\left(\frac{1}{S_y}\right)^{n-1} S^n \qquad (19)$$

This is the equation which is used to determine the stress in each spring as the model is initially loaded. For the compressive stress-strain relation considered in this investigation the shape parameter is n=10 and the dimensionless yield stress is S_y=0.004. The stress-strain curve is shown in Fig. 6 and is typical of 24S-T aluminum alloy material.

As each of the springs unloads, it leaves the stress-strain curve following a straight line of slope $\frac{dS}{d\epsilon} = 1$. As subsequent loading takes place in either spring the same straight line is retraced and, as the stress reaches a level that puts it on the stress-strain curve again, it follows the curve until further unloading occurs.

The differential equation of motion is developed in

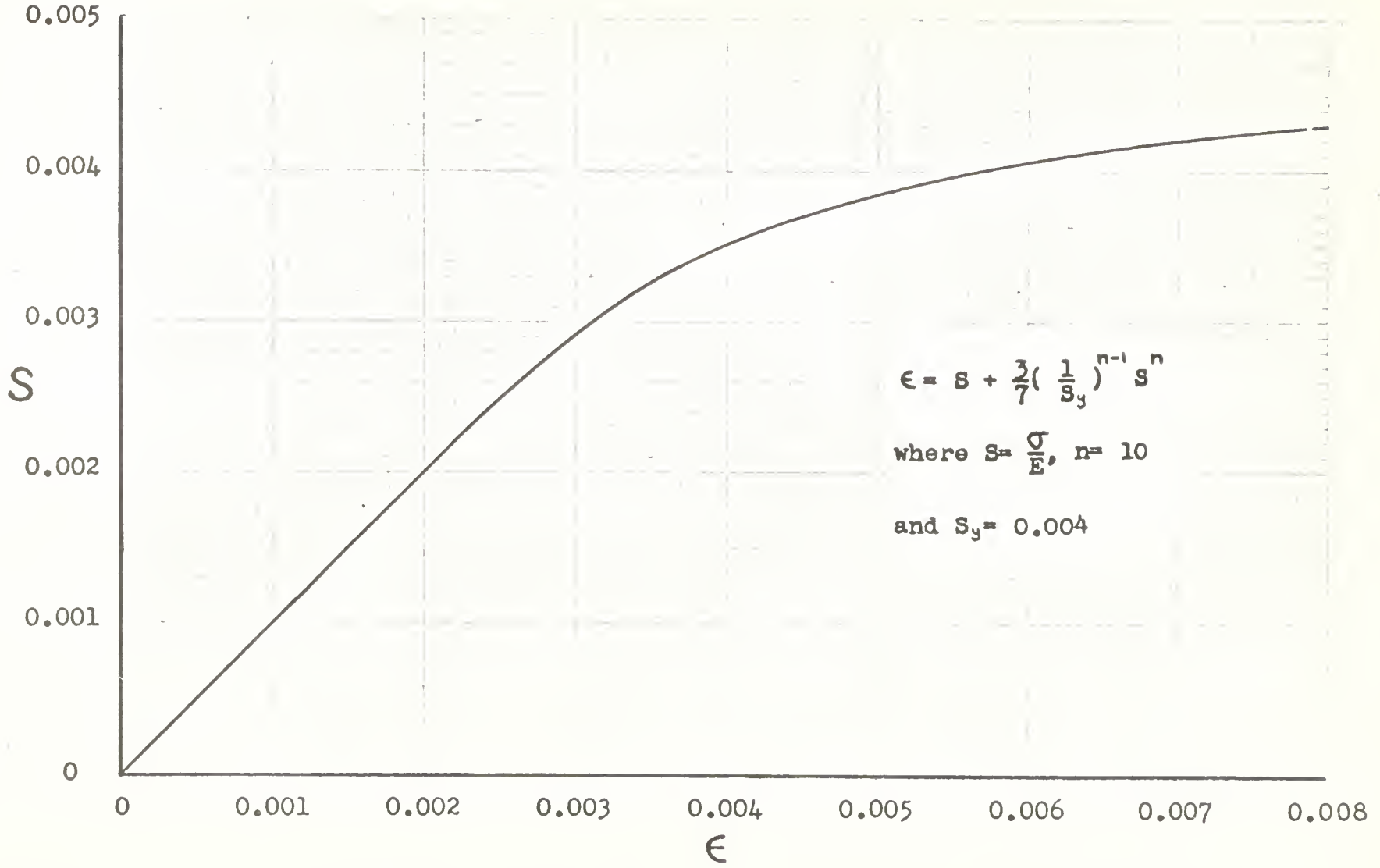

Fig. 6. Dimensionless Ramberg-Osgood Compressive Stress-Strain Curve for the Column Material.

nondimensional form by dividing equation (9) by the eccentricity e and the square of the circular frequency of first mode lateral vibration ω_n^2 and substituting from equation (1) for P. After rearranging terms the equation becomes

$$\frac{1}{\omega_n^2}\frac{d^2(y/e)}{dt^2} = \frac{4}{\pi^4}\left(L/\rho\right)^2\left[\left(\frac{F_1+F_2}{A_1E}\right)\left(\frac{y}{e}+1\right)-\left(\frac{F_1-F_2}{A_1E}\right)\frac{\rho}{e}\right]$$

A dimensionless time T is defined as $T = \omega_n t$, so that $\omega_n^2 (dt)^2 = (dT)^2$. Then $\frac{1}{\omega_n^2}\frac{d^2(y/e)}{dt^2}$ becomes $\frac{d^2(y/e)}{dT^2}$. By making the substitution V for y/e this becomes $\frac{d^2V}{dT^2}$ which is symbolized as $\ddot{V}$. By substituting V and $\ddot{V}$ and recognizing the form $\frac{F}{A_1E}$ as the previously defined non-dimensional stress, the differential equation of motion becomes

$$\ddot{V} = \frac{4}{\pi^4}\left(L/\rho\right)^2\left[\left(S_1+S_2\right)\left(V+1\right)-\left(S_1-S_2\right)\frac{\rho}{e}\right] \qquad (20)$$

The two terms in the brackets can be recognized, respectively, as proportional to the external bending moment due to the force on the end of the column, and the internal bending moment due to the spring forces.

In order to solve this equation it is necessary to specify the forcing function. This is accomplished by specifying the displacement of the ram (as shown in Fig. 1) as a function of time. When the ram is in contact with the column model the ram displacement is the end displacement of the column. If the ram is not in contact with the end of the column, the force is zero ($S_1 = -S_2$) and the column exhibits free vibration.

In either case the conditions of compatibility and dynamic equilibrium are maintained.

The ram displacement is a half-sine pulse of height X and duration τ_f. To enable a selection of dimensionless parameters having a relationship to the column the following dimensionless quantities are defined:

(a) the height of the half-sine ram displacement pulse as a fraction of the Euler end displacement;

$$\alpha = \frac{X}{X_E}$$

(b) the ratio of the natural period τ_n of first mode lateral vibration of the column to the duration τ_f of the half-sine pulse;

$$\beta = \frac{\tau_n}{\tau_f}$$

With these dimensionless quantities and the previously defined dimensionless time. The dimensionless ram displacement becomes

$$\chi = \alpha \sin \tfrac{1}{2}\beta T \qquad \text{for } 0 \leq T \leq \frac{2\pi}{\beta}$$

and (21)

$$\chi = 0 \qquad \text{for } T > \frac{2\pi}{\beta}$$

To determine the maximum force and residual lateral deflection resulting from a specified ram displacement it is necessary to compute the dynamic response of the model to the loading. This is accomplished through a numerical integration process applied to the differential equation of motion and a numerical iteration scheme to satisfy the relations among the strains, stresses, end displacement and lateral deflection.

3. THE NUMERICAL SOLUTION

The equations for the model are solved utilizing FORTRAN programming and a Control Data Corporation 1604 high speed digital computer. The investigation is accomplished with two basic programs, COL 1 and COL 2. The former is employed primarily to obtain graphical output directly to study the dynamic response of the model to a specified loading. Program COL 2 is employed to determine the numerical values of maximum force and residual lateral deflection for a specified loading on the model. The complete programs in FORTRAN language, together with the program notation, are given in Appendix IV.

The numerical integration procedure is the same for both programs, but the program, COL 2, employed to determine maximum values is more comprehensive. For this reason the detailed discussion is limited to this program. A discussion of the differences between these programs follows the detailed discussion. Figure 7 is a simplified block diagram of Program COL 2 and Fig. 8 is a simplified block diagram of the subroutine used in both programs to determine the stress from the strain.

Referring to Fig. 7, the input to the program includes the following dimensionless parameters:

(a) L/ρ (slenderness ratio) and e/ρ (eccentricity ratio) to prescribe the column model.

(b) α (ram pulse height) and ζ (ratio of natural period of first mode lateral vibration to ram pulse duration) to prescribe the forcing function on the model.

Fig. 7. Simplified Block Diagram of Computer Program COL 2

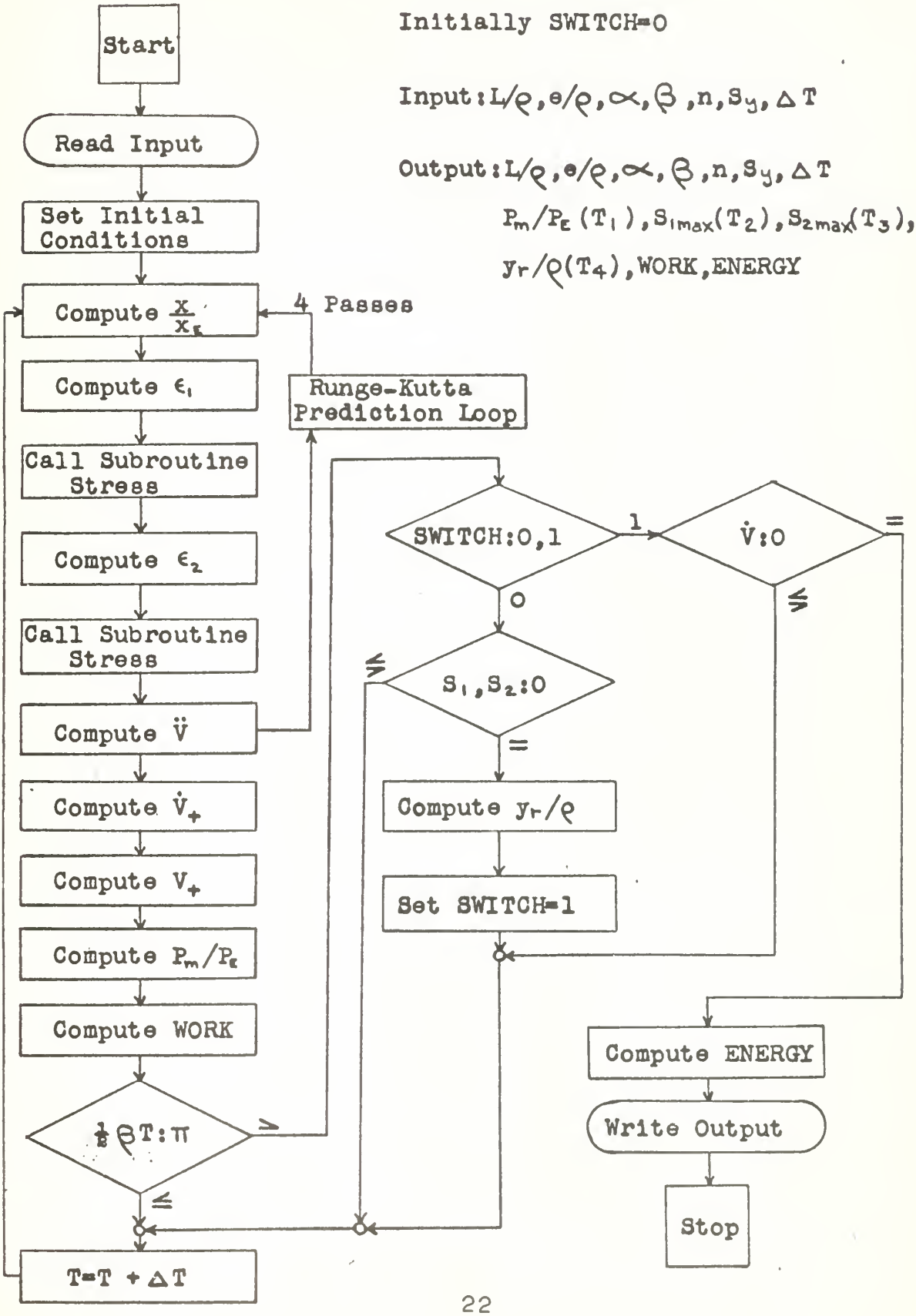

(c) n (Ramberg-Osgood shape parameter) and S_y (yield stress of the material) to prescribe the compressive stress-strain curve.

(d) ΔT (time increment) to prescribe the incremental values in the numerical integration process.

The initial conditions are then set to start the numerical integration process.

Henceforth, the dimensional quantities and the dimensionless quantities are referred to synonomously except where confusion may result, i.e., lateral deflection for dimensionless lateral deflection, etc.

The numerical integration scheme used in the programs is a Runge-Kutta process /10/. This process predicts the lateral deflection V and the lateral velocity $\dot{V}$ at a time $T+\Delta T$ from four estimates of the lateral acceleration $\ddot{V}$ calculated in the time increment ΔT. Accuracy is of the order of $(\Delta T)^3$. Within this predictor loop further calculations are made to satisfy the relations among the strains, stresses, end displacement and lateral deflection.

The ram displacement is computed from equation (21). The values of ram displacement and of lateral deflection are then used to determine the strain in Spring 1 from equation (17). The main program then calls Subroutine STRESS. Because this routine is written with dummy variable inputs to accommodate the strains and stresses in both Spring 1 and Spring 2, the following discussion is presented based on a general strain ϵ and a general dimensionless stress S.

Subroutine STRESS, shown in Fig. 8, is entered with the present value of strain ϵ and the previous values of stress S_a and strain ϵ_a calculated for the preceding time $T-\Delta T$. The solid curve in Fig. 9 represents the dimensionless compressive stress-strain curve. The dashed vertical lines indicated by A, B, and C in the figure are representative of conditions which must be considered in arriving at a value for the stress S from a value of the strain ϵ.

Referring now to Figs. 8 and 9, if the present value of strain is negative this condition is represented by A. The spring has unloaded from the stress-strain curve following a straight line with a slope equal to unity and the stress is calculated from

$$S = S_a + (\epsilon - \epsilon_a) \qquad (22)$$

This equation is also used to determine the stress S if $\epsilon=0$. If ϵ is positive there are three possibilities to be considered. These are:

(a) loading is occurring along the compressive stress-strain curve;

(b) unloading is occurring on a unity slope line;

(c) loading is occurring on a unity slope line.

To determine which of these possibilities exists the incremental change in strain, $\Delta\epsilon = \epsilon - \epsilon_a$, is calculated. If this quantity is negative this condition is represented by B. The spring is unloading on a unity slope line and the stress is calculated from equation (22). If the incremental

Fig. 8. Simplified Block Diagram of Computer Program for Subroutine STRESS.

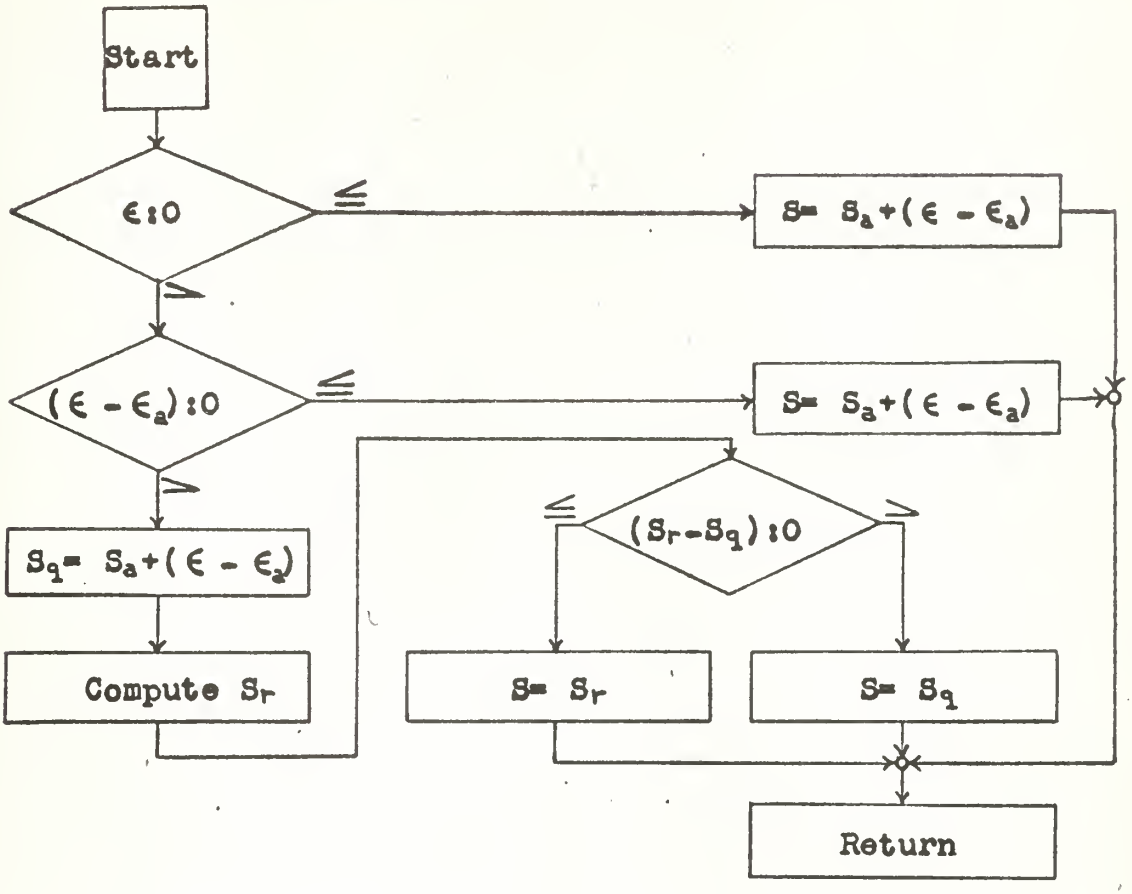

Fig. 9. Stress-Strain Considerations in Computer Program for Subroutine STRESS.

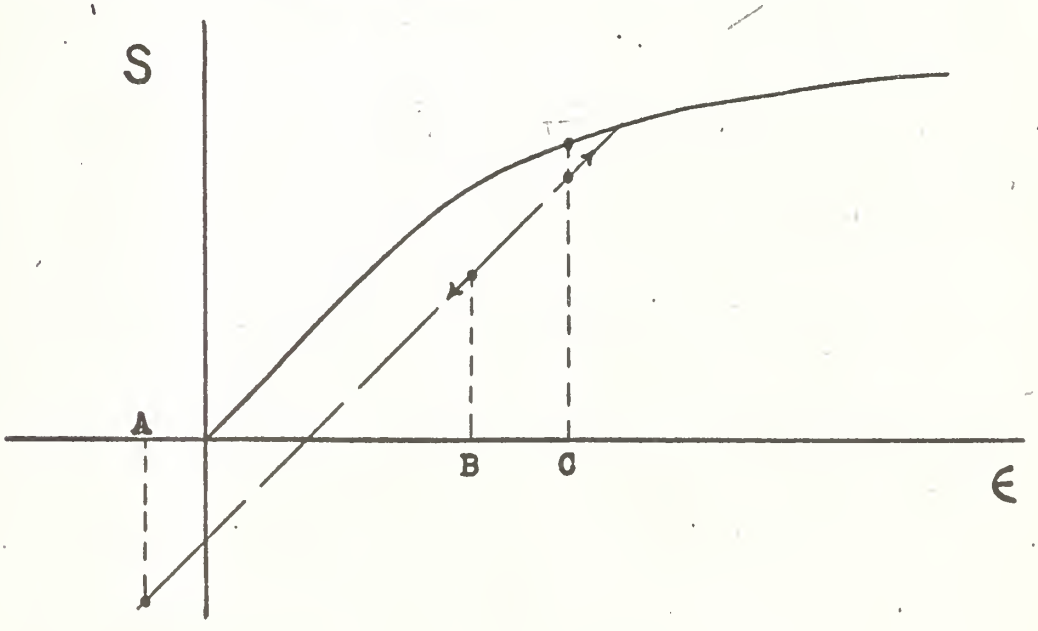

change in strain is positive two possibilities exist. Either the stress is on the compressive stress-strain curve or the stress is increasing on a unity slope line. This situation is represented by C in Fig. 9. The stress level is determined by calculating a value of stress from equation (22) and by calculating a value of stress from the Ramberg-Osgood equation (19) and then selecting the smaller of these two values as the stress existing in the spring. If the incremental change in strain is zero, the stress S is equal to S_3.

To calculate the value of stress from the Ramberg-Osgood equation it is necessary to compute the real, positive root of the equation. This is accomplished by a Newton-Raphson iteration /10/ where the strain ϵ is used as the initial estimate for the root S_r. The stress S could have been determined from the strain ϵ each time by calculating a value from equation (22) and a value from the Ramberg-Osgood equation (19) and selecting the smaller value. However, this would involve an iteration for each stress calculation, thus increasing the computer time. Therefore, this method was not used.

After S_1 is determined the value for the strain ϵ_2 is calculated from equation (18). The main program again calls Subroutine **STRESS** to determine the value of S_2.

At this point the program calculates the sum S_1+S_2, which is directly proportional to the force on the end of the model, to determine if it is compressive (positive) or

tensile (negative). As previously discussed for the model configuration (Fig. 1), the ram cannot transmit a tensile force to the model. Therefore, if this sum is negative the program initiates an iterative interpolation scheme to determine the end displacement of the model which will cause the sum S_1+S_2 to be zero. This involves recalculating the strains and then the stresses for each end displacement until the force is zero. The model is then in a state of free vibration. This free vibration continues until the ram again contacts the column or until the calculation terminates.

Once these states of stress (end force either positive or zero) are determined, the lateral acceleration $\ddot{V}$ is calculated from equation (20). After four passes are made to this point in the program to determine the values for the Runge-Kutta predictions, as previously discussed, the lateral velocity $\dot{V}$ and the lateral deflection V are calculated for the end of the time interval ΔT.

At this point the program computes the force which can be shown to be

$$\frac{P}{P_E} = \frac{4}{\pi^4}\left(L/\rho\right)^2\left(S_1 + S_2\right)$$

and a continuous check is made to determine the maximum value of this quantity which is stored for print-out. This continuous check is also made to determine the maximum value of compressive stress in each of the springs. These values are stored for use in strain energy calculations to be made later.

A continuous check is also made to determine the extreme stress (tensile or compressive) in each spring for print-out. The program then calculates the ram work done on the model for the preceding time increment and adds this quantity to the previous work done by the ram.

This whole process continues until the ram displacement pulse has terminated and the column is left in a state of free vibration. Then a continuous check is initiated to determine the time at which $S_1=S_2=0$. The lateral deflection at this point is the residual deflection y_r in the model, as the lateral acceleration, the longitudinal end force and the internal moment are all zero, and the residual strains determine the permanent deformation that has resulted.

After the residual deflection has been calculated a switch is set to detour this portion of the program. The new path includes a continuous check to determine the time at which the lateral velocity is zero (point of extreme lateral deflection and zero kinetic energy). At this point the net energy input to each of the springs is calculated from the area under the stress-strain curve using the present values of stress and the previously stored maximum values of the compressive stress. This energy is a combination of the strain energy of plastic deformation and of the potential energy due to existing elastic strain in the model. This energy should be equal to the ram work done on the model.

When the energy has been calculated the program then

prints all input quantities and the results. The results include the values of P_m/P_E , y_r/ρ , S_{1max} , S_{2max} and the time T that each of these occur, as well as the work and energy. The times are included to complement the time plots from the other program as an aid in visualizing some of the dynamic behavior and to determine the problem time termination of the program.

The program employed to obtain graphical output directly is Program COL 1 (the FORTRAN language listing is given in Appendix IV). This program differs basically from Program COL 2 described in the preceding paragraphs in that it stores the variable quantities for each time T in array form instead of storing only the maximum values. These array quantities are then available for Subroutine GRAPH (not shown in the listing but available on the FORTRAN Library Tape at the U.S. Naval Postgraduate School, and also available from the Control Data Corporation). Subroutine GRAPH is designed to accept a maximum of 900 points for each variable to be plotted. Thus the program is written to calculate only 900 points while maintaining the necessary accuracy for the numerical integration process compatible with the time increment ΔT.

In addition to the input data required in Program COL 2, axis scaling and multiple curve data, graph title data and curve label data are required for Program COL 1. In addition to the graphical output the program prints the input quantities and the values of T, x/x_E, ϵ_1 , ϵ_2 , S_1 , S_2, y/ρ and P/P_E for every fifteenth point. As all of these quantities

have been stored as 900 point arrays any combination of these variables may be plotted as a function of another. Subroutine **GRAPH** converts these 900 point arrays to input data on a magnetic tape for a Control Data Corporation 160 computer which is programmed to provide output as input to a plotter.

An example of one set of curves used in the investigation is shown in Appendix I. The example includes three graphs with two curves on each graph. The first graph is a plot of ϵ_1 and ϵ_2 versus T. The second graph is a plot of S_1 and S_2 versus T and the third graph is a plot of y/ρ and P/P_E versus T. Other examples of graphical output are shown in Appendices II and III. However, the graphs shown in Appendix II, which are for very slow loading approaching the static case, have been obtained with a modified version of the program. The modification includes calculating 1800 points to maintain the accuracy for the numerical integration process, then re-storing every other point of the 1800 point arrays as 900 point arrays to accomodate Subroutine **GRAPH**.

4. RESULTS AND DISCUSSION

a. Character of the response

An understanding of the results is dependent upon an appreciation of the distinctive features of the loading and their effects upon the response. Loading is accomplished by a forced displacement of one end of the column in the form of a half-sine pulse. This pulse is characterized by the dimensionless parameters α and β. The quantity α is the ratio of the displacement pulse height to that end displacement which, in the absence of lateral deflection, corresponds to the Euler buckling load. The parameter β is the ratio of the first mode natural period of lateral vibration of the column model to the pulse duration. Thus, α measures the amplitude of the loading and β measures its rapidity.

Consider the very slow loading ($\beta << 1$) of a slender column to a maximum end displacement beyond the Euler critical value ($\alpha > 1$). At axial loads above the Euler limit the straight form of the column is unstable. To initiate lateral deflection of the column model the end pins are eccentrically located. The effect of this eccentricity is to produce bending at loads below the stability limit of the column. The maximum force (P_m) developed in the column becomes less than the Euler load (P_E). However, for very slow loading the maximum force developed in the column model is the static maximum load. Increasing values of α above

that corresponding to the Euler critical value do not change the value of the maximum force P_m.

For increasing loading rates (increasing values of β) the lateral motion of the column is retarded by the inertia of the mass and any meaningful correspondence to static behavior is lost. However, the maximum force developed in the column is related to the rate of loading. Also, under pulse loading the inelastic column recovers from a deflected position with an amount of residual deflection and retains a capacity to sustain further load. This capacity may be measured in terms of the amount of residual deflection y_r which results from the loading. This residual deflection is equivalent to additional eccentricity for any subsequent loading. The maximum force P_m and the residual deflection y_r appear to be the most important performance criteria for the dynamic behavior of the inelastic column subjected to a pulse loading. Dimensionless forms of these two quantities are utilized in the graphical form of the results.

b. Range of variables

Solutions for P_m/P_E (maximum force) and for y_r/ρ (residual deflection) have been obtained for a range of β from 0.01 to 1.0 and for a range of α dependent on the column slenderness ratio. The results include solutions for three values of column slenderness ratio (L/ρ) and two values of eccentricity ratio (e/ρ). For slenderness ratios of 70 and 50 the minimum pulse height considered was $\alpha = 1$. For a slenderness

ratio of 100 the minimum pulse height considered was $\alpha = 2$. For values of α less than these, inelastic action is insignificant. The maximum values of α considered are based on the maximum value of tensile stress occurring in the column model springs. For the investigation the stress-strain relationship after departure from the compressive stress-strain curve is considered linear into the tensile stress region. For this reason the maximum tensile stresses in the column are limited to values near the nominal yield stress of the column material. For slenderness ratios of 70 and 50 the maximum pulse height considered was $\alpha = 2.5$. For a slenderness ratio of 100 the maximum pulse height considered was $\alpha = 4$. For values of α greater than these the maximum value of tensile stress occurring in the column model is considerably in excess of the nominal yield stress for some rates of loading.

c. Maximum force

Figure 10 is a plot of families of curves of maximum force P_m/P_E versus β for a constant pulse height α. The families include slenderness ratios of 100, 70, and 50 for an eccentricity ratio of 0.05. Figure 11 is a plot of the same families of curves for an eccentricity ratio of 0.01. The lower limit of $\beta = 0.01$ is for slow loading rates approaching the static case. The upper limit of $\beta = 1.0$ is approaching the region where axial inertia effects become important in the elastic column as reported by Taylor /5/. As the inelastic column model does not include the effects of axial inertia $\beta = 1.0$

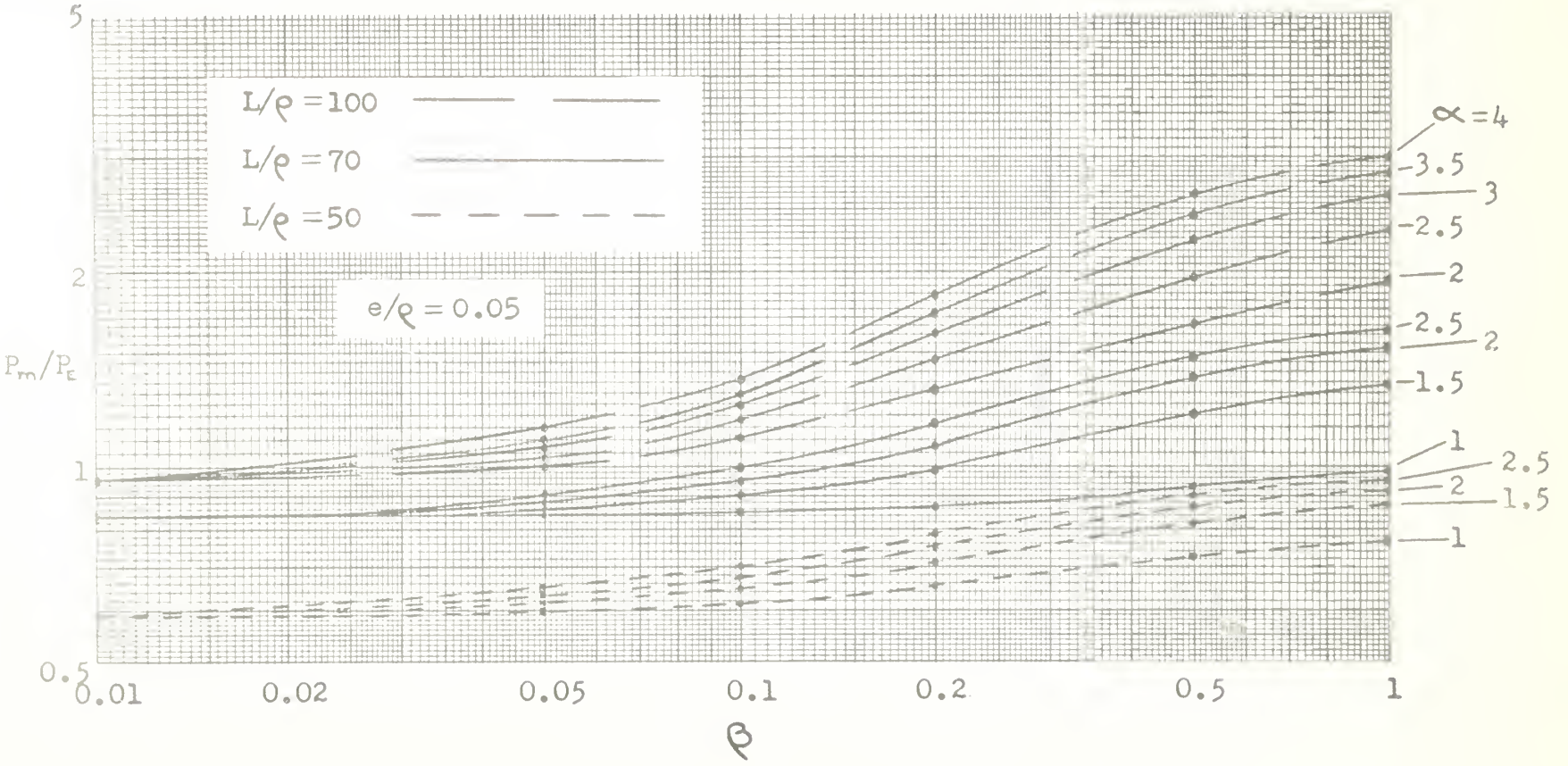

Fig. 10. Values of maximum force P_m/P_E vs. β (α constant, $e/\rho = 0.05$) for column slenderness ratios L/ρ of 100, 70, and 50.

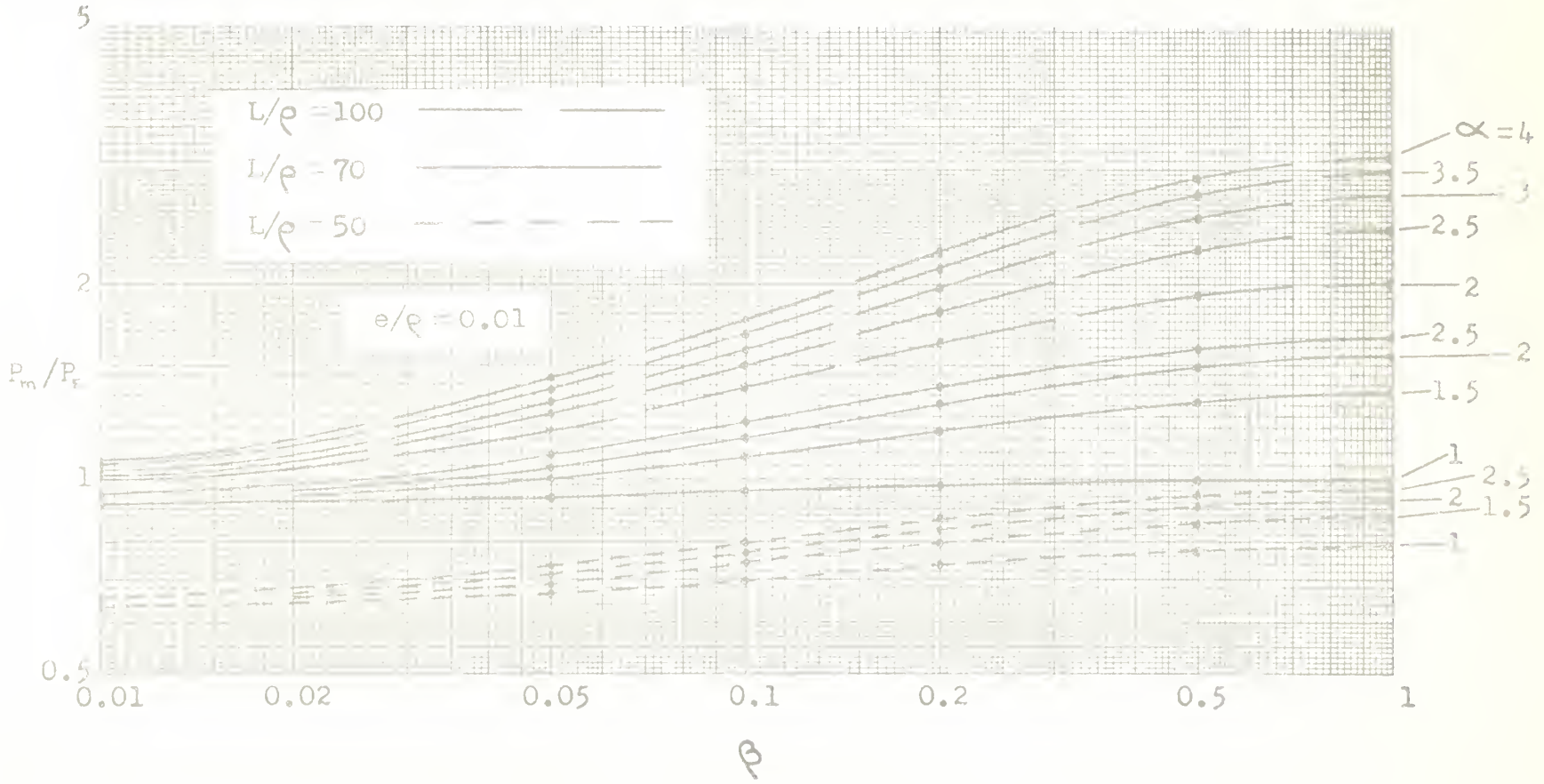

Fig. 11. Values of maximum force P_m/P_E vs. β (α constant, $e/\rho = 0.01$) for column slenderness ratios L/ρ of 100, 70, and 50.

is the upper limit considered in this study.

Figures 10 and 11 show that as the rate of loading is increased the maximum force developed in the column increases. This is due to the delay in the development of lateral deflection because of lateral inertia. These figures also indicate that as the rate of loading is decreased the maximum force developed in the column approaches a limit asymptotically. In Fig. 10 this limit may be observed for each slenderness ratio as all of the curves converge to a single value at $\beta = 0.01$. This limit is the static load capacity of the column for an eccentricity ratio of 0.05. In Fig. 11 this limit is not attained. The spread of points indicates that for this eccentricity ($e/\rho = 0.01$) there is considerable dynamic effect at $\beta = 0.01$. However, the curves of minimum α for each slenderness ratio at $\beta = 0.01$ appear to approach a limit of the static load capacity of the column for an eccentricity ratio of 0.01. A comparison of these figures confirms that as the eccentricity increases the maximum force developed in the column decreases.

d. Slow loading

It is possible to make some observations concerning the values obtained at the low end of the β range by considering the static case of a centrally loaded inelastic column. For this case the maximum load the column can support is between the tangent modulus load P_T and the reduced modulus load P_R. In terms of the Euler load the dimensionless

tangent modulus load is

$$\frac{P_T}{P_E} = \frac{E_T}{E} \tag{23}$$

where E_T is the tangent modulus or the local slope of the compressive stress-strain diagram. The tangent modulus defines the value of stress at which bending begins for the static case of a centrally loaded inelastic column. In terms of the model constants developed previously this critical stress is

$$\sigma_{cr} = \frac{\pi^4}{8} \frac{E_T}{(L/\rho)^2}$$

or in terms of dimensionless stress this becomes

$$S_{cr} = \frac{\pi^4}{8} \frac{E_T}{E} \left(\frac{1}{L/\rho}\right)^2 \tag{24}$$

The ratio of Young's modulus to the tangent modulus in terms of the Ramberg-Osgood parameters is

$$\frac{E}{E_T} = 1 + \frac{n\,(1-0.7)}{0.7} \left(\frac{S}{S_y}\right)^{n-1} \tag{25}$$

where n = 10 (the shape parameter) and S_y = 0.004 (the dimensionless compressive yield stress) are the parameters used in the investigation. By choosing a value of S_{cr} and substituting this for S in equation (25) the ratio E/E_T is determined. By substituting the values of this ratio and S_{cr} in equation (24) the slenderness ratio is determined. In this way a value of the ratio E_T/E is determined corresponding to each of the slenderness ratios 100, 70, and 50. This value of E_T/E equals P_T/P_E from equation (23).

In terms of the Euler load the dimensionless reduced modulus load is

$$\frac{P_R}{P_E} = \frac{E_R}{E} \tag{26}$$

where E_R is the reduced modulus. The reduced modulus defines a maximum value of stress which can be approached but not exceeded for the static case of a centrally loaded inelastic column. In terms of the model constants developed previously this critical stress is

$$\sigma_{cr} = \frac{\pi^4}{8} \frac{E_R}{(L/\rho)^2}$$

or in terms of dimensionless stress this becomes

$$S_{cr} = \frac{\pi^4}{8} \frac{E_R}{E} \left(\frac{1}{L/\rho}\right)^2 \tag{27}$$

The reduced modulus is dependent on the tangent modulus and the geometry of the column. For the column model it can be shown that the reduced modulus is

$$E_R = \frac{2 E E_T}{E + E_T}$$

or in dimensionless form this becomes

$$\frac{E_R}{E} = \frac{2 E_T/E}{1 + E_T/E} \tag{28}$$

and this value is equal to P_R/P_E from equation (26). By choosing a value of S_{cr} and substituting this for S in equation (25) the ratio E_T/E is determined. The ratio E_T/E also determines E_R/E from equation (28). By substituting the values of E_R/E and S_{cr} in equation (27) the slenderness ratio is determined. In this way a value of the ratio E_R/E is determined

corresponding to each of the slenderness ratios 100, 70, and 50. This value of E_R/E equals P_R/P_E from equation (26).

The values of the tangent modulus load and the reduced modulus load determined from these two methods are:

for $L/\rho = 100$, $P_T/P_E = 1.000$ and $P_R/P_E = 1.000$;

for $L/\rho = 70$, $P_T/P_E = 0.969$ and $P_R/P_E = 0.977$;

for $L/\rho = 50$, $P_T/P_E = 0.649$ and $P_R/P_E = 0.691$.

From Figs. 10 and 11 it is seen that in most cases the maximum values at $\beta = 0.01$ are less than the tangent modulus load although the spread of points for an eccentricity ratio of 0.01 indicates that dynamic effects are more pronounced the smaller the eccentricity. For this reason some of the maximum values are greater than the reduced modulus load.

To observe further the effect of eccentricity on the load capacity of the column at very slow loading rates, a study was made to determine the behavior of the column under a ramp displacement of the end at a loading rate corresponding to that available to commercial testing machines. In terms of the parameters previously used to describe the pulse loading of the column the ramp displacement of the head is

$$\chi = \tfrac{1}{2} \alpha \beta T$$

where $\alpha = 1.0$ and $\beta = 0.01$. Computer solution results including a graphical presentation of Strain 1 (ϵ_1) and Strain 2 (ϵ_2) versus force (P/P_E) were obtained for the three column slenderness ratios of 100, 70, and 50 for eccentricity ratios of 0.05, 0.01, and 0.001. The graphical results shown in App.II

exhibit a general resemblance to the experimental strain versus force curves of actual column test data displayed by Shanley /1/. From the results given in Table 1 it is seen that for eccentricity ratios of 0.05 and 0.01 the maximum load is less than the tangent modulus load for all three slenderness ratios considered. However, the maximum load increases with a decrease in the eccentricity ratio. As the eccentricity ratio is decreased to 0.001 the maximum load is greater than the tangent modulus load but less than the reduced modulus load for a slenderness ratio of 50. For a slenderness ratio of 70 there is considerable dynamic effect and the maximum force exceeds the reduced modulus load by a

Table I Computer and Theoretical Static Load Comparison
(For Ramp Loading of Column Model)

		$L/\rho = 100$	$L/\rho = 70$	$L/\rho = 50$
Static P_T/P_E		1.000	0.969	0.649
Static P_R/P_E		1.000	0.977	0.691
Dynamic (Computer) P_m/P_E	for $e/\rho = 0.05$	0.952	0.839	0.584
	for $e/\rho = 0.01$	0.983	0.916	0.633
	for $e/\rho = 0.001$	1.000	0.981	0.665

small amount. For a slenderness ratio of 100 there is considerable dynamic effect also but the solution oscillates about an average maximum value of $P_m / P_E = 1.0$.

The tabulated values of P_m/P_E for an eccentricity ratio of 0.05 for a ramp displacement loading are in agreement with the maximum force values P_m/P_E for pulse loading at $\beta = 0.01$ in Fig. 10. The strain (ϵ_1 and ϵ_2) versus force (P/P_E) curves for the ramp displacement loading for an eccentricity ratio of 0.05 shown in App. II display no dynamic behavior. In Fig. 11 ($e/\rho = 0.01$), where the dynamic effects are more pronounced at $\beta = 0.01$ for pulse loading, the forces on the $\alpha = 1$ curves for slenderness ratios of 70 and 50 agree with these tabulated results. For a slenderness ratio of 100 the smallest value of α considered for pulse loading was 2 and this curve appears to approach a value $P_m/P_E = 0.983$ asymptotically. The strain versus force curves for the ramp displacement loading for an eccentricity ratio of 0.01 shown in App. II display an insignificant amount of dynamic behavior which does not affect the values of maximum force P_m/P_E . Therefore, these values of P_m/P_E may be considered the static load capacity of the inelastic column for eccentricity ratios of 0.05 and 0.01.

Appendix III contains a compilation of the dynamic response curves stress (S_1 and S_2) versus time (T) for a range of β from 0.1 to 1.0 and for an eccentricity ratio $e/\rho = 0.01$. This graphical compilation includes the solutions for the minimum and maximum values of pulse height considered in the

study for all three slenderness ratios. Included with the compilation is a discussion of the more prominent features of the curves.

e. Residual deflection

Figures 12, 13, and 14 are familes of curves showing residual deflection y_r/ρ versus β for a constant pulse height α and for e/ρ = 0.01 and 0.65. Figure 12 is the family for L/ρ = 100, Fig. 13 is the family for L/ρ = 70, and Fig. 14 is the family for L/ρ = 50. The points shown on these curves are from the identical computer solution results as the points shown in Figs. 10 and 11.

From Fig. 12 for L/ρ = 100 it is shown that in general the values of residual deflection increase with the rapidity of loading to a maximum value then decrease abruptly. This abrupt decrease is because of the delay in the development of lateral deflection due to lateral inertia. From Fig. 13 for L/ρ = 70 and Fig. 14 for L/ρ = 50 it is shown that in general the values of residual deflection are essentially constant as the rapidity of loading increases until an abrupt decrease occurs due to the effect of lateral inertia. The exception for α = 1 and L/ρ = 70 is due to the small amount of inelastic action that takes place for this pulse height at all values of β. The amount of residual deflection may be expressed in terms of the amount of inelastic action that occurs. From the graphical compilation of stress versus time curves in App. III and the data compiled in App. V the amount

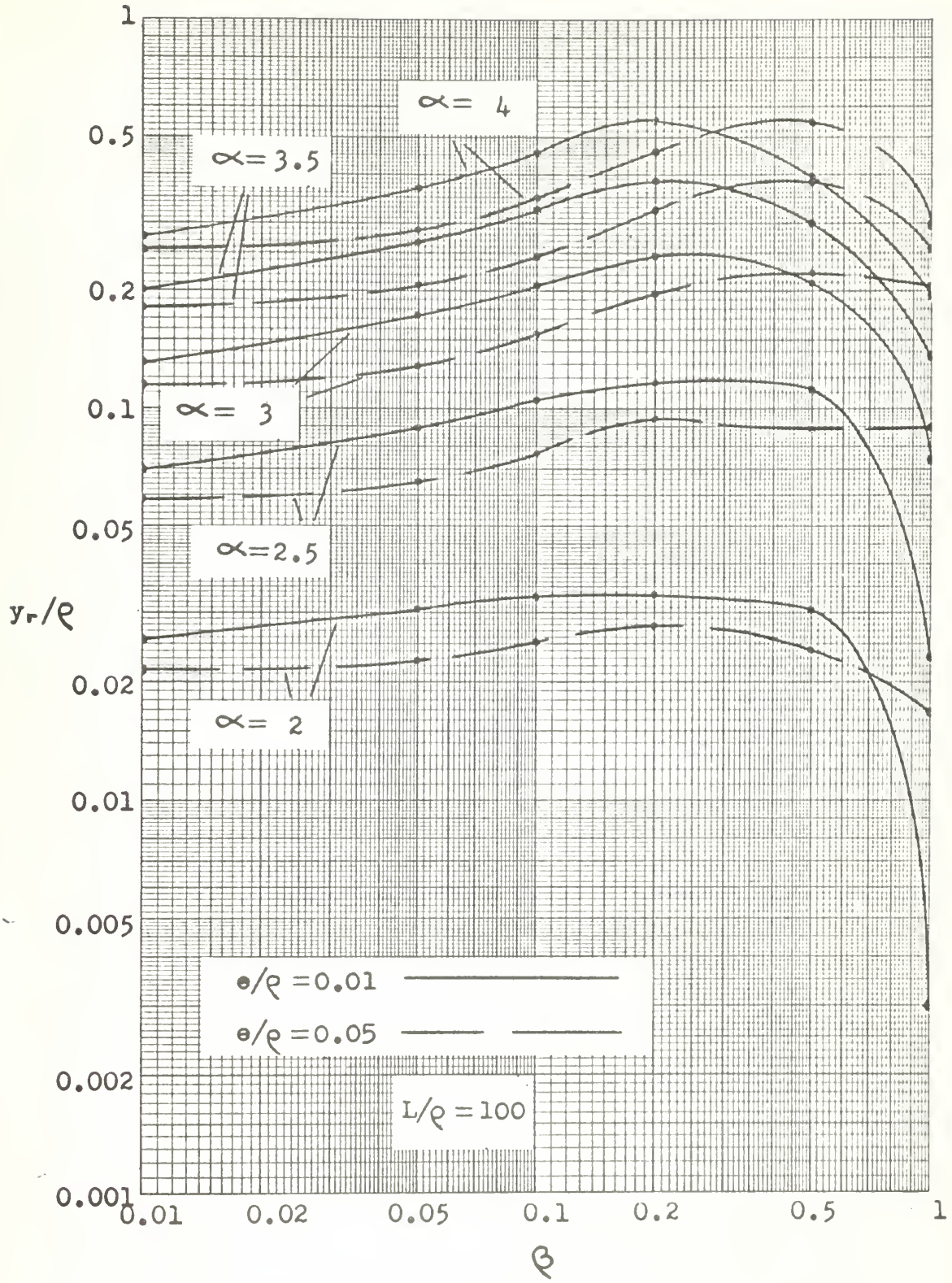

Fig. 12. Values of residual deflection y_r/ρ vs. β (α constant, $e/\rho = 0.01$ and 0.05) for a column slenderness ratio L/ρ of 100

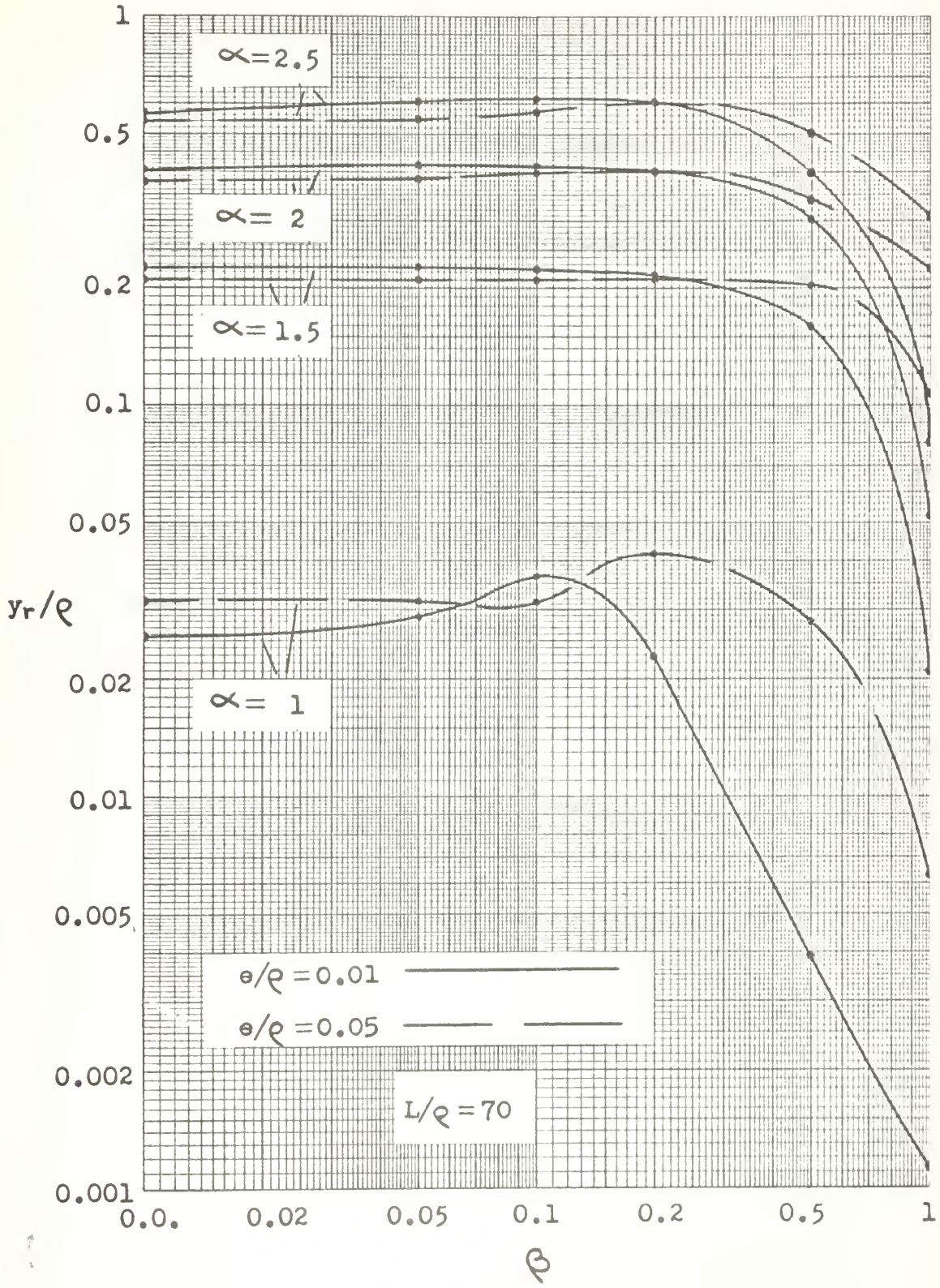

Fig. 13. Values of residual deflection y_r/ϱ vs. β (α constant, $e/\varrho = 0.01$ and 0.05) for a column slenderness ratio L/ϱ of 70.

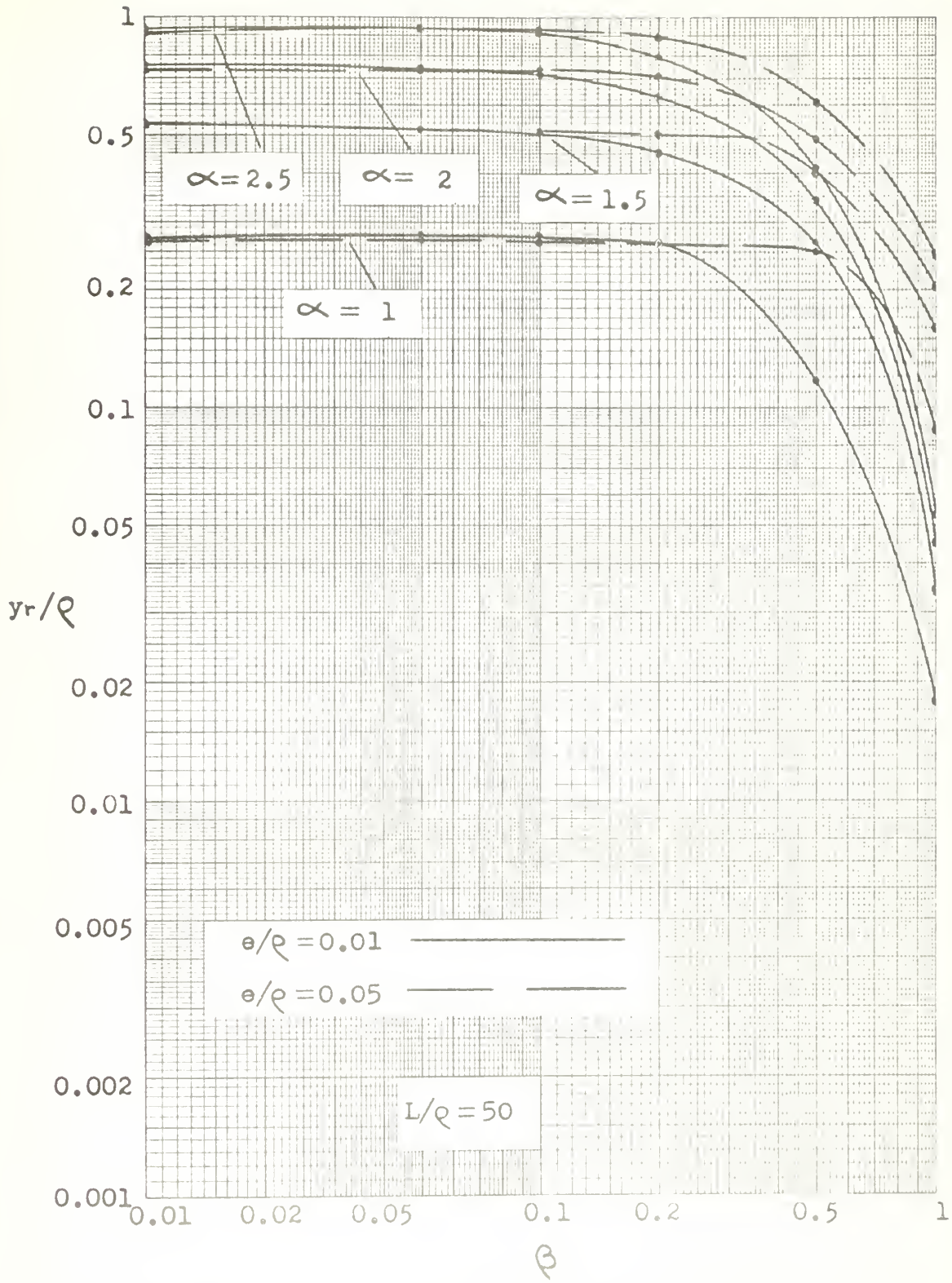

Fig. 14. Values of residual deflection y_r/ρ vs. β (α constant, e/ρ= 0.01 and 0.05) for a column slenderness ratio L/ρ of 50.

of inelastic action may be determined. For a slenderness ratio of 100, inelastic action in the column is limited to maximum compressive stress levels below the value of the yield stress for all solutions considered in the investigation. For a slenderness ratio of 50, inelastic action, in general, occurs at much higher maximum compressive stress levels-near or above the yield stress. For a slenderness ratio of 70, inelastic action occurs at maximum compressive stress levels intermediate to those for slenderness ratios of 100 and 50.

A comparison of Fig. 12, 13, and 14 indicates that as the slenderness ratio decreases the effect of eccentricity on the values of residual deflection is less pronounced. However, decreasing eccentricity causes a shift of the residual deflection curves to longer pulse durations (smaller values of β). This is because dynamic behavior is more pronounced the smaller the eccentricity and lateral inertia effects become more important at slower loading rates. It may also be observed from these residual deflection curves that the maximum values of residual deflection do not necessarily occur at the slowest loading rates. The minimum values of residual deflection generally occur at the fastest loading rates. The only exceptions are for the columns of largest slenderness ratio ($L/\rho = 100$) and largest eccentricity ($e/\rho = 0.05$). However, the residual deflections appear to follow the same trend but are limited by the maximum value of the parameter β = 1.0(shortest pulse duration considered in the investigation).

5. CONCLUSIONS

From the results discussed in the preceding section, the following conclusions may be drawn for the rates of loading considered in the investigation:

(a) The inelastic column model, together with a high speed digital computer and the peripheral plotting equipment, provides a sound and reasonable method for the study of the dynamic behavior of inelastic columns.

(b) For very slow loading (long pulse duration) the model exhibits behavior in agreement with Shanley's postulates.

(c) As eccentricity is reduced, the lateral response is slowed. Accordingly, columns with very small eccentricity show significant dynamic effects at quite slow loading rates.

(d) Within the range of pulse durations studied, the maximum load increases monotonically with decreasing pulse duration.

(e) The ratio of maximum dynamic load to static load capacity decreases as the slenderness ratio is reduced.

(f) Within the range of pulse durations studied, the smallest residual deflections generally accompany the shortest pulse durations.

6. BIBLIOGRAPHY

1. F. R. Shanley, Inelastic Column Theory. Journal of the Aeronautical Sciences, Vol. 14, No. 5, May 1947, pp 261-268.

2. N. J. Hoff, The Dynamics of the Buckling of Elastic Columns. Journal of Applied Mechanics, March 1951, pp 68-74.

3. N. J. Hoff, S. V. Nardo, and B. Erickson, The Maximum Load Supported by an Elastic Column in a Rapid Compression Test. Proceedings of the First U.S. National Congress of Applied Mechanics, 1952, pp 419-423

4. E. Sevin, On the Elastic Bending of Columns Due to Dynamic Axial Forces Including Effects of Axial Inertia. Journal of Applied Mechanics, March 1960, pp 125-131.

5. L. H. Taylor, Jr., Elastic Columns Under Half Sine Pulse Loading. Thesis, U.S. Naval Postgraduate School, Monterey, California, 1962.

6. G. Gerard and H. Becker, Column Behavior Under Conditions of Impact. Journal of the Aeronautical Sciences, Vol. 19, No. 1, January 1952, p 58.

7. J. P. Chawla, Numerical Analysis of the Process of Buckling of Elastic and Inelastic Columns. Proceedings of the First U.S. National Congress of Applied Mechanics, 1952, pp 435-441.

8. W. A. Brooks, Jr. and T. W. Wilder, III, The Effect of Dynamic Loading on the Strength of an Inelastic Column. National Advisory Committee for Aeronautics, Technical Note 3077, 1954.

9. W. Ramberg and W. R. Osgood, Description of Stress-Strain Curves by Three Parameters. National Advisory Committee for Aeronautics, Technical Note 902, 1943.

10. G. A. Korn and T. M. Korn, Mathematical Handbook for Scientists and Engineers. McGraw Hill Book Company, 1961.

APPENDIX I

Example of Graphical Output from Program COL 1

Graphical Notation

The computed points on the graphs are the values of the dimensionless variables developed in the basic equations. The graphical notation is as follows:

Symbol on Graph	Corresponding Symbols in the basic equations
SLENDERNESS	L/ρ
ECC	e/ρ
ALPHA	α
BETA	β
STRAIN 1	ϵ_1
STRAIN 2	ϵ_2
STRESS 1	S_1
STRESS 2	S_2
DEFLECTION	y/ρ
FORCE	P/P_E
TIME	T

Each of the curves on the graph is labeled to correspond to the terms in the graph title. The x-axis is the axis of abscissas and the y-axis is the axis of ordinates. The numbers specifying the coordinates are integer numbers located to the right of the coordinate on the x-axis and above the coordinate on the y-axis. The scale quantity is the value of the first marked coordinate from the origin in either the x-direction or the y-direction expressed in powers of ten

to locate the decimal point. The symbol E in the scale value indicates that the number following is the exponential power of ten to be applied to the basic scale value, i.e., 1.00E+01 is $1.00 \times 10^{+1}$.

Discussion of the curves

On pages I-5 to I-7 following this discussion are shown curves of ϵ_1, ϵ_2, S_1, S_2, y/ρ and P/P_E versus T. These curves are the solutions for the inelastic column model dynamic response to a ram pulse loading with the following parameters:

(a) slenderness ratio, $L/\rho = 100$

(b) eccentricity ratio, $e/\rho = 0.05$

(c) ram pulse height, $\alpha = 4.0$

(d) ram pulse duration in terms of $\beta = 0.2$,

$T_f = 2\pi/\beta = 10\pi$

The discussion includes some of the more prominent features of the dynamic behavior of the column model under ram pulse loading.

A comparison of the strain versus time curves with the stress versus time curves indicates the amount of inelastic action that takes place in Spring 1 and Spring 2. In Spring 1 the compressive stress level increases above that in Spring 2 as the amount of bending increases. The internal bending moment in the column model is directly proportional to $S_1 - S_2$. As the amount of bending increases Spring 2 departs from the compressive stress-strain curve along a straight

line with unit slope and continues into the tensile stress region. The values of stress in Spring 2 remain on this straight line for the remainder of the solution. The compressive stress level in Spring 1 continues to increase to a point where it also departs from the compressive stress-strain curve along a straight line as the internal bending moment increases and the force decreases to zero. This force is directly proportional to $S_1 + S_2$. When the force becomes zero the end of the column has departed from the ram which exhibits a half-sine pulse displacement. The column model is then in a state of free vibration until the end again makes contact with the ram. The compressive stress level in Spring 1 again returns to values on the compressive stress-strain curve. This alternate departure and contact between the column and the ram continues until the ram displacement pulse nears its termination. The column then continues in a state of free vibration where $S_1 = -S_2$. The amount of residual deflection may then be determined from the mean value of the deflection or from the deflection at the time when $S_1 = S_2 = 0$. At this point the internal forces and the internal bending moment in the column model are zero.

The effect of eccentricity on the dynamic behavior of the column model with all other parameters remaining the same may be observed by comparing the stress versus time curves in this appendix with the stress versus time curves on page III-13 where the eccentricity ratio is 0.01. It may

be noted that the essential differences in these curves are that the maximum compressive stress levels attained in Spring 1 and Spring 2 are greater for the smaller eccentricity. Also, contact between the ram and the column terminates sooner for the smaller eccentricity.

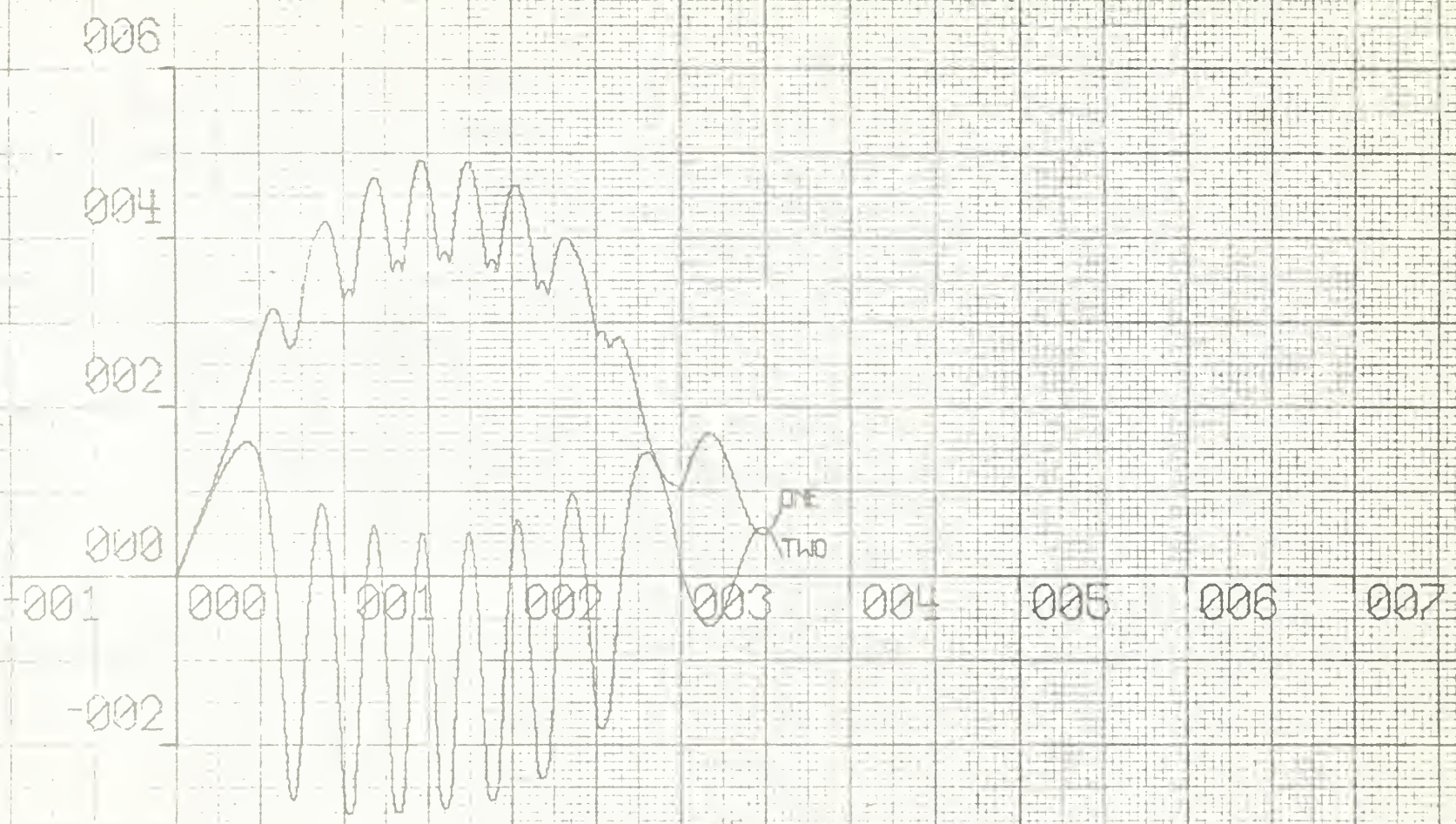

X AXIS SCALE = 1.00E+01
Y AXIS SCALE = 2.00E-03

DEFIBAUGH INELASTIC COLUMN (SLENDERNESS=100,ECC=0.05,ALPHA=4.0,BETA=0.2)

STRAIN 1 AND STRAIN 2 VERSUS TIME

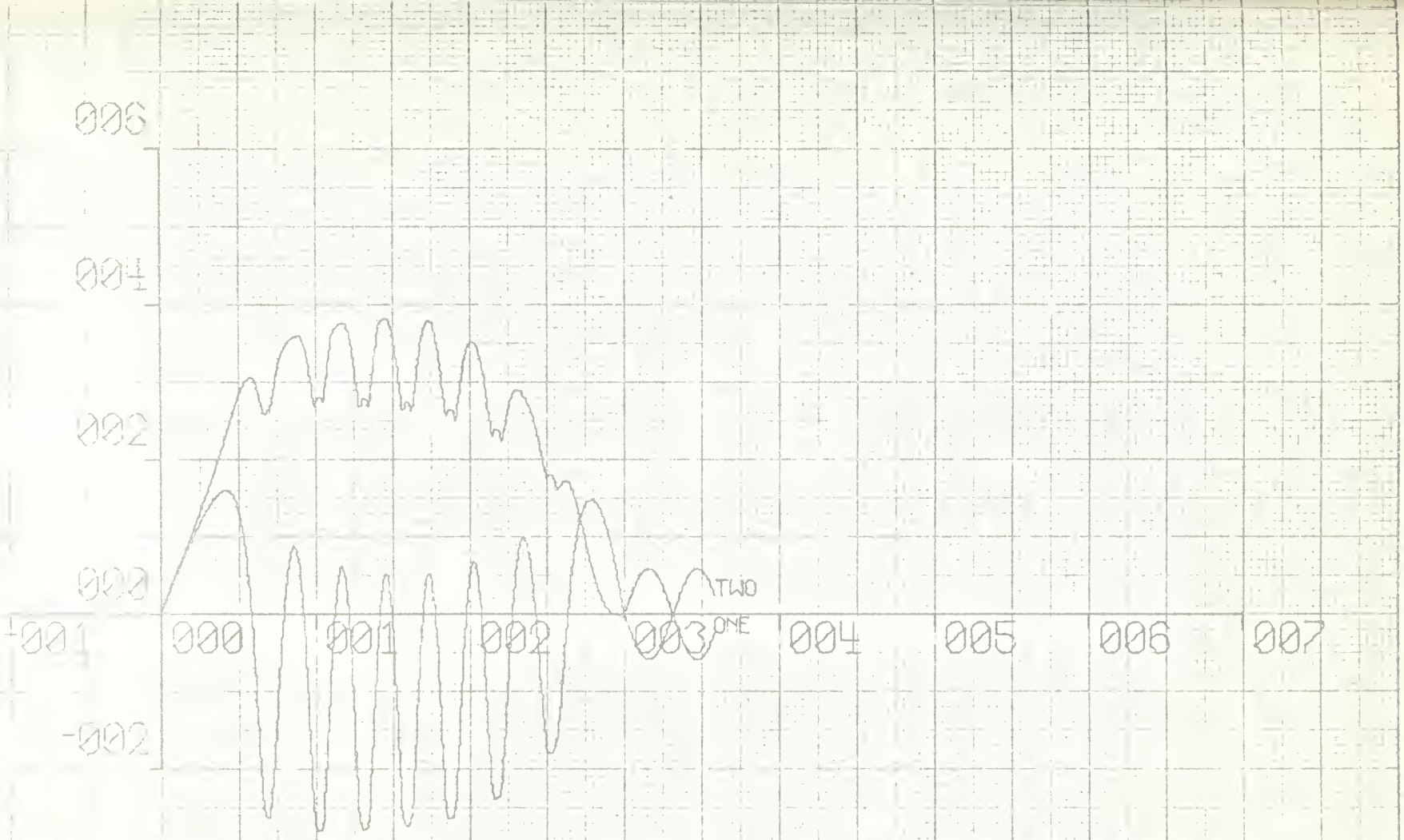

X AXIS SCALE = 1.00E+01
Y AXIS SCALE = 2.00E-03

DEFIB-LON INELASTIC COLUMN (SLENDERNESS=100,ECC=0.05,ALPHA=4.0,BETA=0.2)
STRESS 1 AND STRESS 2 VERSUS TIME

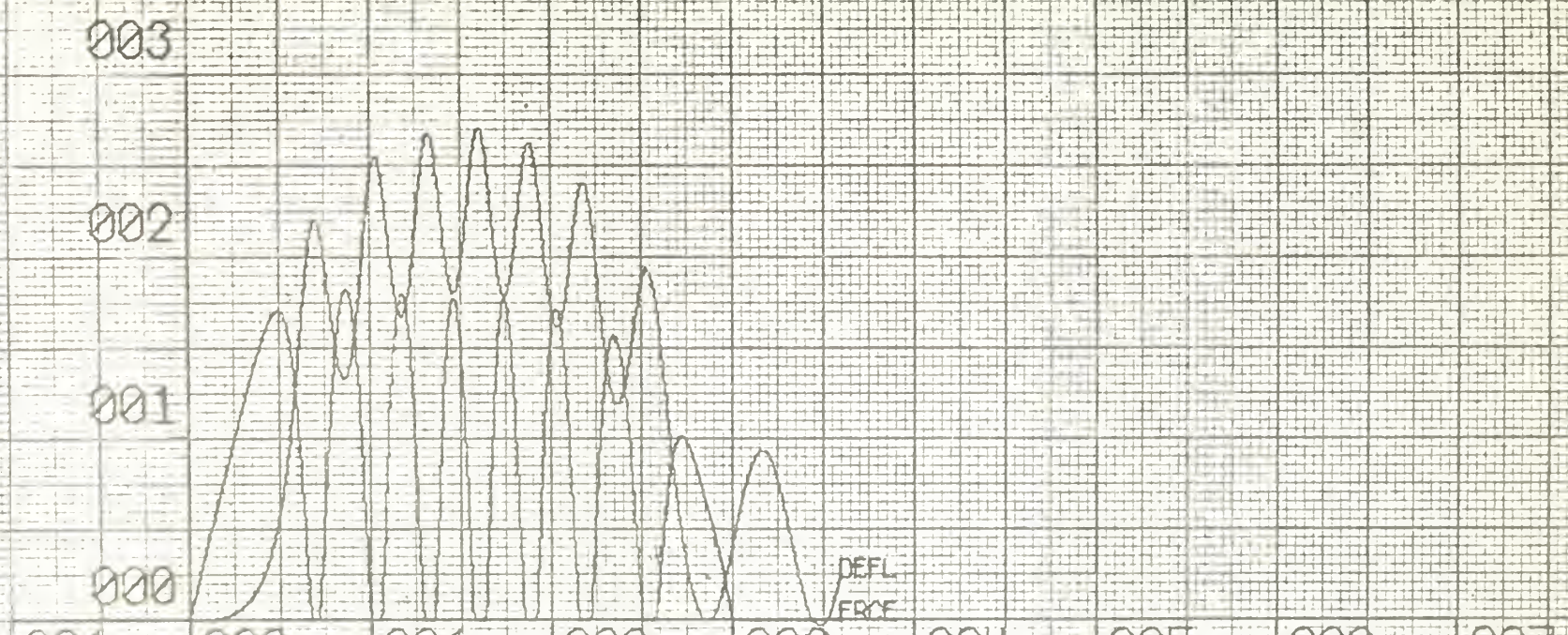

X AXIS SCALE = 1.00E+01

Y AXIS SCALE = 1.00E+00

DEFIBAUGH-INELASTIC COLUMN (SLENDERNESS=100,ECC=0.05,ALPHA=4.0,BETA=0.2)

DEFLECTION AND FORCE VERSUS TIME

APPENDIX II

Theoretical and Computer Solution Graphical Comparisons of Maximum Loads for the Static Case

The notation for the graphs displayed in this appendix is explained in App. I.

The graphs on pages II-3 to II-11 folowing this discussion are the curves ϵ_1 and ϵ_2 versus P/P_{cr} for the three slenderness ratios considered in the study. As previously mentioned, the loading for the study in this appendix is a ramp displacement of the end of the column model at a displacement rate comparable to that in commercial testing machines. The study includes eccentricity ratios of 0.05, 0.01, and 0.001 for each of the slenderness ratios. The tabulated results of this study are shown in Table I in Section 4.

In addition to the previous comments made concerning the results, it may also be seen from the graphs that for all slenderness and eccentricity ratios considered an amount of bending takes place before strain reversal occurs in Spring 2 and before the maximum load is reached. This was essentially Shanley's point in proving the fallacy of the reduced-modulus theory for column action. As stated by Shanley /1/,

> .....the reduced-modulus theory is not correct for predicting the maximum load up to which a perfect column will remain straight. This is because

it is possible for the column to bend simultaneously with increasing axial load. Under such conditions it is possible to have bending without introducing any strain reversal, upon which the reduced-modulus theory depends.

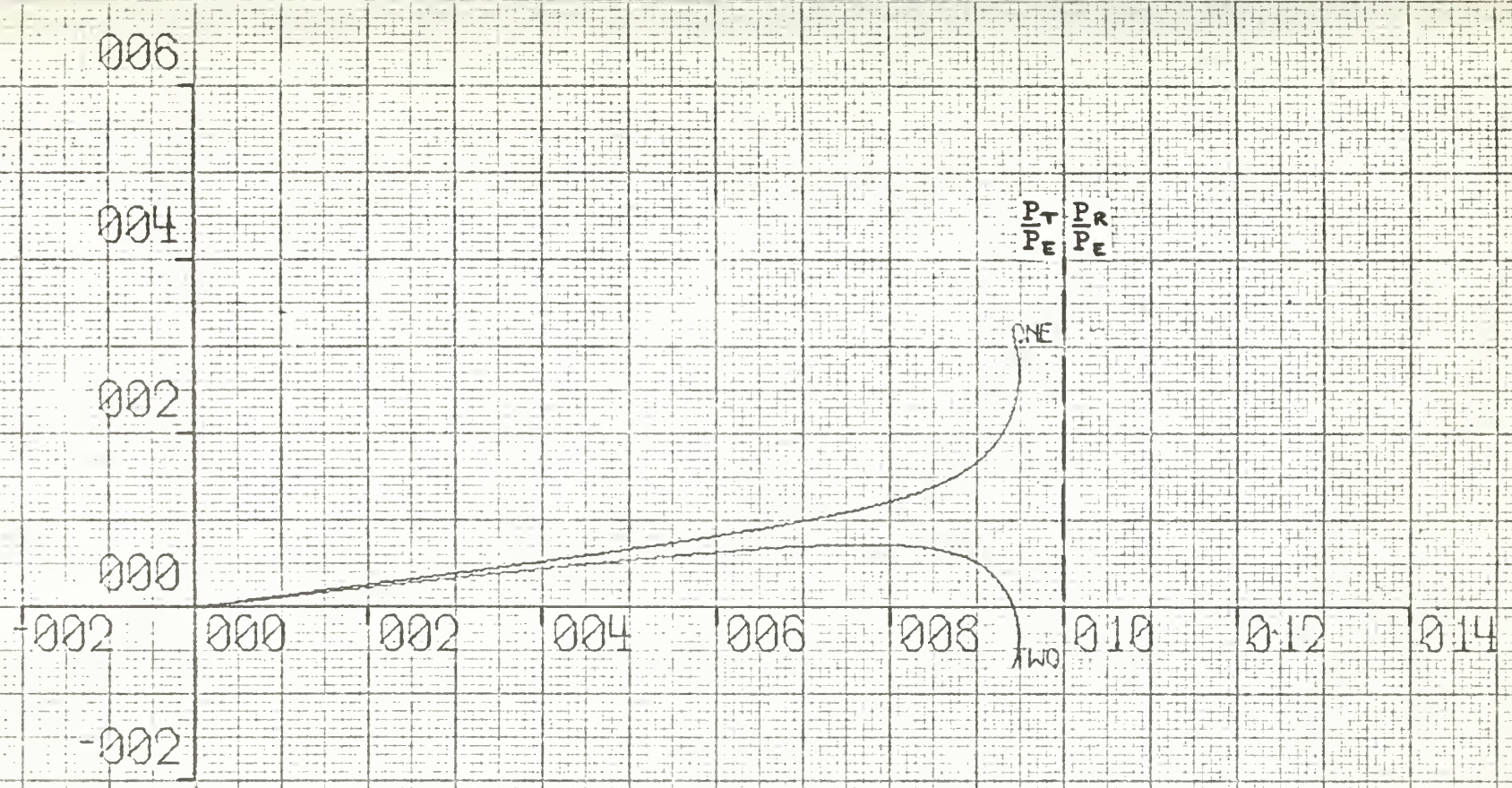

X AXIS SCALE = 2.00E-01

Y AXIS SCALE = 2.00E-03

DEFIBAUGH-INELASTIC COLUMN (SLENDERNESS=100,ECC=0.05,ALPHA=1.0,BETA=0.01)

STRAIN 1 AND STRAIN 2 VERSUS FORCE

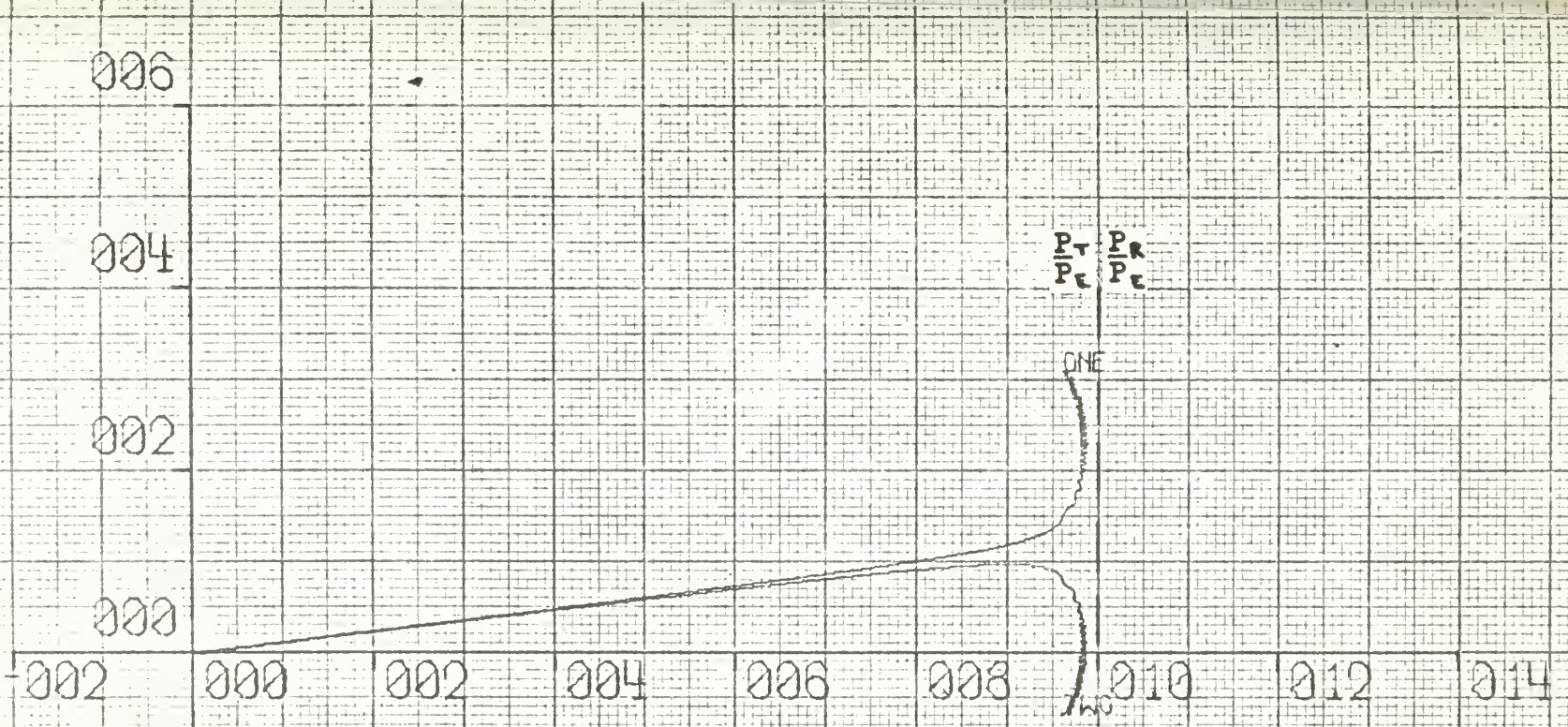

X AXIS SCALE = 2.00E-01

Y AXIS SCALE = 2.00E-03

DEFIBAUGH-INELASTIC COLUMN (SLENDERNESS=100, ECC=0.01, ALPHA=1.0, BETA=0.01)

STRAIN 1 AND STRAIN 2 VERSUS FORCE

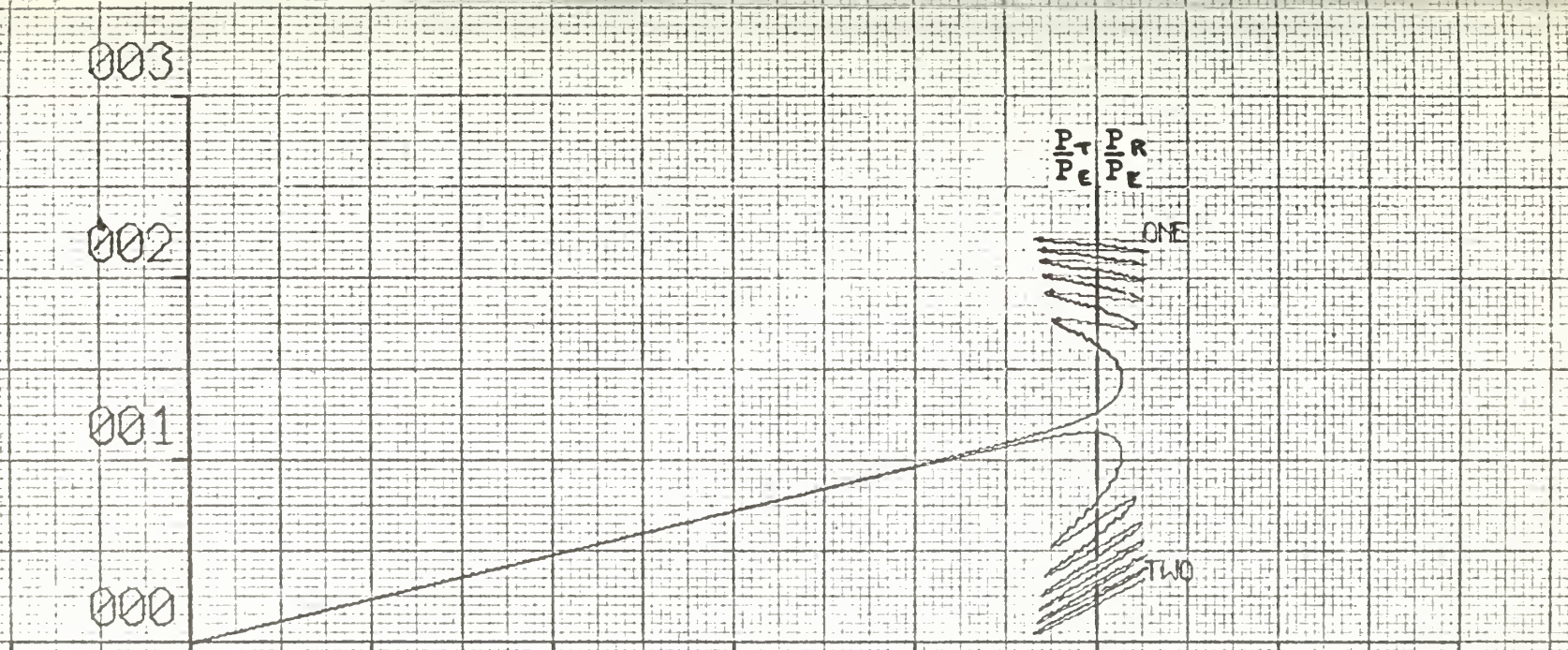

X AXIS SCALE = 2.00E-01

Y AXIS SCALE = 1.00E-03

DEFIBAUCH-INELASTIC COLUMN (SLENDERNESS=100, ECC=0.001, ALPHA=1.0, BETA=0.01)

STRAIN 1 AND STRAIN 2 VERSUS FORCE

015
010
005
000
-005
-002
000
002
004
006
008
010
012
014
$\frac{P_T}{P_E}$ $\frac{P_R}{P_E}$
ONE
X AXIS SCALE = 2.00E-01
Y AXIS SCALE = 5.00E-03
DEFIBAUGH-INELASTIC COLUMN (SLENDERNESS= 20, ECC=0.85, ALPHA=1.0, BETA=0.0)
STRAIN 1 AND STRAIN 2 VERSUS FORCE

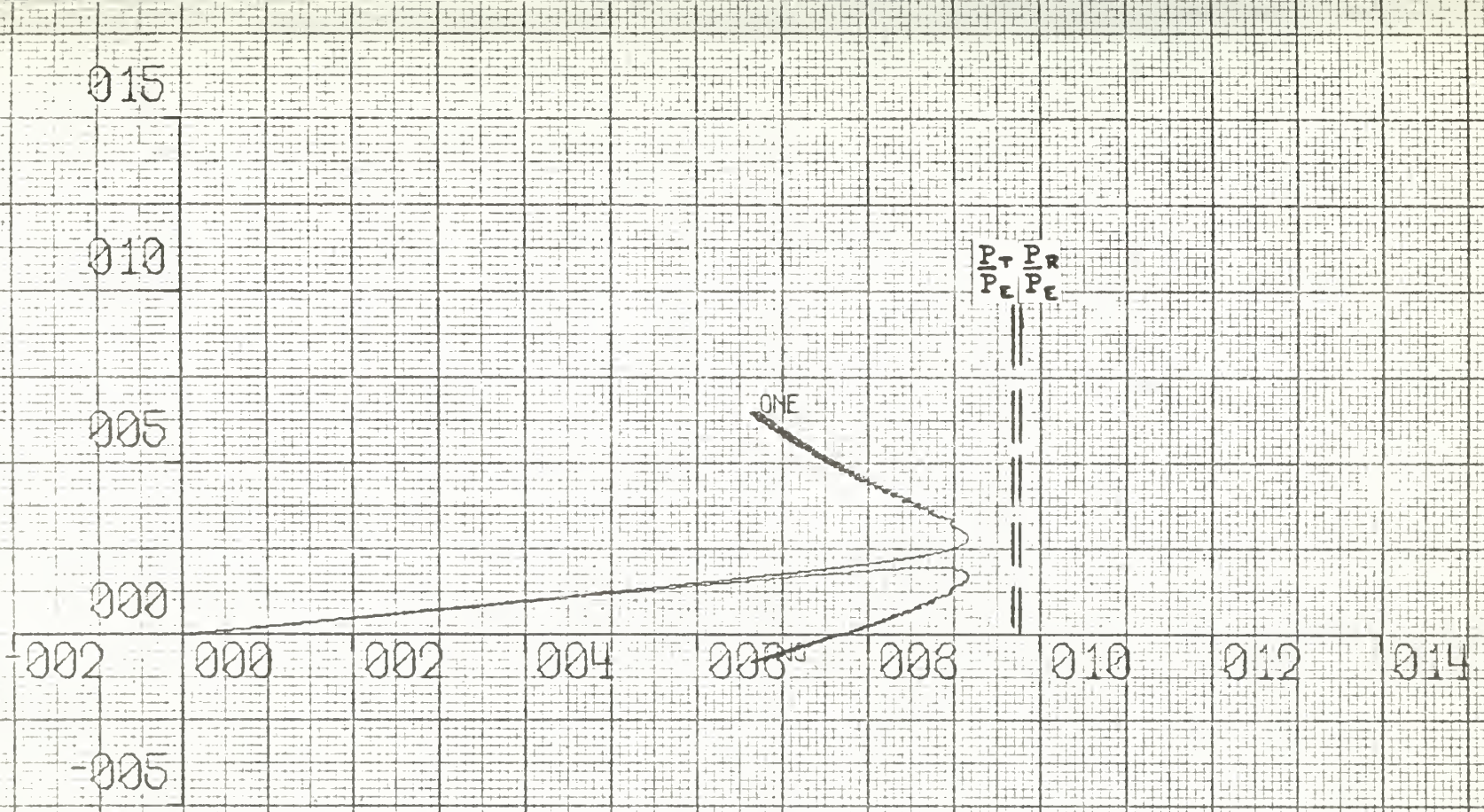

X AXIS SCALE = 2.00E-01

Y AXIS SCALE = 5.00E-03

DEFIBAUGH-INELASTIC COLUMN (SLENDERNESS= 20,ECC=0.01,ALPHA=1.0,BETA=0.01)

STRAIN 1 AND STRAIN 2 VERSUS FORCE

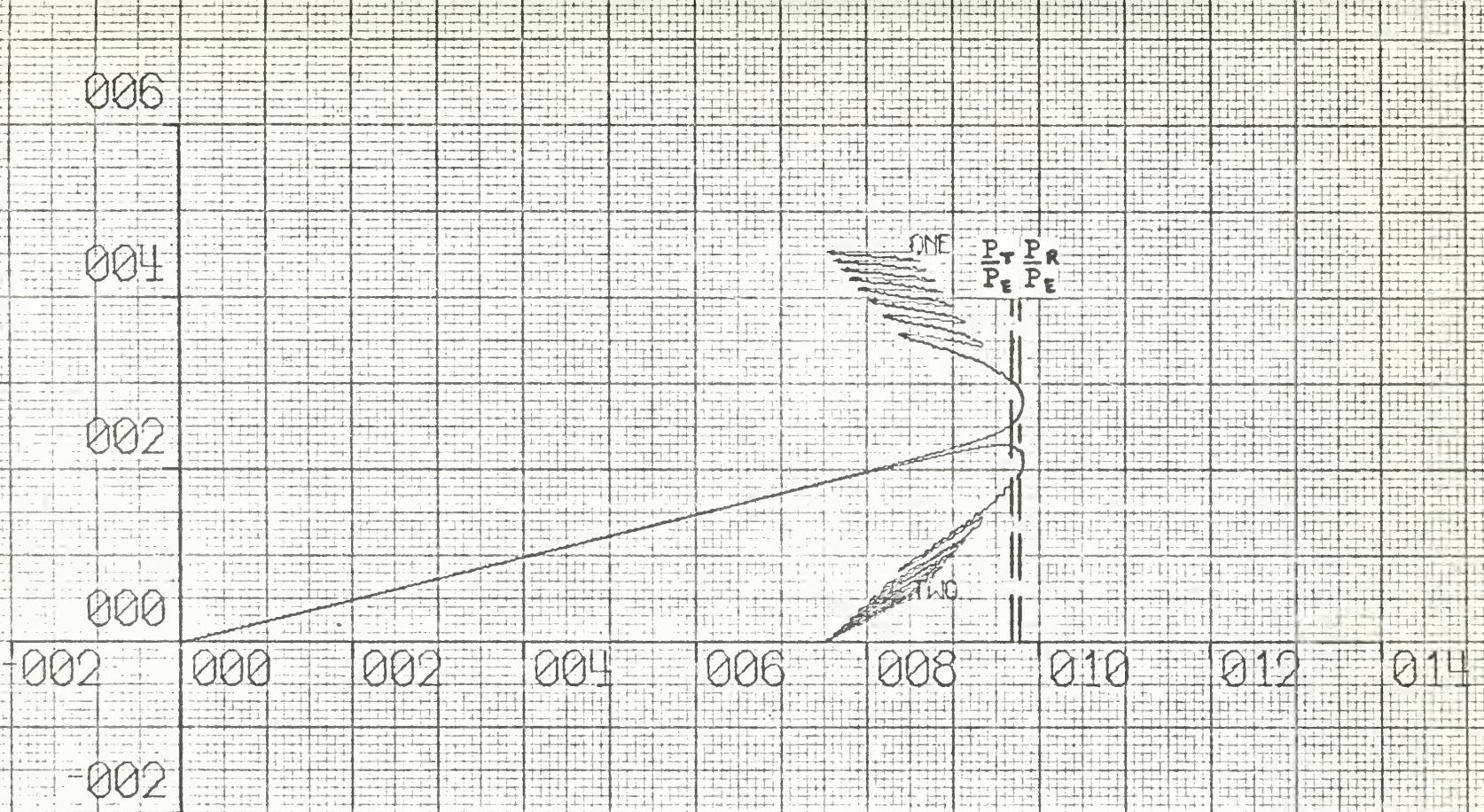

X AXIS SCALE = 2.00E-01

Y AXIS SCALE = 2.00E-03

DEFIBAUGH-INELASTIC COLUMN (SLENDERNESS= 70,ECC=0.001,ALPHA=1.0,BETA=0.01)

STRAIN 1 AND STRAIN 2 VERSUS FORCE

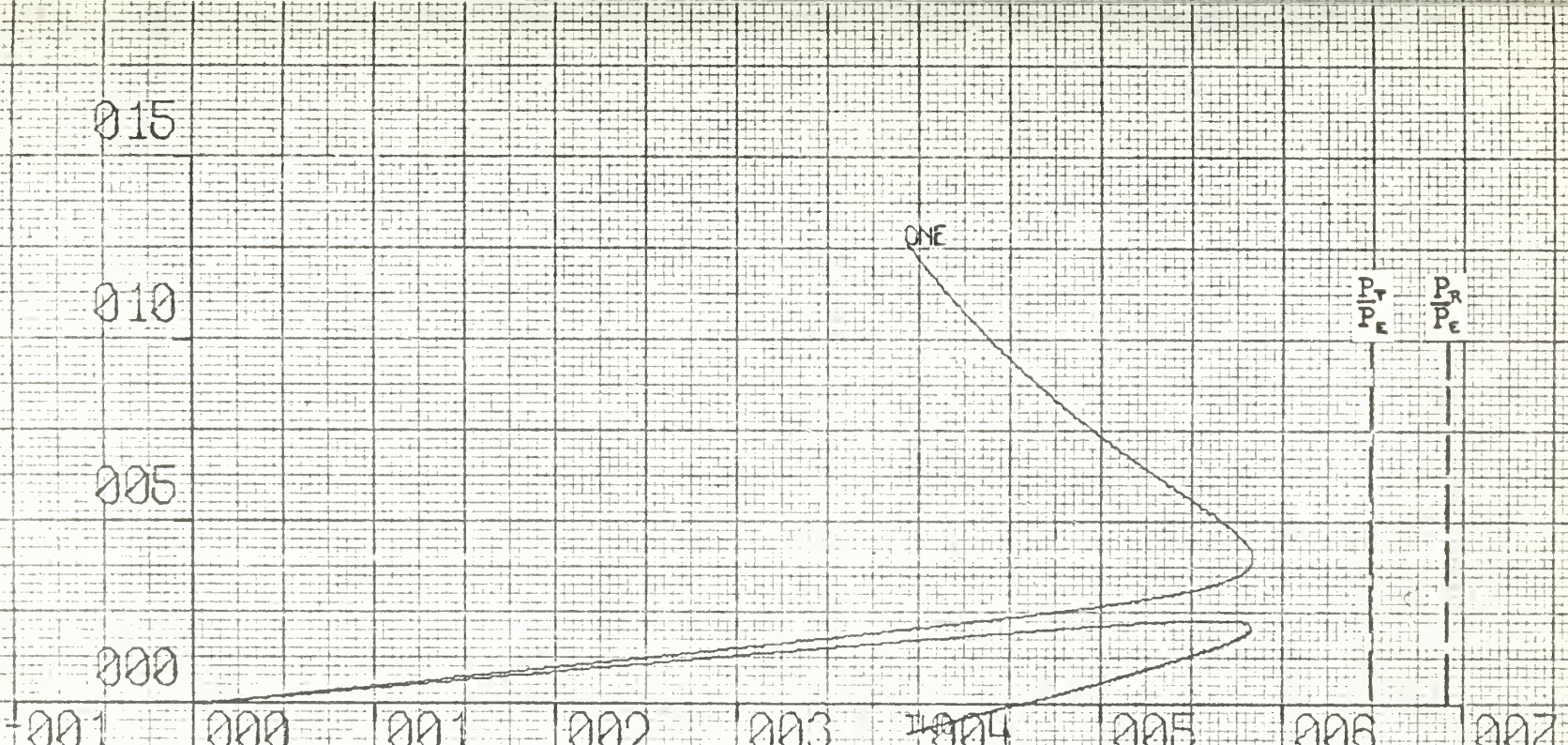

X AXIS SCALE = 1.00E-01

Y AXIS SCALE = 5.00E-03

DEFIBAUGH-INELASTIC COLUMN (SLENDERNESS= 50.,ECC=0.05,ALPHA=1.0,BETA=0.01)

STRAIN 1 AND STRAIN 2 VERSUS FORCE

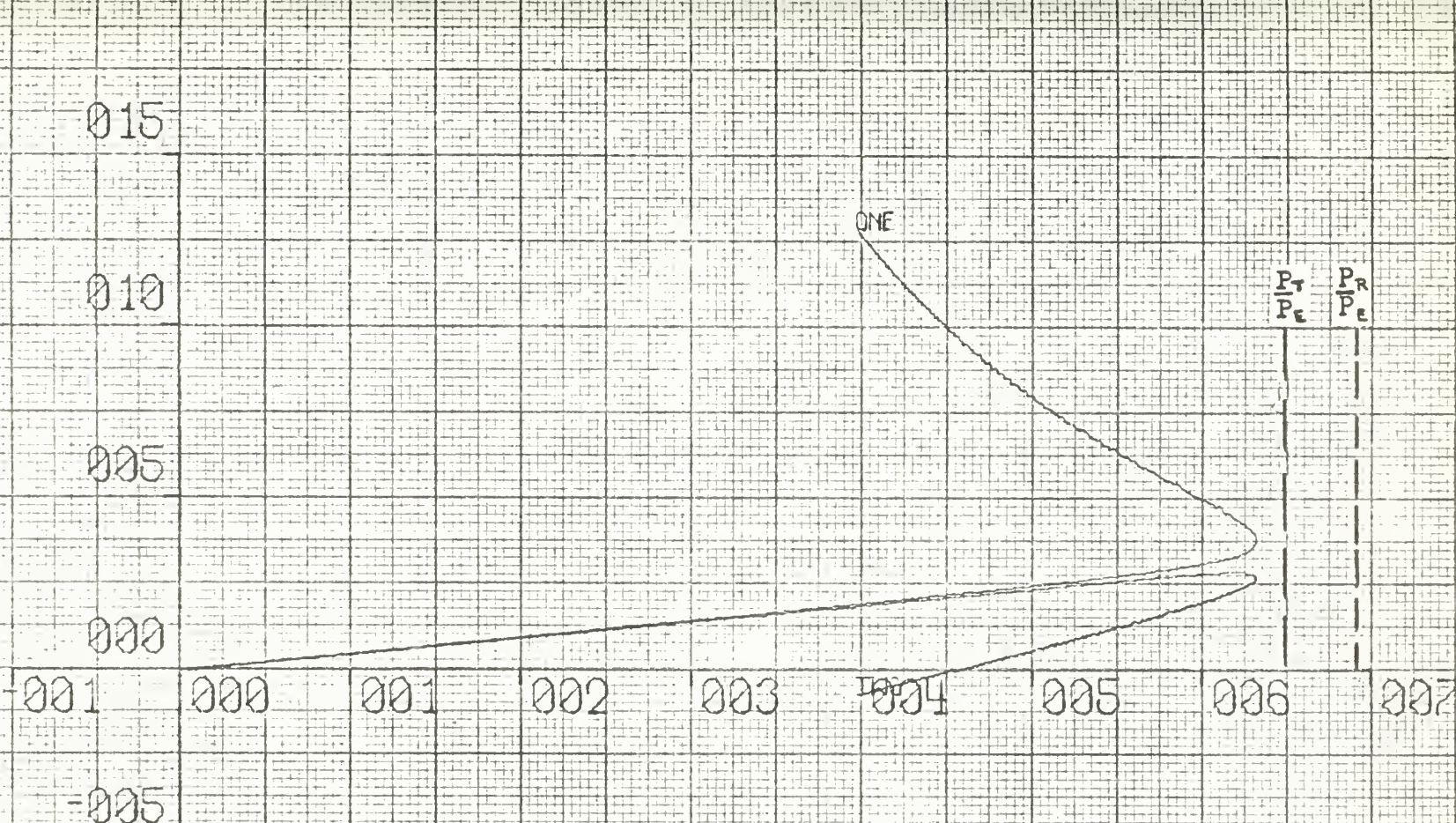

X AXIS SCALE = 1.00E-01
Y AXIS SCALE = 5.00E-03

DEFIBAUGH-INELASTIC COLUMN (SLENDERNESS= 50,ECC=0.01,ALPHA=1.0,BETA=0.01)

STRAIN 1 AND STRAIN 2 VERSUS FORCE

015
010
005
000
005
001
000
001
002
003
004
005
006
007
PT/PE PR/PE
ONE
TWO
X AXIS SCALE = 1.00E-01
Y AXIS SCALE = 5.00E-03
DEFLECTION-INELASTIC COLUMN (SLENDERNESS= 50.ECC=0.00,ALPHA=1.0,BETA=0.0)
STRAIN 1 AND STRAIN 2 VERSUS FORCE

APPENDIX III

Column Model Dynamic Response Curves

The notation for the graphs displayed in this appendix is explained in App. I.

The graphical compilation on pages III-3 to III-26 following this discussion gives the curves S_1 and S_2 versus T for β = 0.1, 0.2, 0.5 and 1.0 and for an eccentricity ratio e/ρ = 0.01. Included in the compilation are the solutions for the minimum and maximum values of ram pulse height α considered in the investigation for all three slenderness ratios. The graphical solutions are grouped by slenderness ratio with the solution for the maximum value of α followed by the solution for the minimum value of α for a single β value. The order of the β values is 0.1, 0.2, 0.5 and 1.0, that is, from the longest pulse duration of loading to the shortest pulse duration of loading considered in the compilation.

A discussion of some of the prominent features of the dynamic behavior of the column model under ram pulse loading is included in App. I where the curves of ϵ_1, ϵ_2, S_1, S_2, y/ρ and P/P_E versus T are displayed for one computer solution. The following is a discussion of some of the more prominent features of the dynamic behavior of the column model in terms of the stress curve compilation in this appendix.

In general the amount of inelastic action in the column model is inversely related to the slenderness ratio. For a slenderness ratio of 100 inelastic action is limited to com-

pressive stress levels below the value of the yield stress. For a slenderness ratio of 50 the maximum conpressive stress levels are near or above the yield stress. For a slenderness ratio of 70 inelastic action occurs at maximum compressive stress levels intermediate to those for slenderness ratios of 50 and 100.

It may also be noted that, in general, contact is lost between the ram and the end of the column (when $S_1 = - S_2$) before the loading pulse nears its termination for β values of 0.2 and 0.5 and slenderness ratios of 70 and 50. For a slenderness ratio of 100 this occurs at values of β = 0.1, 0.2 and 0.5.

It may be seen that the value of maximum tensile stress in Spring 2 exceeded the value of the nominal yield stress (S_y = 0.004) for the β values of 0.2 and 0.5 and α = 2.5 for a slenderness ratio of 50.

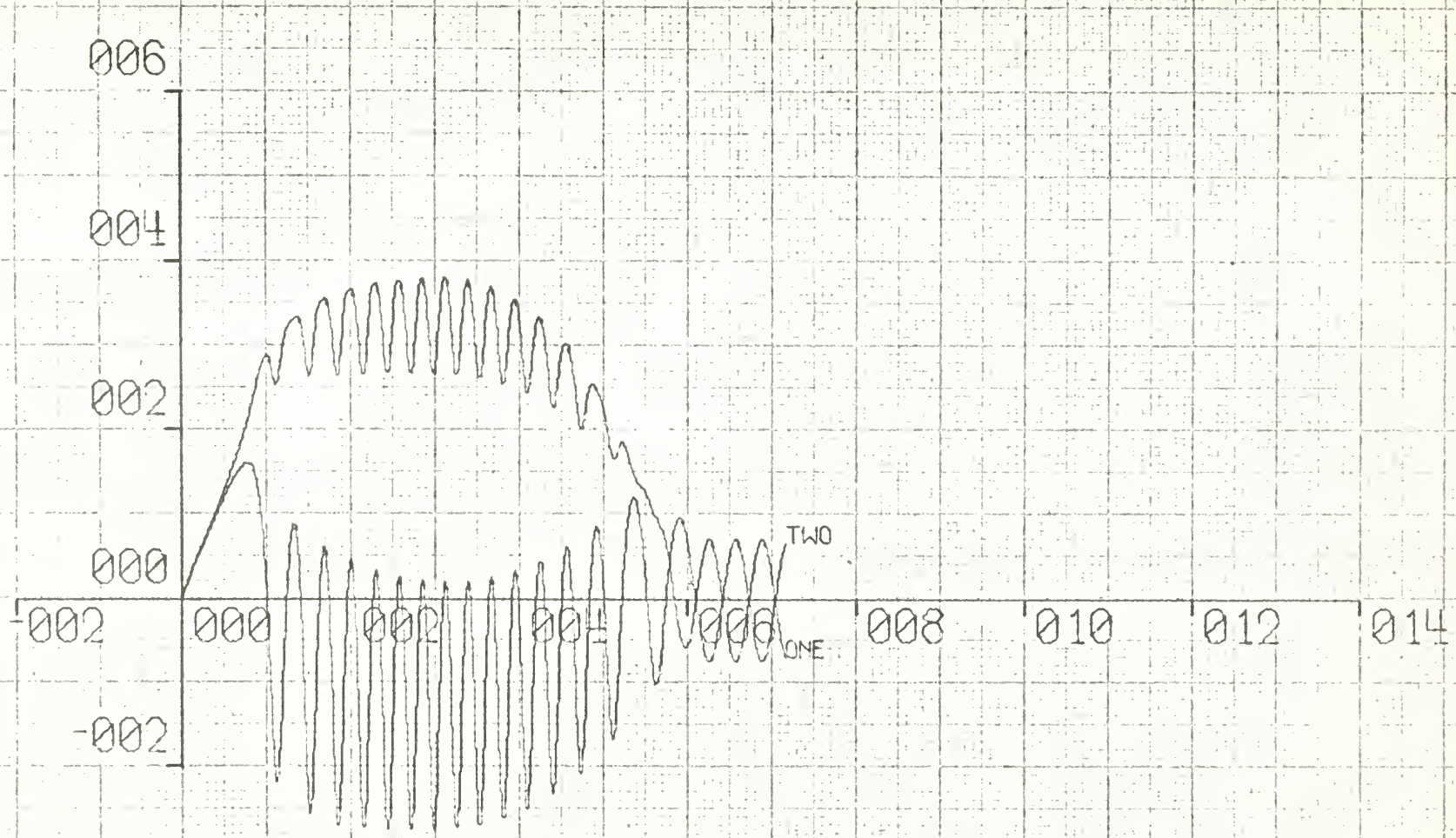

X AXIS SCALE = 2.00E+01
Y AXIS SCALE = 2.00E-03

DEFIBAUGH-INELASTIC COLUMN (SLENDERNESS=100,ECC=0.01,ALPHA=4.0,BETA=0.1)

STRESS 1 AND STRESS 2 VERSUS TIME

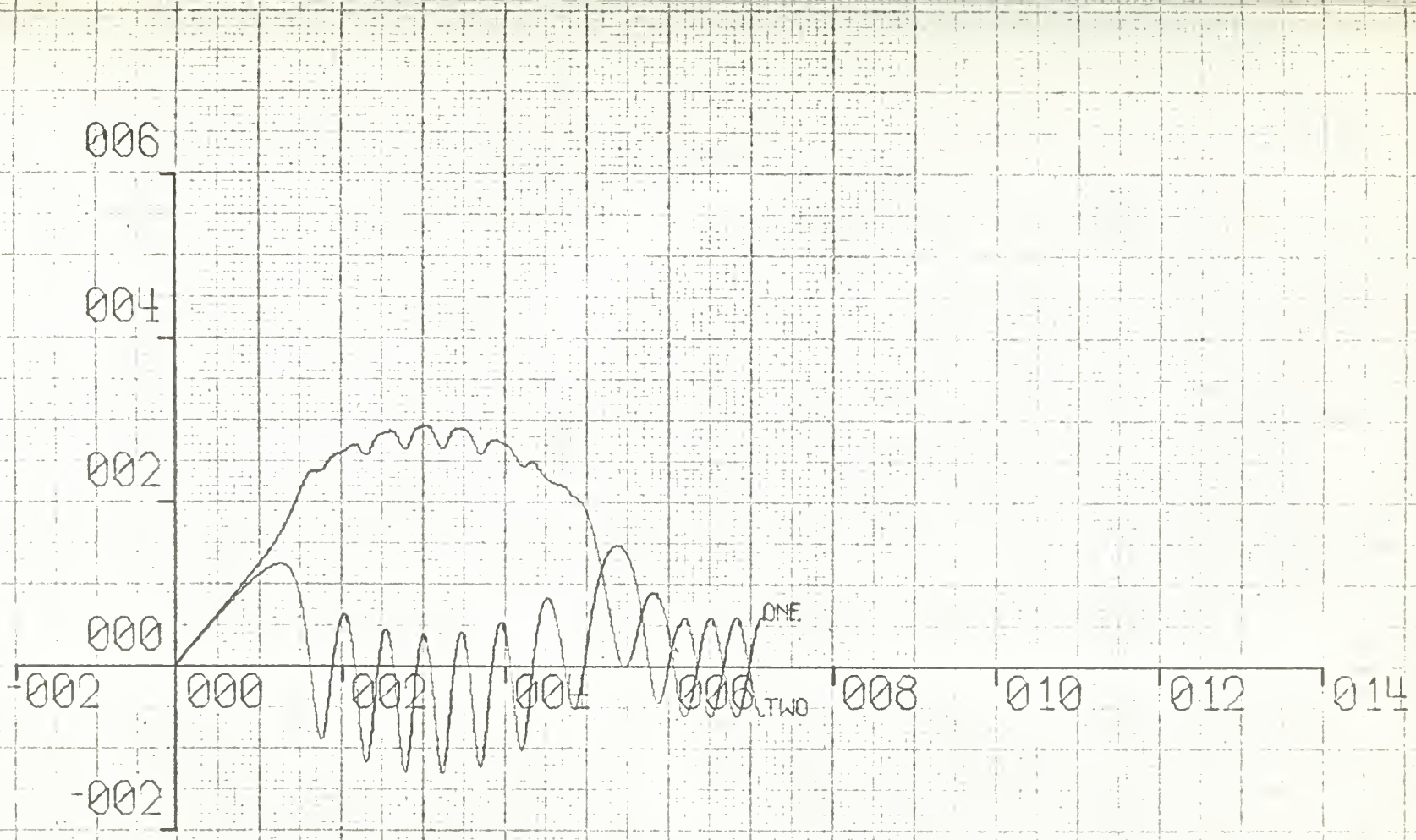

X AXIS SCALE = 2.00E+01

Y AXIS SCALE = 2.00E-03

DEFIBAUCH-INELASTIC COLUMN (SLENDERNESS=100,ECC=0.01,ALPHA=2.0,BETA=0.1)

STRESS 1 AND STRESS 2 VERSUS TIME

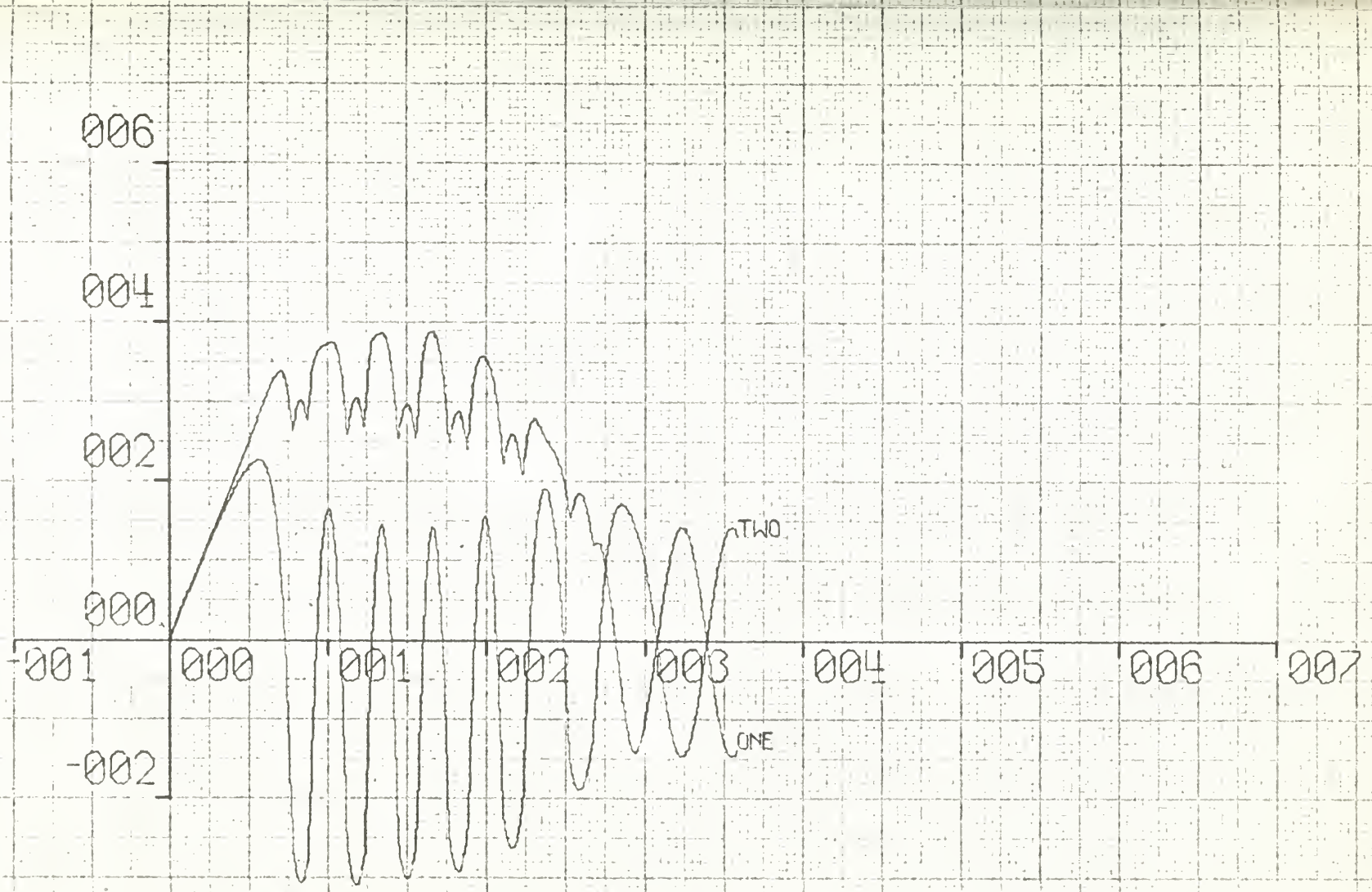

X AXIS SCALE = 1.00E+01
Y AXIS SCALE = 2.00E-03

DEFIBAUGH-INELASTIC COLUMN (SLENDERNESS=100,ECC=0.01,ALPHA=1.0,BETA=0.2)

STRESS 1 AND STRESS 2 VERSUS TIME

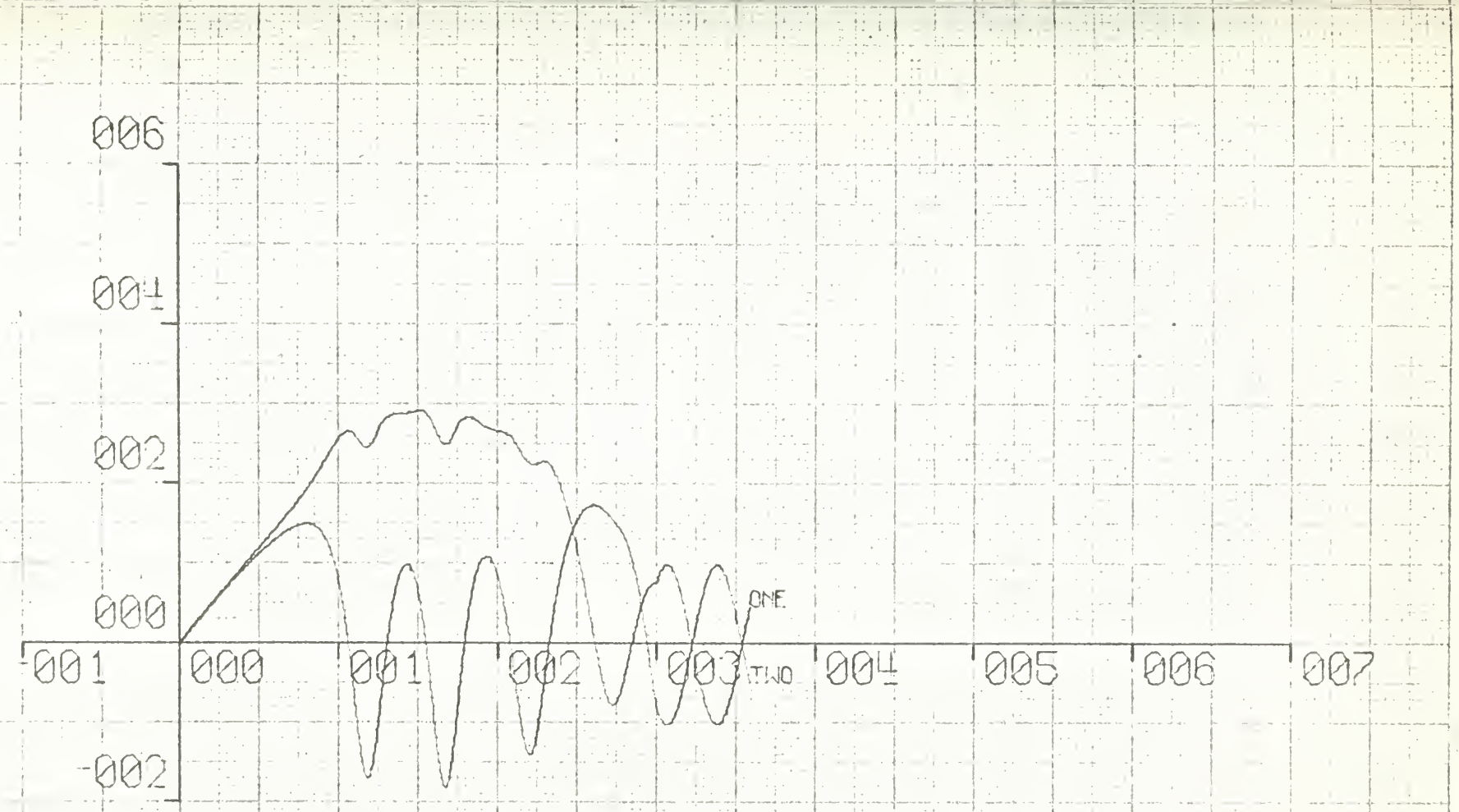

X AXIS SCALE = 1.00E+01
Y AXIS SCALE = 2.00E-03

DEFIBAUGH-INELASTIC COLUMN (SLENDERNESS=100,ECC=0.01,ALPHA=2.0,BETA=0.2)
STRESS 1 AND STRESS 2 VERSUS TIME

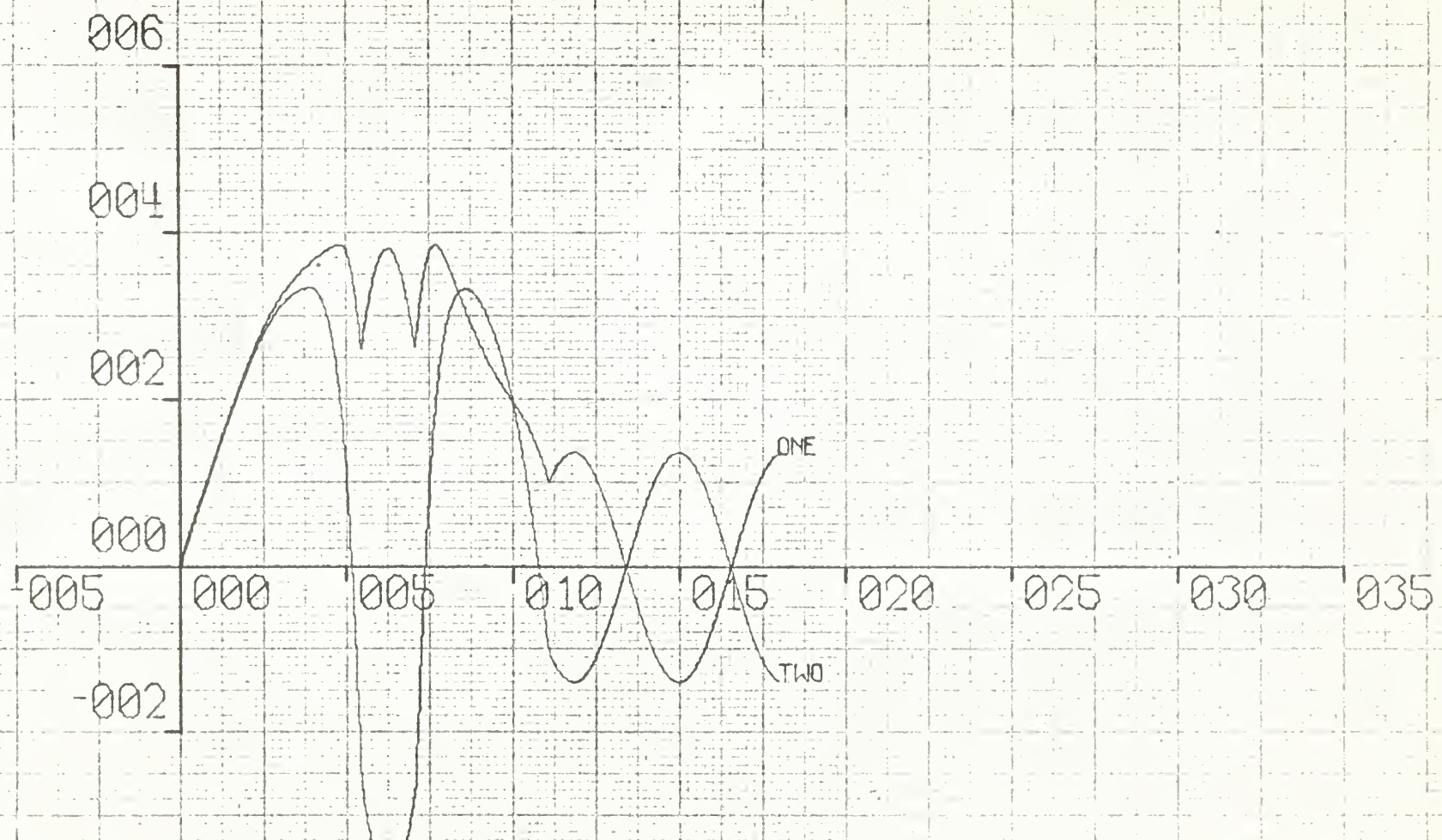

X AXIS SCALE = 5.00E+00
Y AXIS SCALE = 2.00E-03

DEFIBAUGH-INELASTIC COLUMN (SLENDERNESS=100,ECC=0.01,ALPHA=4.0,BETA=0.5)

STRESS 1 AND STRESS 2 VERSUS TIME

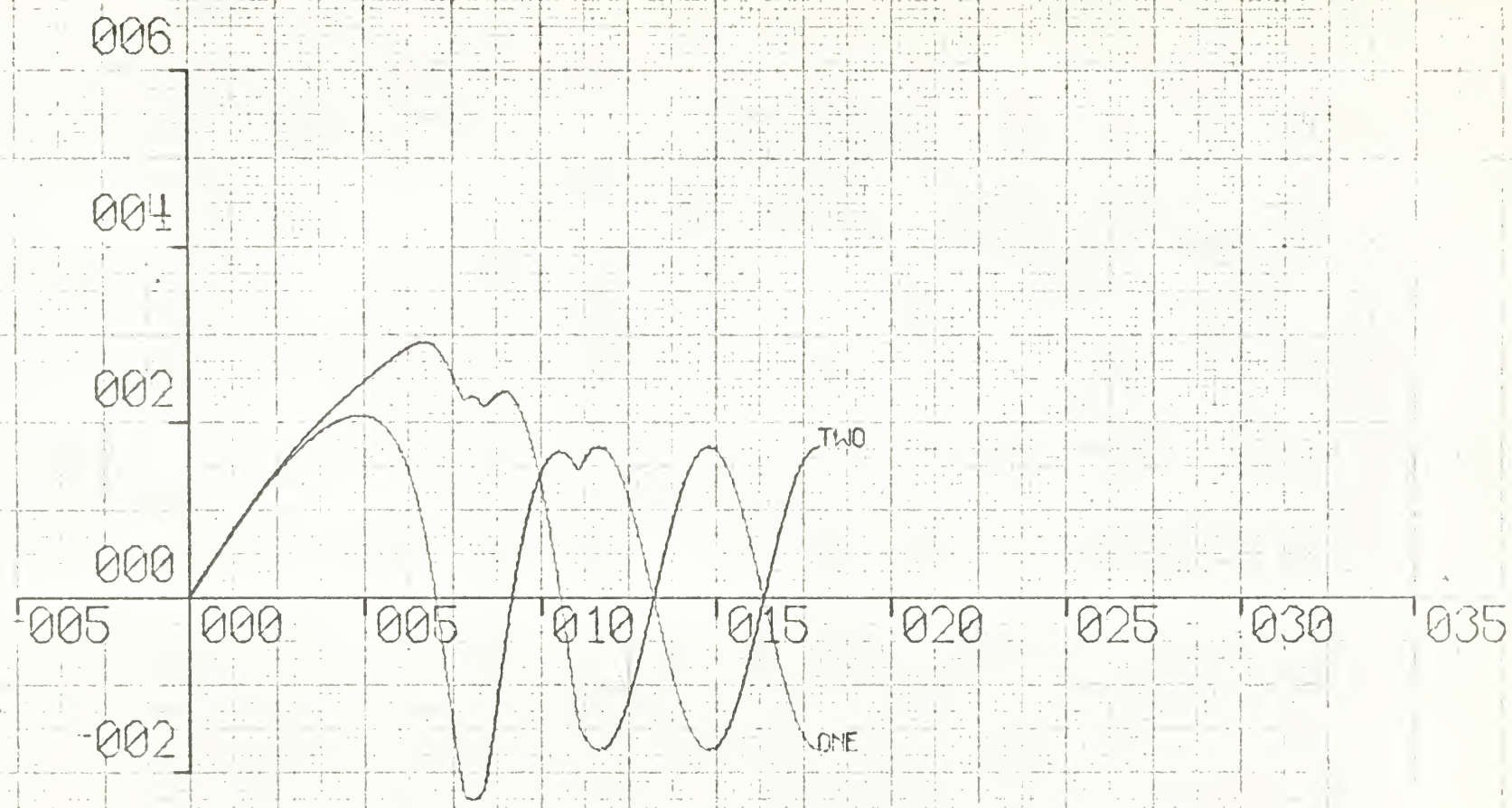

X AXIS SCALE = 5.00E+00
Y AXIS SCALE = 2.00E-03

DEFIBRUCH-INELASTIC COLUMN (SLENDERNESS=100,ECC=0.01,ALPHA=2.0,BETA=0.5)

STRESS 1 AND STRESS 2 VERSUS TIME

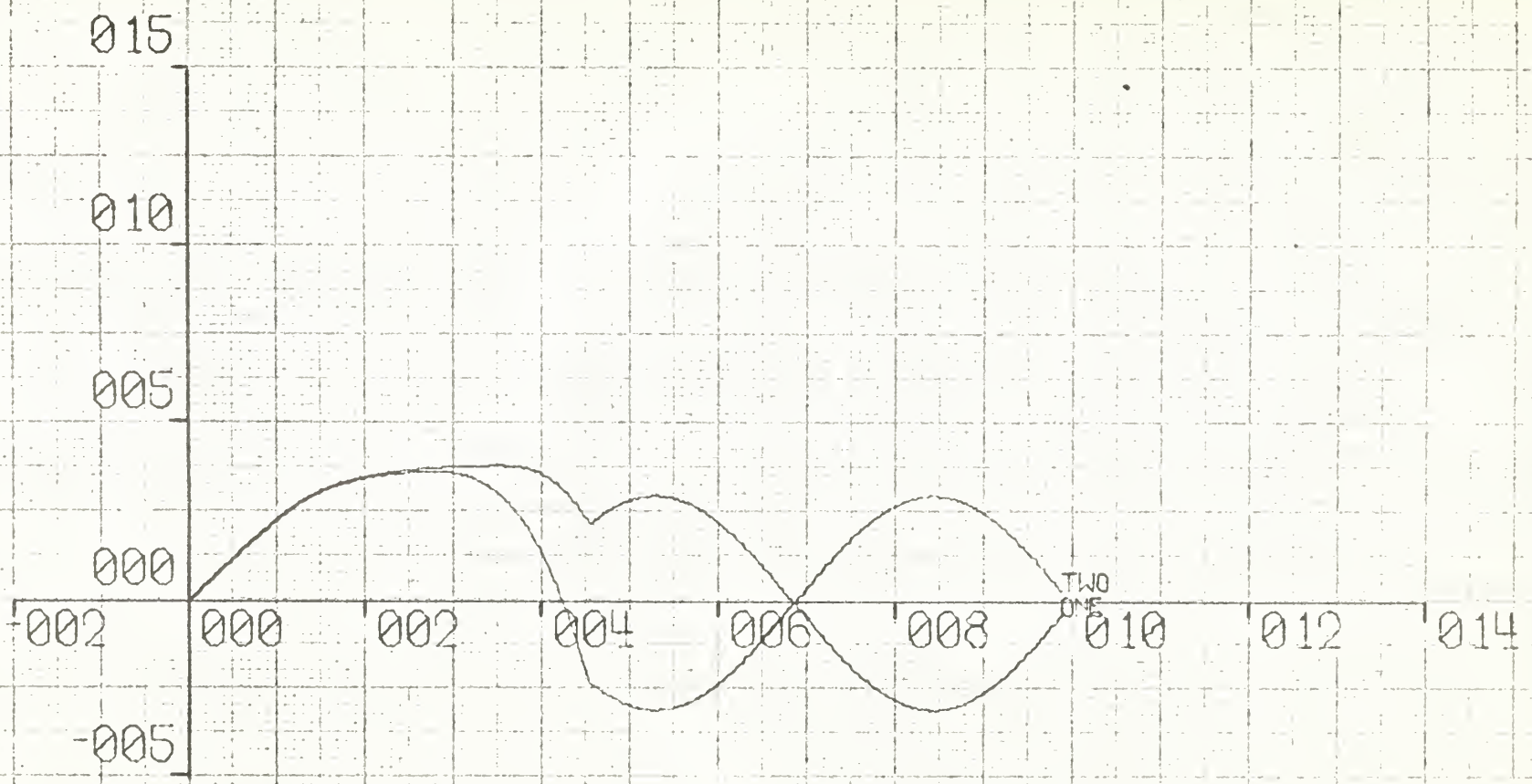

X AXIS SCALE = 2.00E+00
Y AXIS SCALE = 5.00E-03

DEFIBAUCH-INELASTIC COLUMN (SLENDERNESS=100,ECC=0.01,ALPHA=4.0,BETA=1.0)
STRESS 1 AND STRESS 2 VERSUS TIME

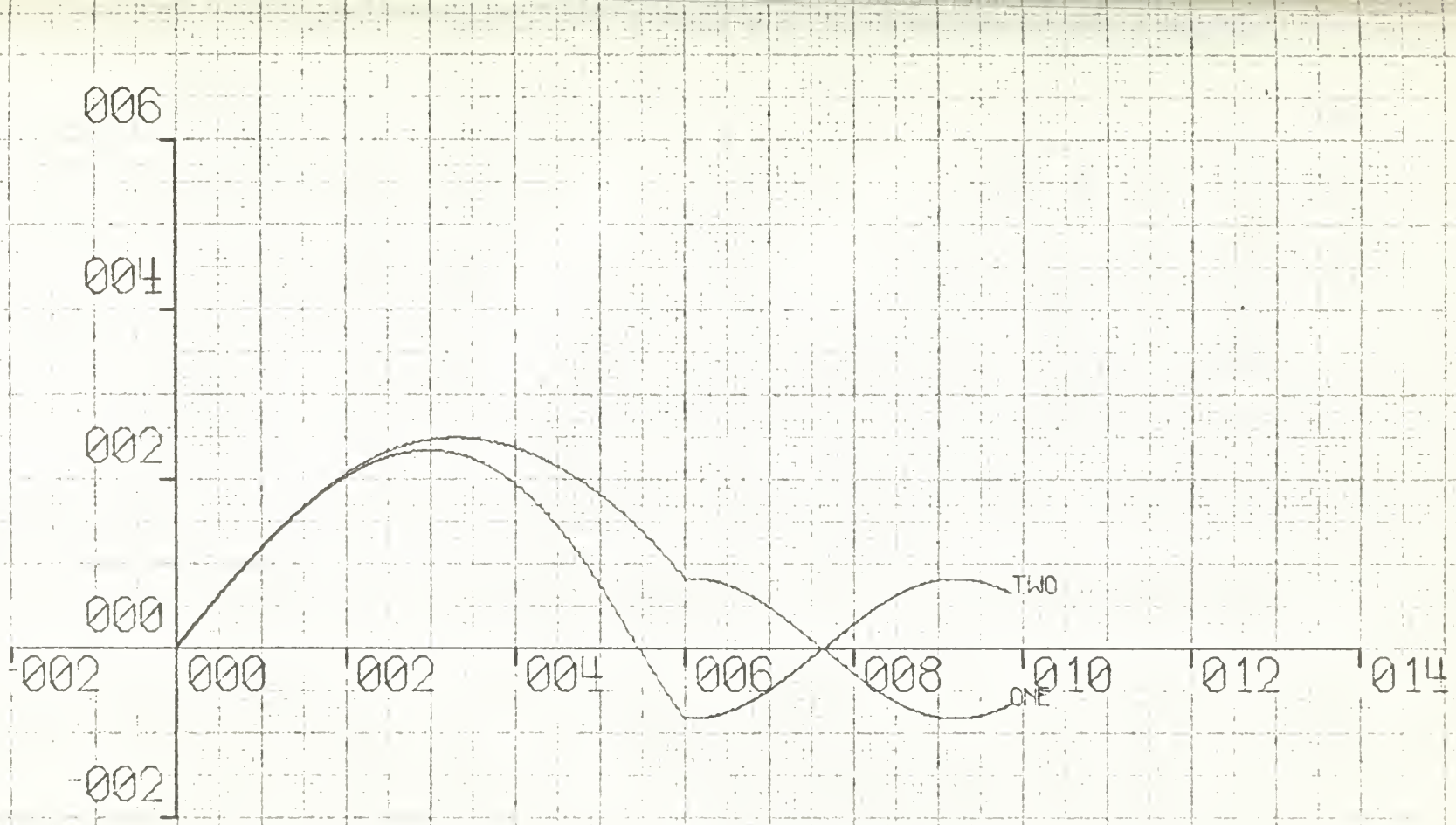

X AXIS SCALE = 2.00E+00
Y AXIS SCALE = 2.00E-03

DEFIBRUCH INELASTIC COLUMN (SLENDERNESS=100,ECC=0.01,ALPHA=2.0,BETA=1.0)

STRESS 1 AND STRESS 2 VERSUS TIME

X AXIS SCALE = 2.00E+01

Y AXIS SCALE = 2.00E-03

DEFIBRICH-INELASTIC COLUMN (SLENDERNESS= 70,ECC=0.01,ALPHA=2.5,BETA=0.1)

STRESS 1 AND STRESS 2 VERSUS TIME

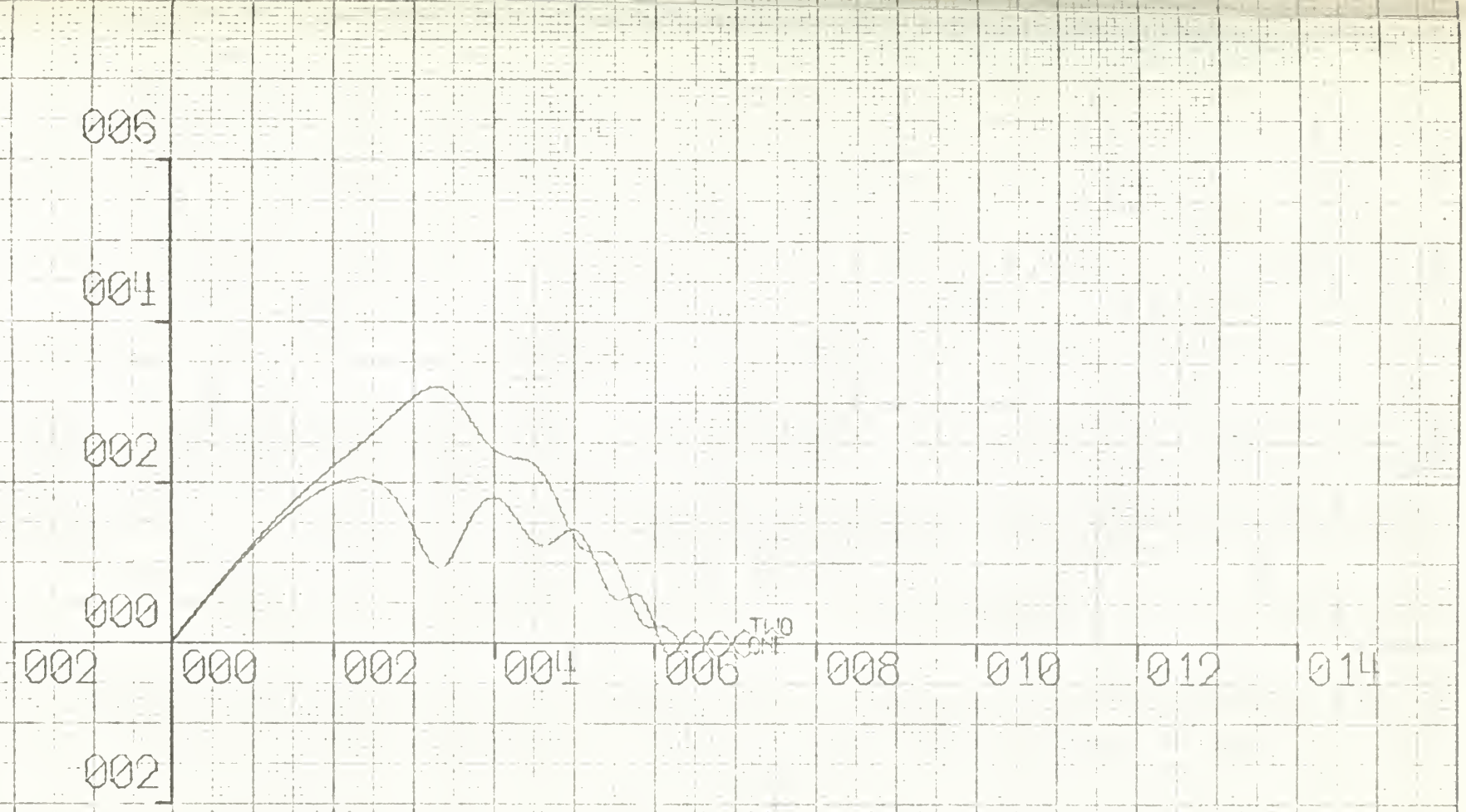

X AXIS SCALE = 2.00E+01
Y AXIS SCALE = 2.00E 03

DEFIBRUSH INELASTIC COLUMN (SLENDERNESS= 70.,ECC=0.01,ALPHA=1.0,BETA=0.1)

STRESS 1 AND STRESS 2 VERSUS TIME

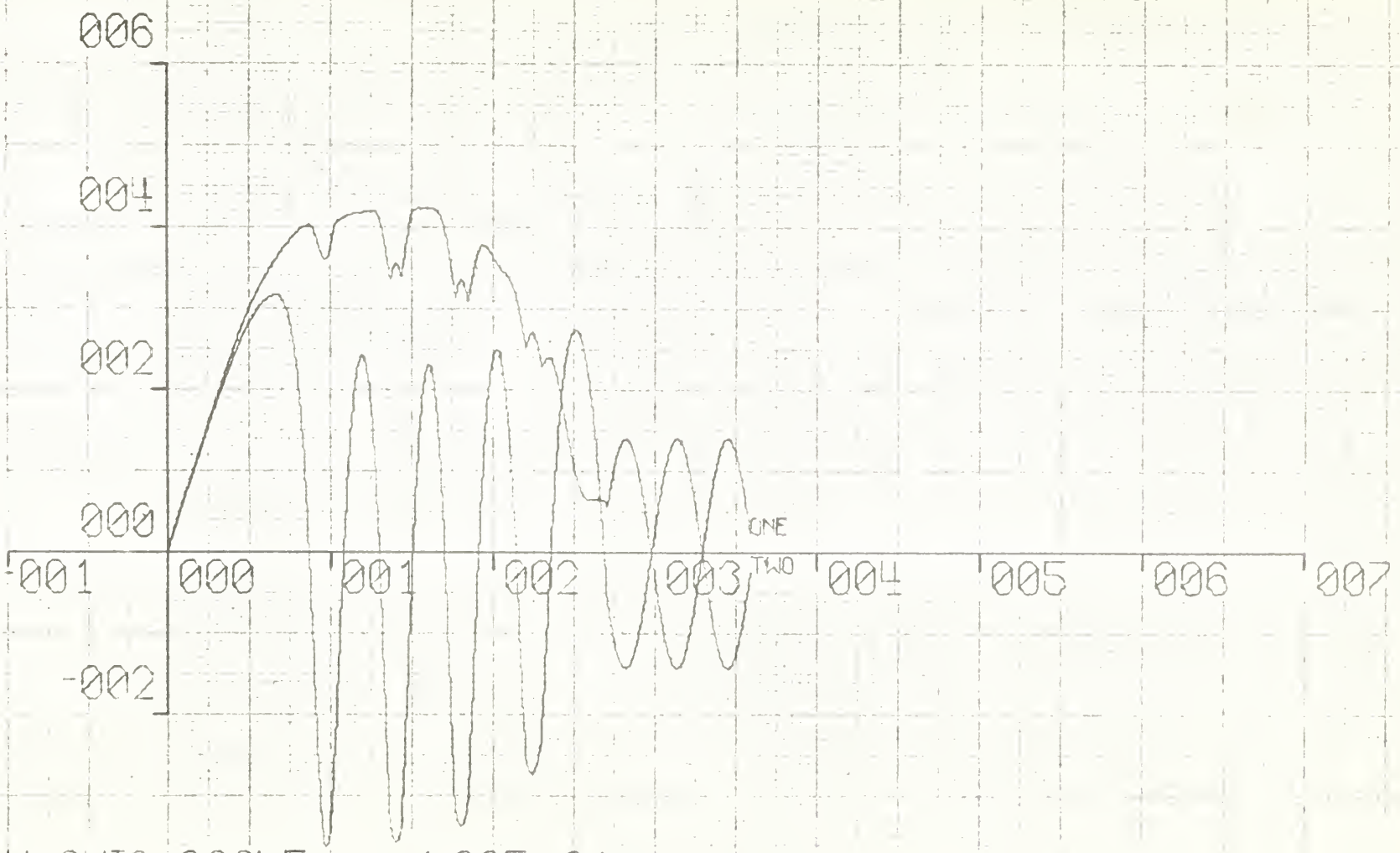

X AXIS SCALE = 1.00E+01
Y AXIS SCALE = 2.00E-03

DEFIBAUCH-INELASTIC COLUMN (SLENDERNESS= 70,ECC=0.01,ALPHA=2.0,BETA=0.2)
STRESS 1 AND STRESS 2 VERSUS TIME

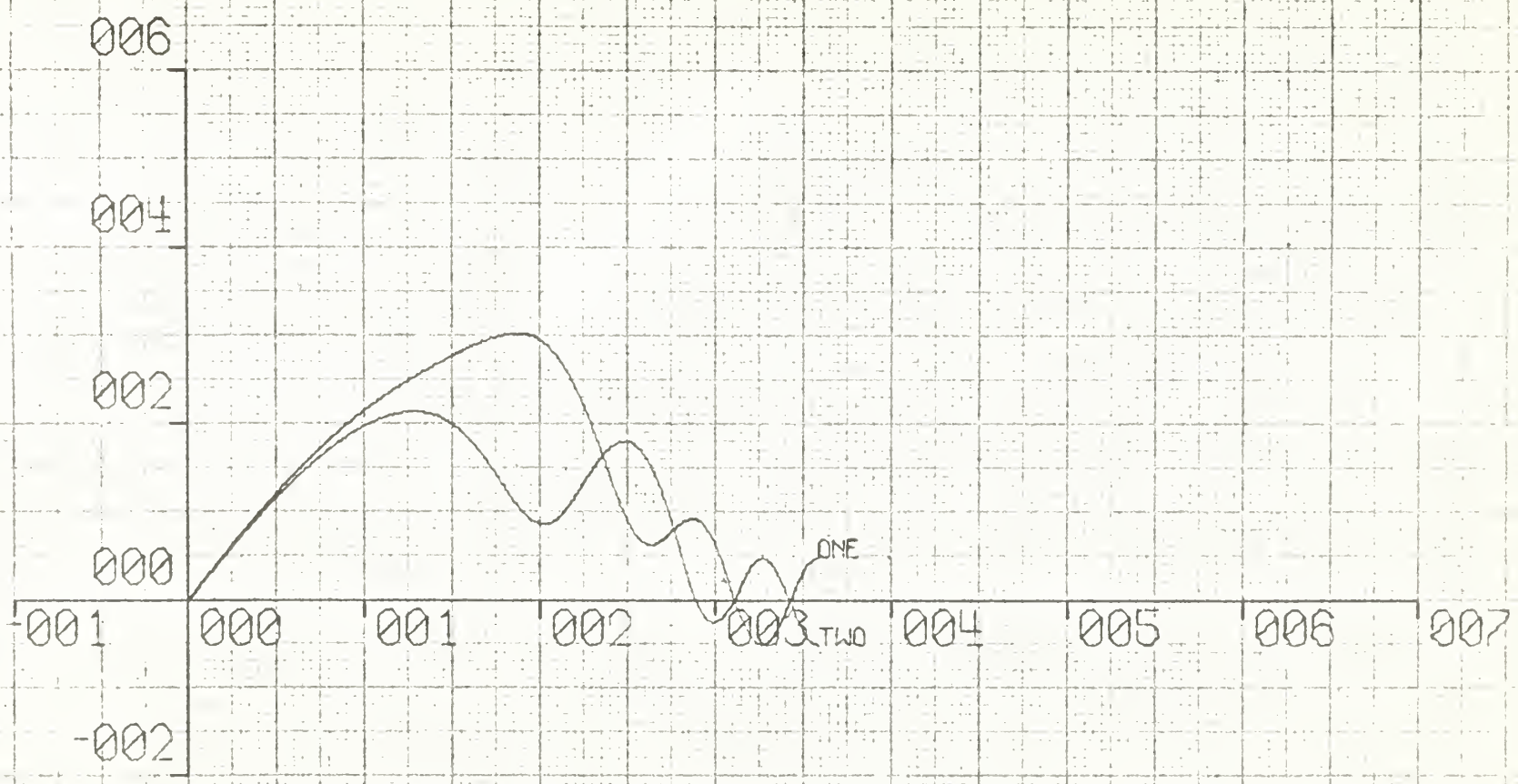

X AXIS SCALE = 1.00E+01
Y AXIS SCALE = 2.00E-03

DEFIBAUGH-INELASTIC COLUMN (SLENDERNESS= 70,ECC=0.01,ALPHA=1.0,BETA=0.2)

STRESS 1 AND STRESS 2 VERSUS TIME

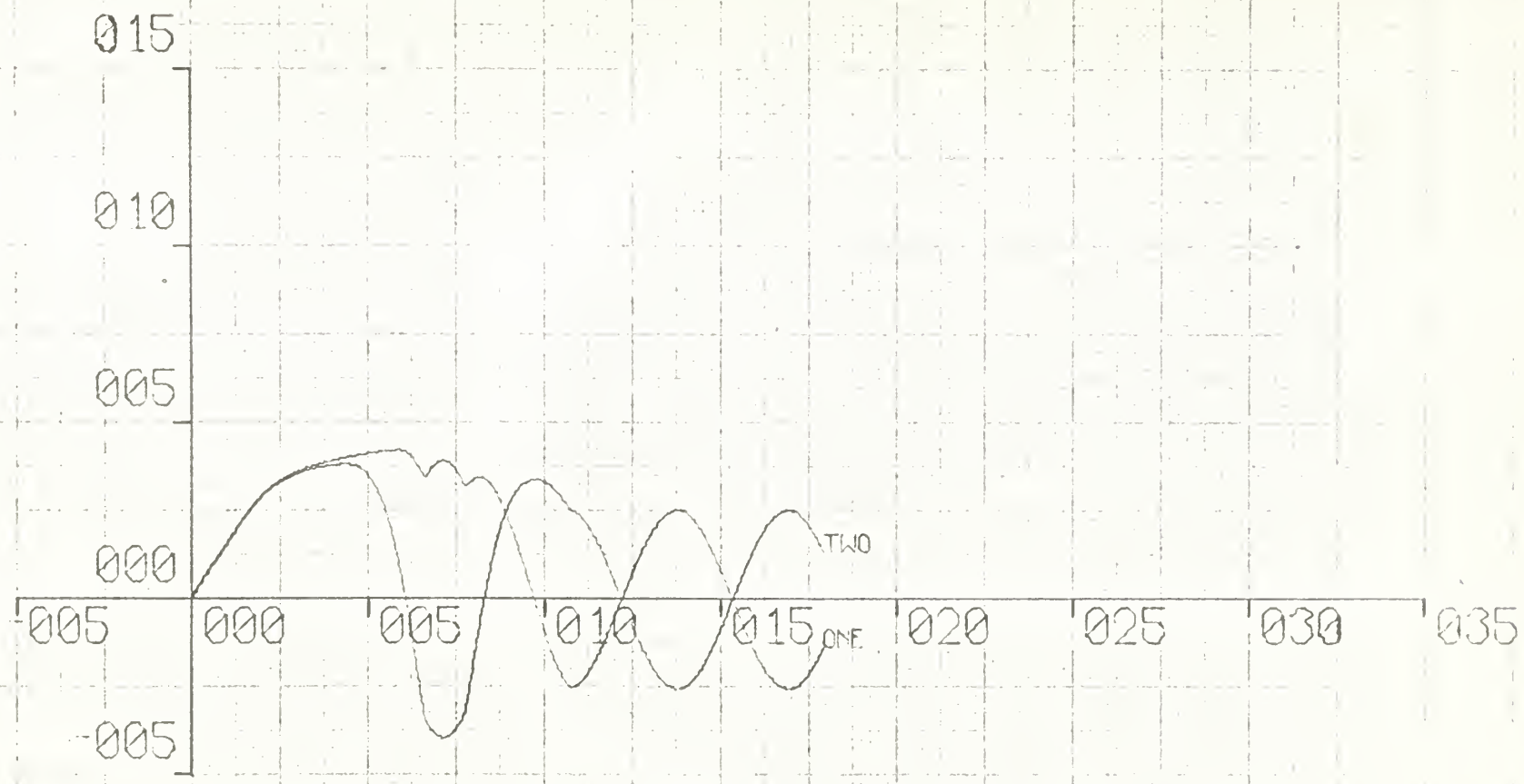

X AXIS SCALE = 5.00E+00
Y AXIS SCALE = 5.00E-03

DEFIBAUGH-INELASTIC COLUMN (SLENDERNESS= 70,ECC=0.01,ALPHA=0.5,BETA=0.5)

STRESS 1 AND STRESS 2 VERSUS TIME

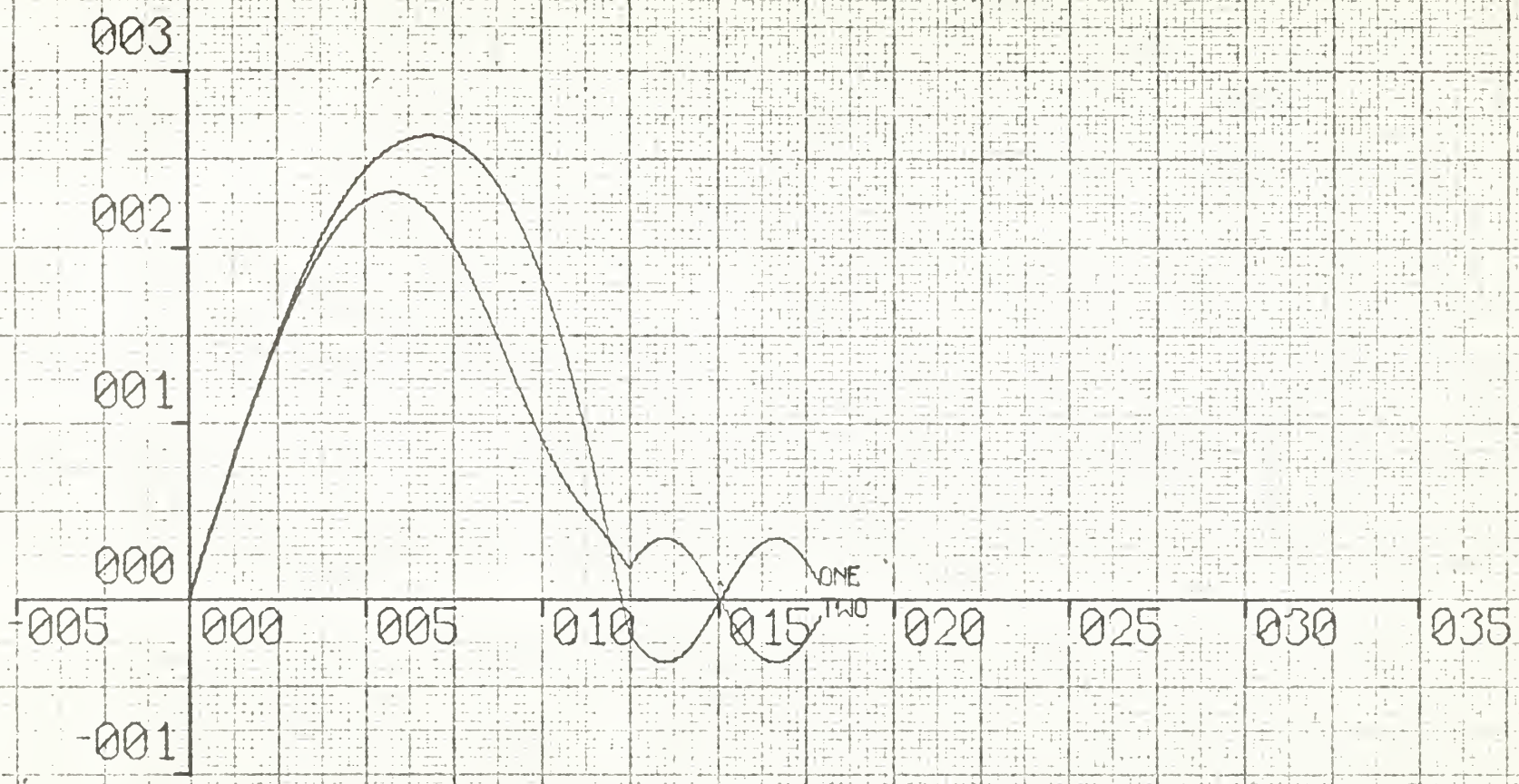

X AXIS SCALE = 5.00E+00

Y AXIS SCALE = 1.00E-03

DEFIBAUCH-INELASTIC COLUMN (SLENDERNESS= 70,ECC=0.01,ALPHA=1.0,BETA=0.5)

STRESS 1 AND STRESS 2 VERSUS TIME

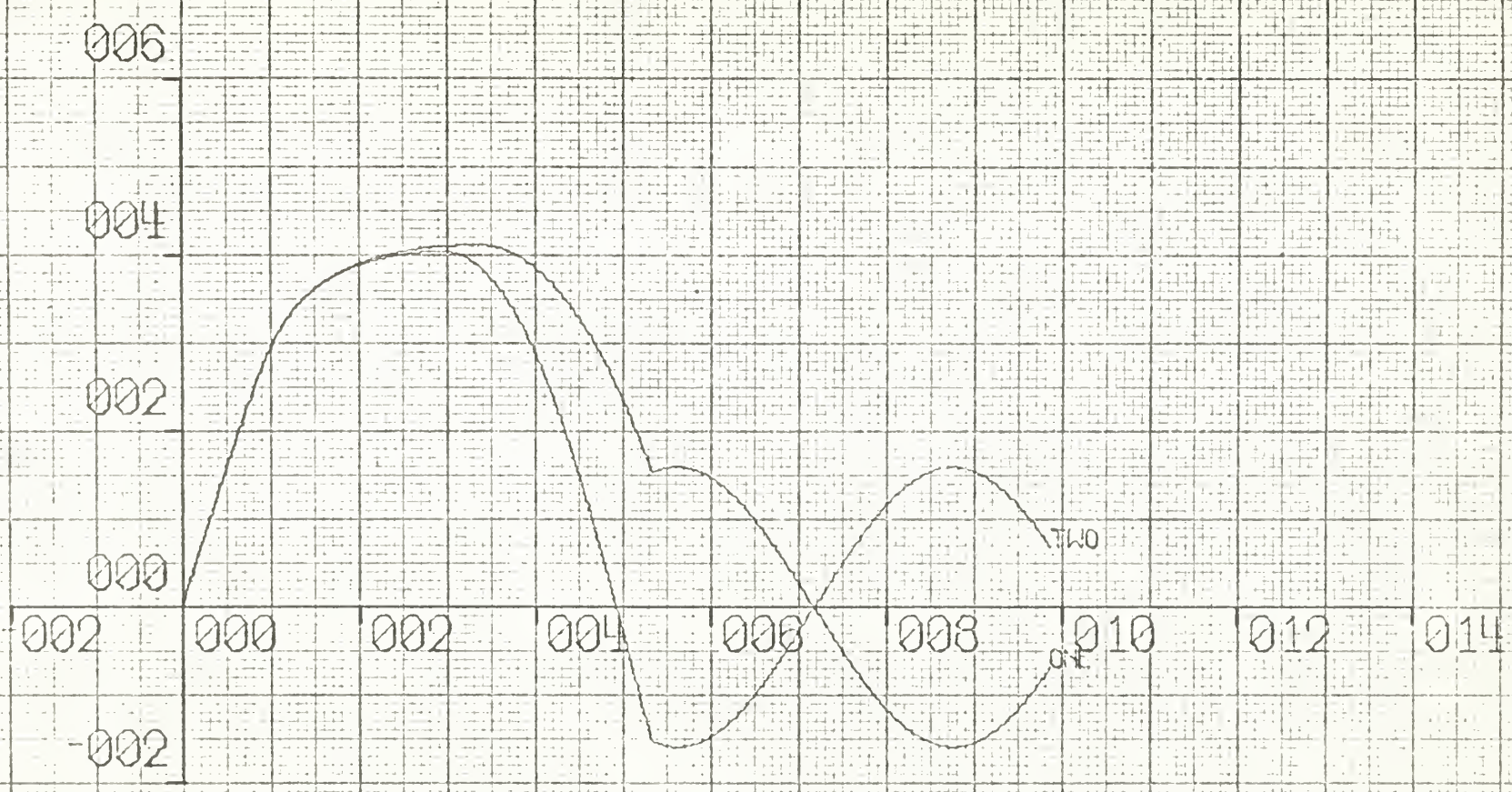

X AXIS SCALE = 2.00E+00

Y AXIS SCALE = 2.00E-03

DETIBAUGH-INELASTIC COLUMN (SLENDERNESS= 20,ECC=0.01,ALPHA=2.5,BETA=1.0)

STRESS 1 AND STRESS 2 VERSUS TIME

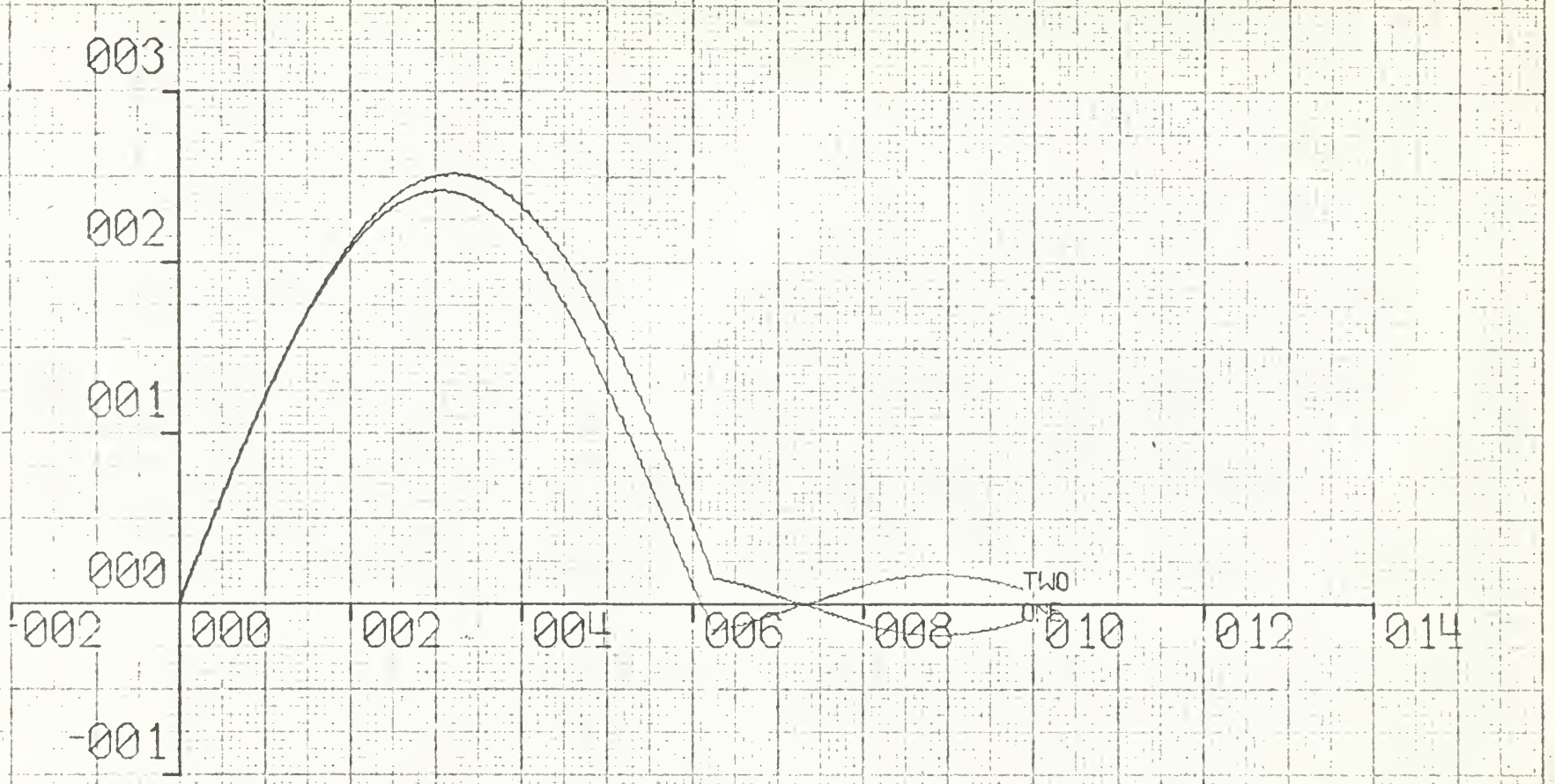

X AXIS SCALE = 2.00E+00
Y AXIS SCALE = 1.00E-03

DEFIBAUCH-INELASTIC COLUMN (SLENDERNESS= 70,ECC=0.01,ALPHA=1.0,BETA=1.0)

STRESS 1 AND STRESS 2 VERSUS TIME

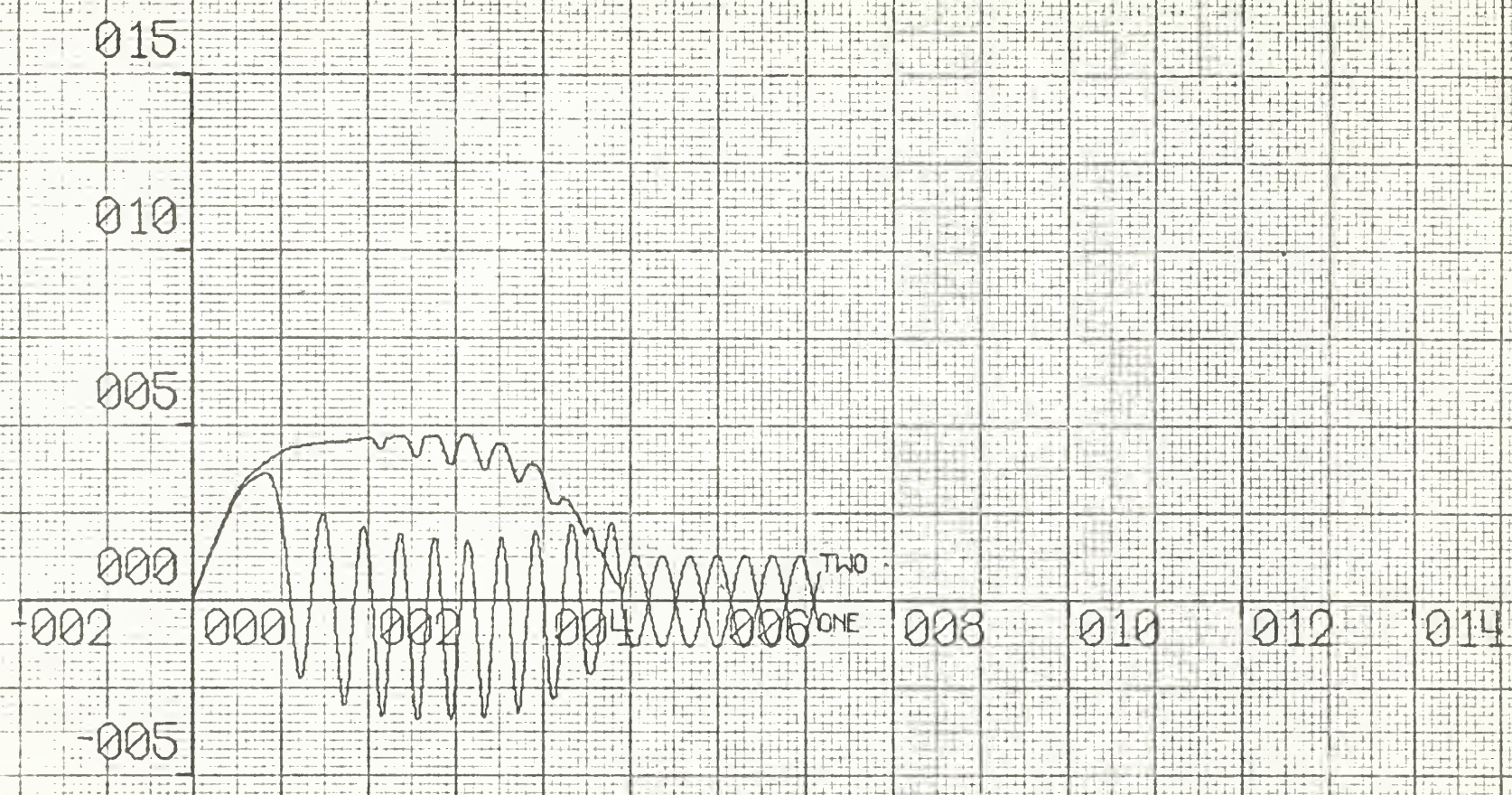

X AXIS SCALE = 2.00E+01

Y AXIS SCALE = 5.00E-03

DEFIBAUGH-INELASTIC COLUMN (SLENDERNESS= 50,ECC=0.01,ALPHA=2.5,BETA=0.1)

STRESS 1 AND STRESS 2 VERSUS TIME

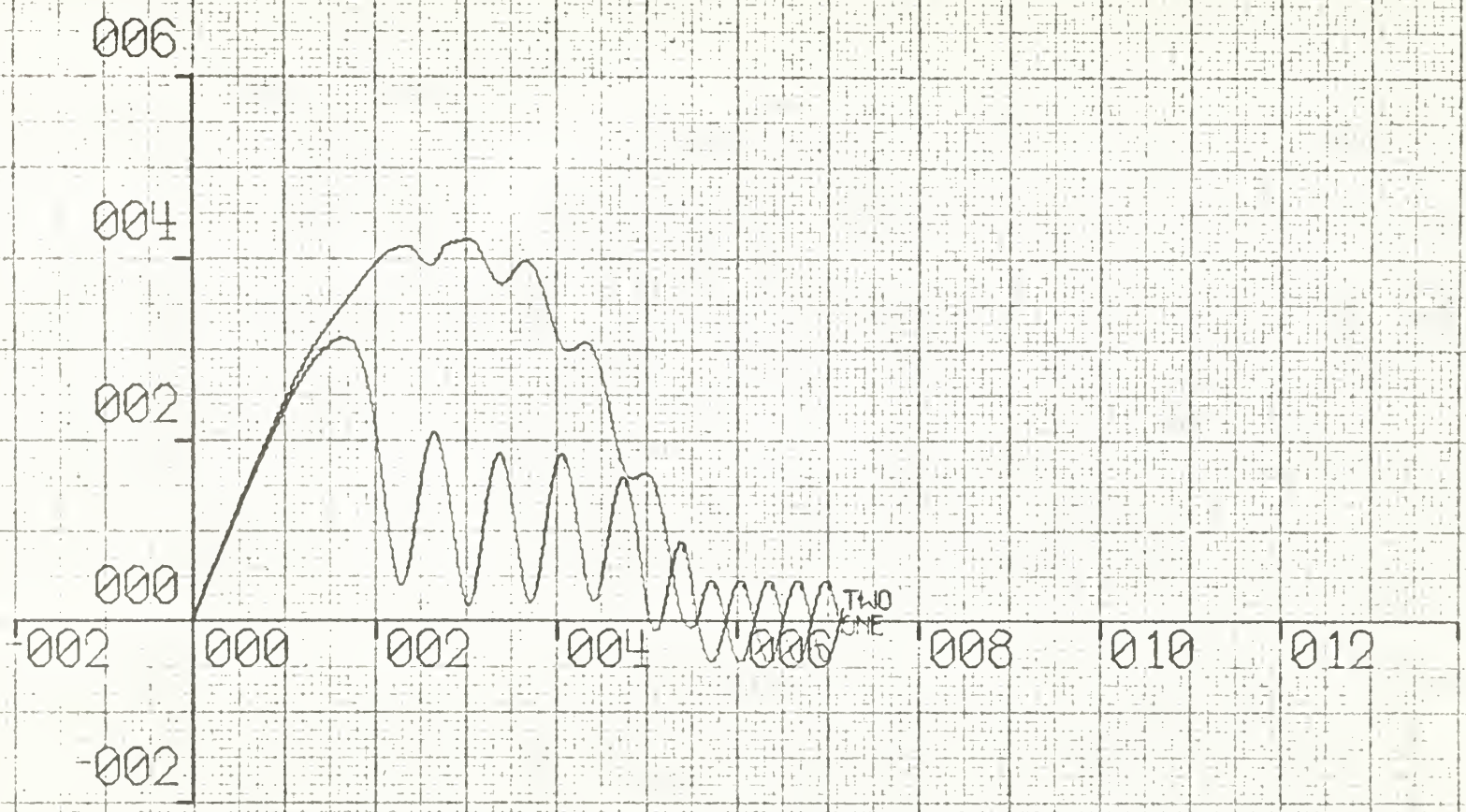

X AXIS SCALE = 2.00E+01

Y AXIS SCALE = 2.00E-03

DEFIBAUGH-INELASTIC COLUMN (SLENDERNESS= 50,ECC=0.01,ALPHA=1.0,BETA=0.1)

STRESS 1 AND STRESS 2 VERSUS TIME

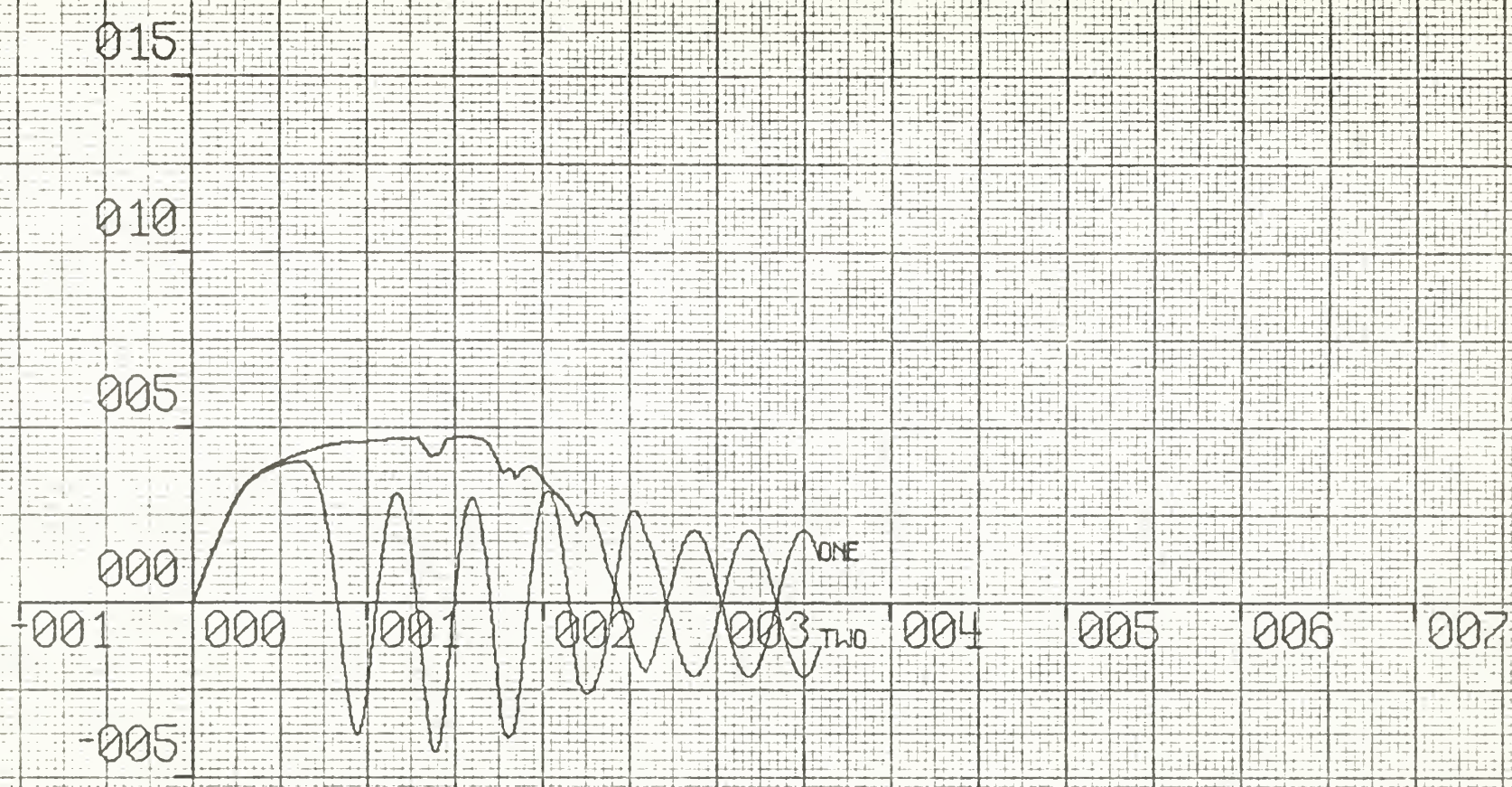

X AXIS SCALE = 1.00E+01
Y AXIS SCALE = 5.00E-03

DEFIBAUGH-INELASTIC COLUMN (SLENDERNESS= 50,ECC=0.01,ALPHA=2.5,BETA=0.2)

STRESS 1 AND STRESS 2 VERSUS TIME

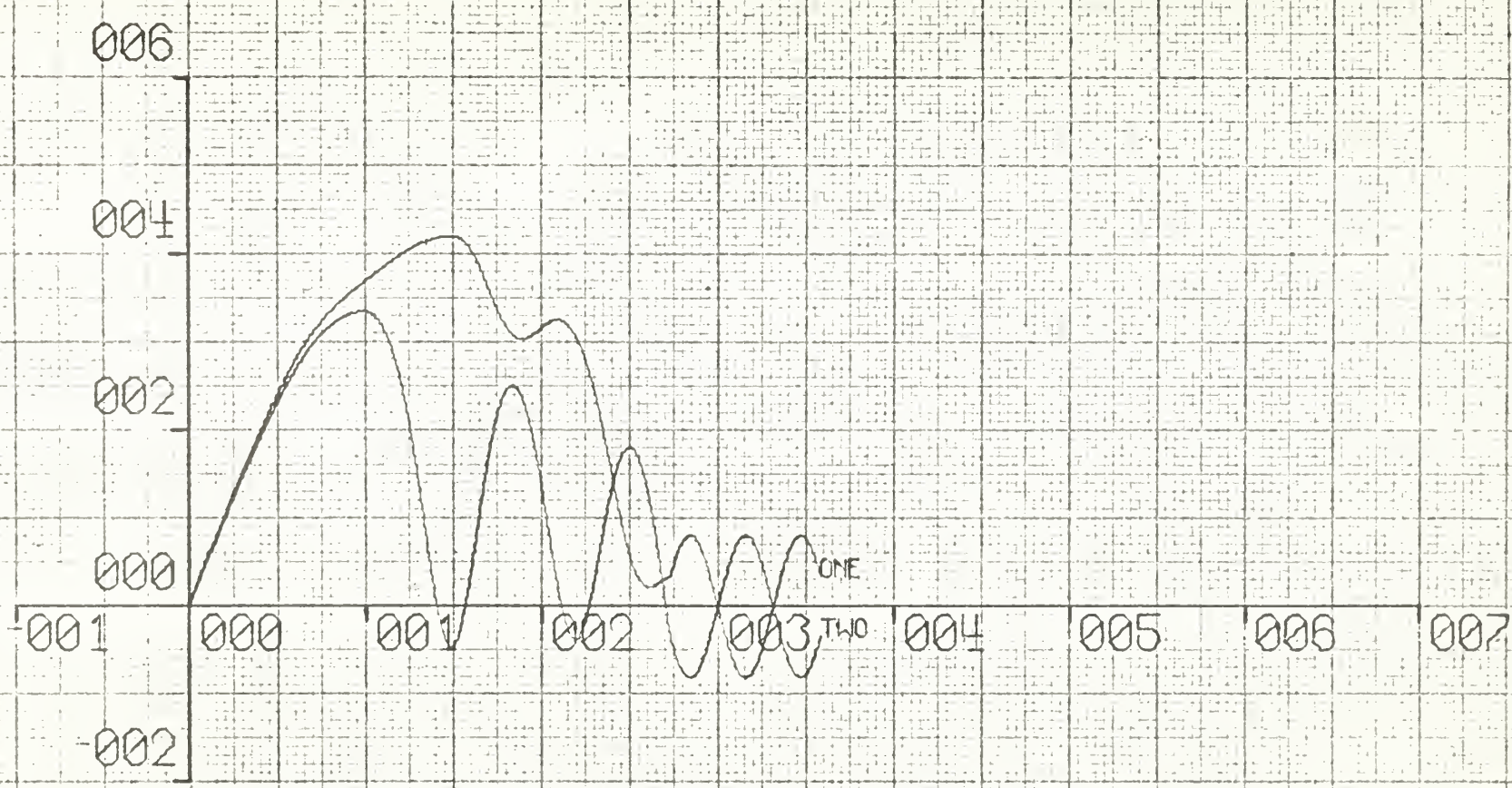

X AXIS SCALE = 1.00E+01

Y AXIS SCALE = 2.00E-03

DEFIBAUCH INELASTIC COLUMN (SLENDERNESS= 50,ECC=0.01,ALPHA=1.0,BETA=0.2)

STRESS 1 AND STRESS 2 VERSUS TIME

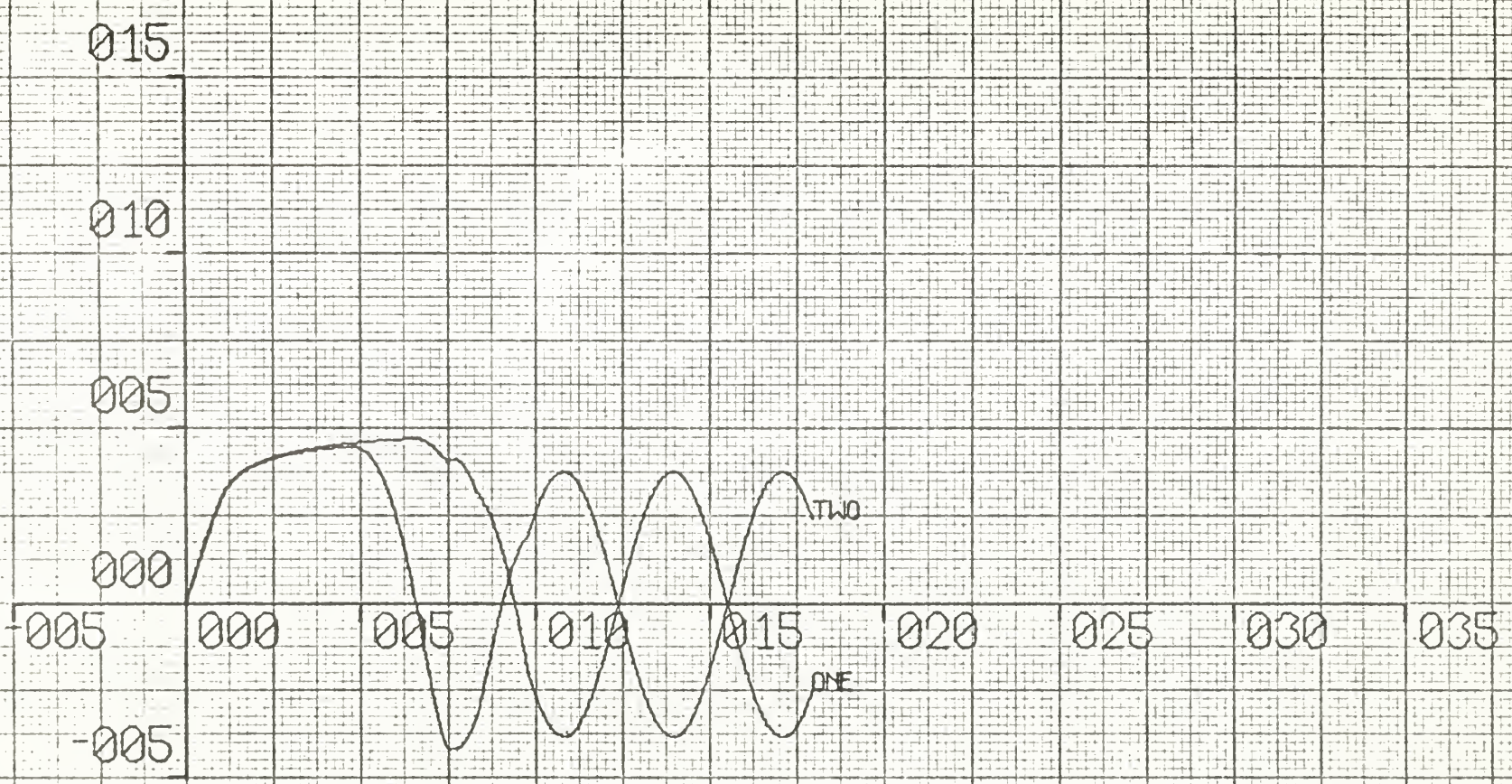

X AXIS SCALE = 5.00E+00

Y AXIS SCALE = 5.00E-03

DEFIBAUGH-INELASTIC COLUMN (SLENDERNESS= 50,ECC=0.01,ALPHA=2.5,BETA=0.5)

STRESS 1 AND STRESS 2 VERSUS TIME

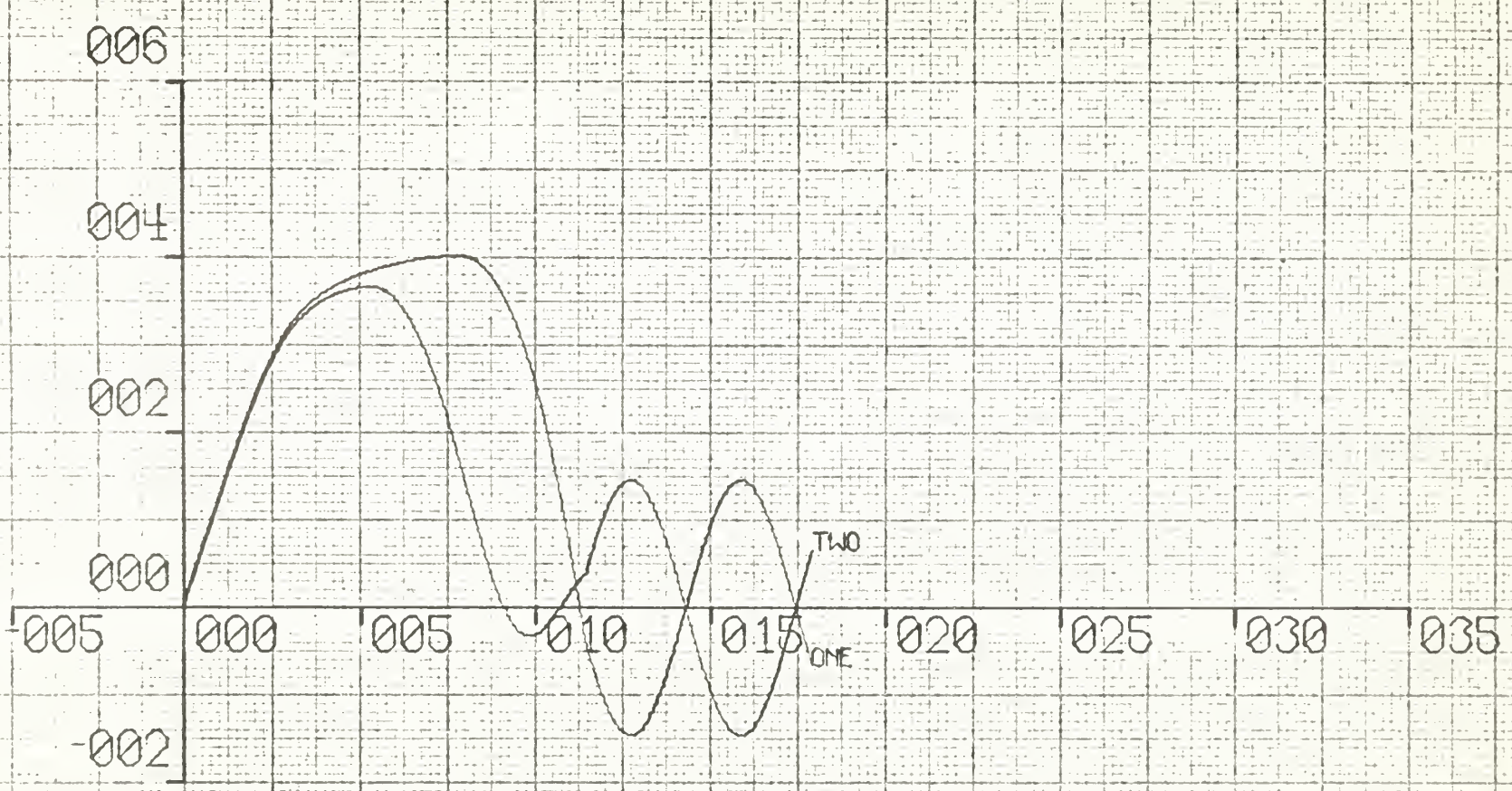

X AXIS SCALE = 5.00E+00

Y AXIS SCALE = 2.00E-03

DEFIBAUCH-INELASTIC COLUMN (SLENDERNESS= 50,ECC=0.01,ALPHA=1.0,BETA=0.5)

STRESS 1 AND STRESS 2 VERSUS TIME

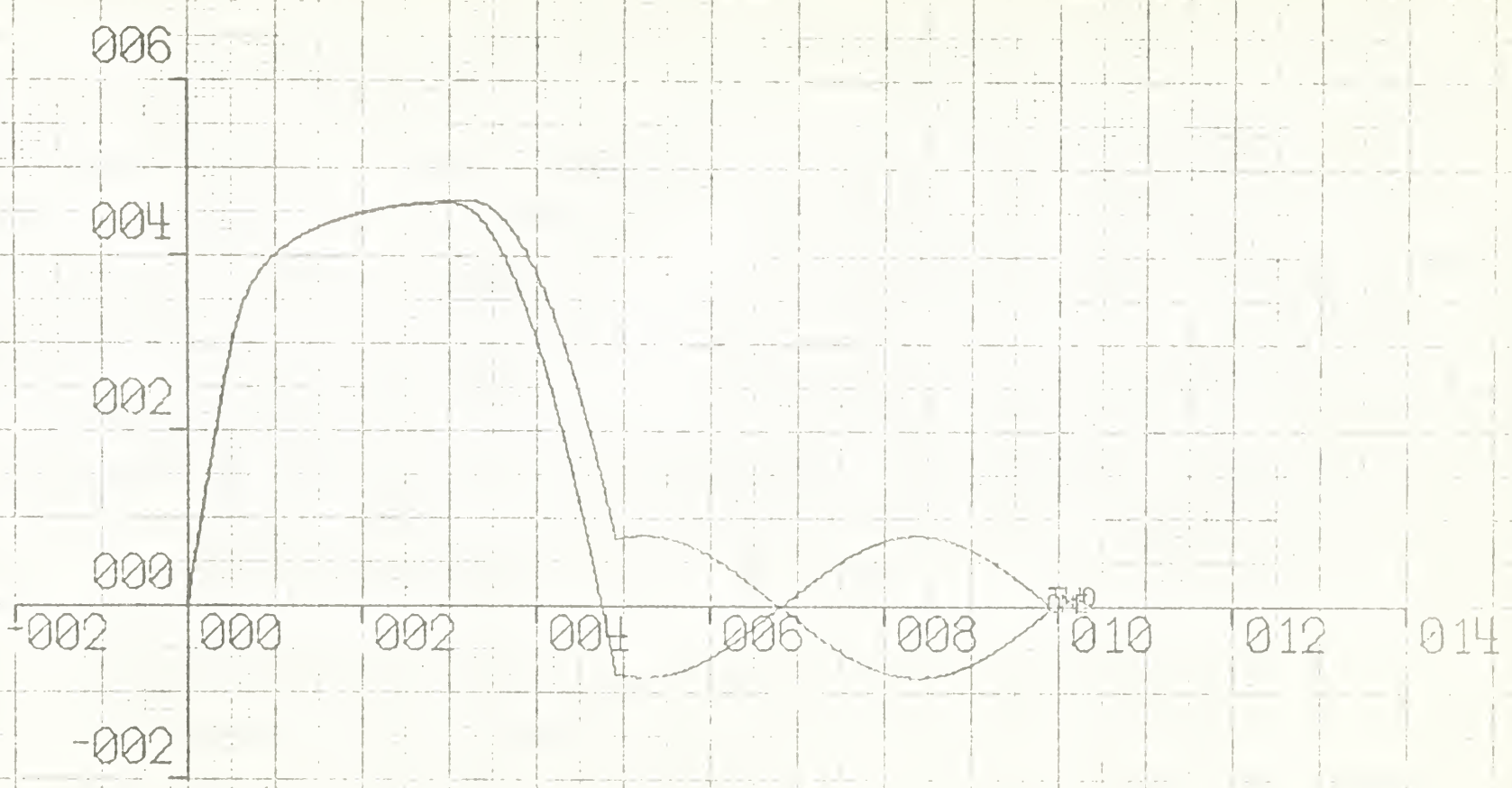

X AXIS SCALE = 2.00E+00
Y AXIS SCALE = 2.00E-03

DEFIBAUGH-INELASTIC COLUMN (SLENDERNESS= 80,ECC=0.01,ALPHA=2.5,BETA=1.0)

STRESS 1 AND STRESS 2 VERSUS TIME

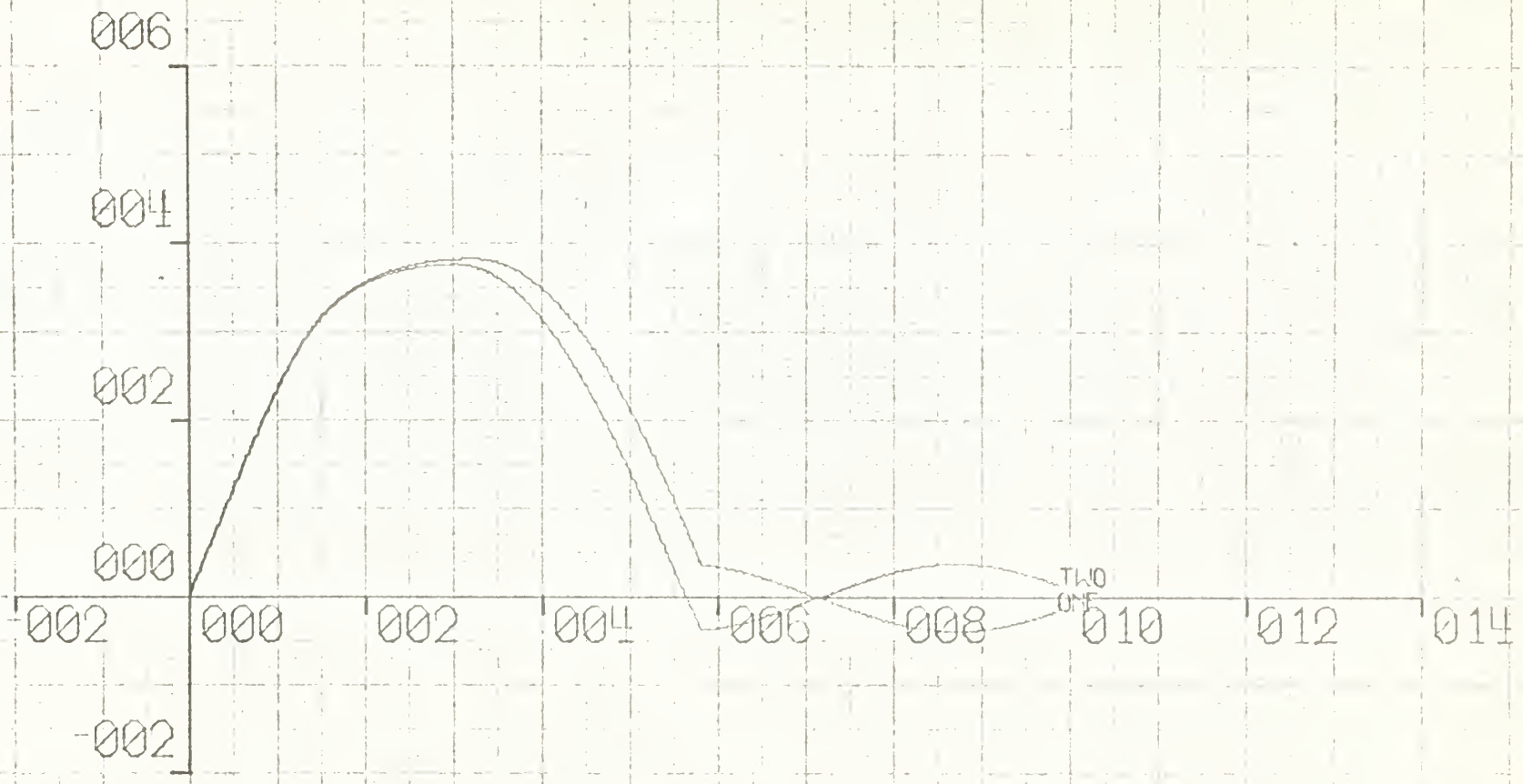

X AXIS SCALE = 2.00E+00
Y AXIS SCALE = 2.00E-03

DEFIE-RUCH-INELASTIC COLUMN (SLENDERNESS= 50,ECC=0.01,ALPHA=1.0,BETA=1.0)

STRESS 1 AND STRESS 2 VERSUS TIME

APPENDIX IV

Computer Programs and Notation

a. General

The FORTRAN language computer programs, together with the notation, and the program operating instructions for both Program COL 1 and Program COL 2 are included in the following pages. The discussion and a listing of Program COL 1 are included on pages IV - 2 to IV - 10. The discussion and a listing of Program COL 2 are included on pages IV - 11 to IV - 20. The FORTRAN language format for each of the programs is in standard FORTRAN language to be used with a standard FORTRAN compiling routine. The program language is compatible with any of the large machine FORTRAN compiling systems including the IBM 7090 and the CDC 1604 systems. Each line in the listing is the information contained on one 80 column IBM card where columns 1-5 contain any statement number, column 6 is used to indicate a continuation card, columns 7-72 contain the FORTRAN statement, and columns 73-80 are used for card identification only. Although the notation is basically the same, the subscript notation is different for each program. Program COL 1 stores a number of variable quantities in array form for print-out and to accommodate Subroutine GRAPH, whereas, Program COL 2 stores only one value of the variable quantities for print-out.

b. Notation for Program COL 1

In the notation for Program COL 1 the subscript J refers to quantities within the Runge-Kutta prediction loop which are calculated for intermediate times within the time increment ΔT. The subscript I refers to the quantities corresponding to each time T(I). The notation for Program COL 1 is as follows:

Computer program notation for Program COL 1

Computer Program Term	Corresponding terms in table of symbols	Computer Program term	Corresponding terms in table of symbols
A	n	SIGY	S_y
ALPHA	α	SIG1(J)	S_1
BETA	β	SIG2(J)	S_2
DDV(J)	$\ddot{V}$	SLNESS	L/ρ
DEFL(I)	V	STRN1(I)	ϵ_1
DELT	ΔT	STRN2(I)	ϵ_2
DISPL(I)	x/x_E	STRS1(I)	S_1
ECC	e/ρ	STRS2(I)	S_2
EPSI1(J)	ϵ_1	T(I)	T
EPSI2(J)	ϵ_2	VEL	$\dot{V}$
FORCE(I)	P/P_E	X(J)	x/x_E

c. Operating instructions for Program COL 1

The output from Program COL 1 includes the print-out and the array quantities necessary for Subroutine GRAPH. The listing for Program COL 1 does not include Subroutine

GRAPH. However, a listing of Subroutine GRAPH and instructions for its use may be obtained from the Control Data Corporation. To use the program to obtain the print-out quantities without the graphical output remove the cards CALL GRAPH. To operate Program COL 1 without Subroutine GRAPH use the cards including Subroutine STRESS in the order shown in the listing followed by one blank card, then the input data card.

The read-write statements in the listing are written for magnetic tape input and output as follows:

(1) Input (READ INPUT TAPE 2)

The input to the program is contained on one card (7E10.3) and includes the following seven quantities in order:

Input quantity	Format
SLNESS (L/ϱ)	E10.3
ALPHA (α)	E10.3
ECC (e/ϱ)	E10.3
BETA (β)	E10.3
A (n)	E10.3
SIGY (S_y)	E10.3
DELT (ΔT)	E10.3

If Subroutine GRAPH is used axis scaling and multiple curve data, graph title data and curve label data in addition to the above are also needed in the input.

(2) Output (WRITE OUTPUT TAPE 4)

The output includes the input quantities and the variable quantities for every fifteenth point as follow:

Output Quantity	Format
SLNESS (L/ρ)	F5.0
ALPHA (α)	F5.2
ECC (e/ρ)	F5.3
BETA (β)	F4.2
A (n)	F5.1
SIGY (S_y)	F6.3
DELT (ΔT)	F5.3
T	F5.2
DISPL (x/x_E)	E14.4
STRN1 (ϵ_1)	E14.4
STRN2 (ϵ_2)	E14.4
STRS1 (S_1)	E14.4
STRS2 (S_2)	E14.4
DEFL (y/ρ)	E14.4
FORCE (P/P_E)	E14.4

```
      PROGRAM COL 1
C PROGRAM TC DETERMINE INELASTIC CCLUMN RESPONSE TO HALF-SINE
C RAM DISPLACEMENT PULSE APPLIEC AT END WITH SMALL ECCENTRICITY
C TO INITIALLY STRAIGHT CCLUMN. WHEN RAM CAUSES TENSION COLUMN
C EXHIBITS FREE VIBRATION.
      ODIMENSION T(900),DISPL(9CC),DEFL(900),STRN1(9C0),STRN2(900),
     1STRS1(900),STRS2(90C),X(4),DCV(4),EPSI1(4),EPSI2(4),SIG1(4),
     2SIG2(4),AK(4,2),C(4),FORCE(900)
      COMMCN A,SIGY
      READ INPUT TAPE 2,5,SLNESS,ALPHA,ECC,BETA,A,SIGY,DELT
    5 FORMAT(7E10.3)
      T(1)=C.C
      DEFL(1)=0.0
      VEL=0.C
      STRN1(C)=0.0
      STRN2(C)=0.0
      STRS1(C)=0.0
      STRS2(C)=0.C
      C(1)=C.0
      C(2)=C.5
      C(3)=C.5
      C(4)=1.C
      KTENS=1
      KONTACT=1
      M=0
```

```
      I=1
   40 DO 70 J=1,4
      TC=T(I)+C(J)*DELT
      VC=DEFL(I)+C(J)*AK(J-1,1)
      IF(0.5*BETA*TC-3.141593)50,55,55
   50 X(J)=ALPHA*SINF(0.5*BETA*TC)
      GO TO 60
   55 X(J)=C.0
  600EPSI1(J)=12.1761/( SLNESS**2 )*(X(J)-0.5*(ECC**2)*VC**2+
     1ECC*VC*(1.0-ECC))
      IF(J-1)62,62,63
   62 CALL STRESS(EPSI1(J),STRN1(I-1),STRS1(I-1),SIG1(J))
      STRN1(I)=EPSI1(1)
      STRS1(I)=SIG1(1)
      GO TO 64
   63 CALL STRESS(EPSI1(J),STRN1(I),STRS1(I),SIG1(J))
  640EPSI2(J)=12.1761/( SLNESS**2 )*(X(J)-0.5*(ECC**2)*VC**2-
     1ECC*VC*(1.0+ECC))
      IF(J-1)65,65,66
   65 CALL STRESS(EPSI2(J),STRN2(I-1),STRS2(I-1),SIG2(J))
      STRN2(I)=EPSI2(1)
      STRS2(I)=SIG2(1)
      GO TO 661
   66 CALL STRESS(EPSI2(J),STRN2(I),STRS2(I),SIG2(J))
  661 IF(KTENS-1)67,665,665
```

```
665 IF(KONTACT-1)67,694,694
 67 IF(M-1)675,68,685
675 X1=X(J)
    P1=SIG1(J)+SIG2(J)
    X(J)=DISPL(I-1)
    M=M+1
    GO TO 60
 68 X2=X(J)
    P2=SIG1(J)+SIG2(J)
    X(J)=X2-(P2/(P2-P1))*(X2-X1)
    M=M+1
    GO TO 60
685 P=SIG1(J)+SIG2(J)
    IF(P)686,688,688
686 IF(10.0**(-8.0)-ABSF(P1))687,693,693
687 X1=X(J)
    P1=P
    X(J)=X2-(P2/(P2-P1))*(X2-X1)
    GO TO 60
688 IF(10.0**(-8.0)-ABSF(P))689,693,693
689 X2=X(J)
    P2=P
    X(J)=X2-(P2/(P2-P1))*(X2-X1)
    GO TO 60
693 M=0
```

```
      KTENS=1
      GO TO 698
  694 IF(SIG1(J)+SIG2(J))695,698,698
  695 IF(0.5*BETA*TC-3.141593)6955,696,696
 6955 KTENS=0
      GO TO 675
  696 KONTACT=0
      GO TO 675
 6980DV(J)=0.0410639*( SLNESS**2 )*((SIG1(J)+SIG2(J))*(VC+1.0)-
     1(SIG1(J)-SIG2(J))/ECC)
      AK(J,1)=DELT*(VEL+C(J)*DELT*DDV(J))
   70 AK(J,2)=DELT*DDV(J)
      DISPL(I)=X(1)
      FORCE(I)=.0410639*( SLNESS**2 )*(STRS1(I)+STRS2(I))
      VEL=VEL+(AK(1,2)+2.0*AK(2,2)+2.0*AK(3,2)+AK(4,2))/6.0
      DEFL(I+1)=DEFL(I)+(AK(1,1)+2.0*AK(2,1)+2.0*AK(3,1)+AK(4,1))/6.0
      IF(I-900)75,80,80
   75 T(I+1)=T(I)+DELT
      I=I+1
      GO TO 40
   80 WRITE OUTPUT TAPE 4,82
   82 FORMAT(1H1)
      WRITE OUTPUT TAPE 4,85,SLNESS,ALPHA,ECC,BETA,A,SIGY,DELT
  850FORMAT(14H   OUTPUT DATA //3X12HSLENDERNESS=F5.0,2X6HALPHA=F5.2,
     12X4HECC=F5.3,2X5H8ETA=F4.2,2X2HA=F5.1,2X5HSIGY=F6.3,2X5HDELT=F5.3
     2   //)
```

```
   WRITE OUTPUT TAPE 4,90
900FORMAT(4X4HTIME,4X12HDISPLACEMENT,4X10HDEFLECTION,4X8HSTRAIN 1,
  16X8HSTRESS 1,6X8HSTRAIN 2,6X8HSTRESS 2,6X5HFORCE//)
   DO 92 I=1,900
92 DEFL(I)=ECC*DEFL(I)
   DO 95 I=1,900,15
950WRITE OUTPUT TAPE 4,98,T(I),DISPL(I),DEFL(I),STRN1(I),STRS1(I),
  1STRN2(I),STRS2(I),FORCE(I)
98 FORMAT(3XF6.2,7E14.4)
   CALL GRAPH(900,T,STRN1,8)
   CALL GRAPH(900,T,STRN2,8)
   CALL GRAPH(900,T,STRS1,8)
   CALL GRAPH(900,T,STRS2,8)
   CALL GRAPH(900,T,DEFL,8)
   CALL GRAPH(900,T,FORCE,8)
   STOP
   END
   SUBROUTINE STRESS(EPSI,EPSIA,SIGA,SIG)
   COMMON A,SIGY
   IF(EPSI)20,20,21
20 SIG=SIGA+(EPSI-EPSIA)
   GO TO 33
21 IF(EPSI-EPSIA)22,22,23
22 SIG=SIGA+(EPSI-EPSIA)
```

```
      GO TO 33
   23 SIGB=SIGA+(EPSI-EPSIA)
      B=3.0/(7.0*(SIGY**(A-1.0)))
      SIG1=EPSI
   24 SIG2=SIG1-(SIG1+B*(SIG1**A)-EPSI)/(A*B*(SIG1**(A-1.0))+1.0)
      IF(ABSF(SIG2*(10.0**(-6.0)))-ABSF(SIG2-SIG1))29,30,30
   29 SIG1=SIG2
      GO TO 24
   30 IF(SIG2-SIGB)31,31,32
   31 SIG=SIG2
      GO TO 33
   32 SIG=SIGB
   33 RETURN
      END
      END
```

d. Notation for Program COL 2

In the notation for Program COL 2 the subscript J refers to quantities within the Runge-Kutta prediction loop which are calculated for intermediate times within the time increment ΔT. The variable quantities ending in B correspond to a time $T - \Delta T$ and the variable quantities ending in A correspond to a time T. The notation for Program COL 2 is as follows:

Computer program notation for Program COL 2

Computer Program Term	Corresponding terms in table of symbols	Computer Program Term	Corresponding terms in table of symbols
A	n	SIG1(J)	S_1
ALPHA	α	SIG2(J)	S_2
BETA	β	SLNESS	L/ρ
DDV(J)	$\ddot{V}$	STRN1A or B	ϵ_1
DEFLA or B	V	STRN2A or B	ϵ_2
DEFLP	y_r/ρ	STRS1A or B	S_1
DELT	ΔT	STRS2A or B	S_2
DISPLA or B	x/x_ϵ	STRS1M	Max S_1 (tensile or compressive)
ECC	e/ρ	STRS2M	Max S_2 (tensile or compressive
EPSI1(J)	ϵ_1	T	T
EPSI2(J)	ϵ_2	VELA or B	$\dot{V}$
PMAX	P_m/P_ϵ	X(J)	x/x_ϵ
SIGY	S_y		

e. Operating instructions for Program COL 2

To operate Program COL 2 use the cards including Subroutine STRESS in the order shown in the listing followed by one blank card, then the input data card.

The read-write statements in the listing are written for magnetic tape input and output as follows:

(1) Input (READ INPUT TAPE 2)

The input to the program is contained on one card (7E10.3) and includes the following seven quantities in order:

Input quantity	Format
SLNESS(L/ϱ)	E10.3
ALPHA (α)	E10.3
ECC (e/ϱ)	E10.3
BETA (β)	E10.3
A (n)	E10.3
SIGY (S_y)	E10.3
DELT (ΔT)	E10.3

(2) Output (WRITE OUTPUT TAPE 4)

The output includes the input quatities and one value of each of the variable quantities including the time T of occurrence of the value as follows:

Output quantity	Format
SLNESS (L/ϱ)	F5.0
ALPHA (α)	E14.4
ECC (e/ϱ)	F5.2
BETA (β)	F4.2
A (n)	F5.1

Output quantity	Format
SIGY (S_y)	F6.3
DELT (ΔT)	F5.3
PMAX (P_m/P_E) T1	E14.4 F6.2
STRS1M ($S_{1\,max}$) T2	E14.4 F6.2
STRS2M ($S_{2\,max}$) T3	E14.4 F6.2
DEFLP (y_r/ρ) T4	E14.4 F6.2

```
      PROGRAM COL 2
C PROGRAM TO DETERMINE RESIDUAL DEFLECTION AND MAXIMUM FORCE
C IN INELASTIC COLUMN RESULTING FROM HALF-SINE RAM DISPLACEMENT
C PULSE APPLIED AT END WITH SMALL ECCENTRICITY TO INITIALLY
C STRAIGHT COLUMN. WHEN RAM CAUSES TENSION COLUMN EXHIBITS FREE
C VIBRATION.
      DIMENSION X(4),DDV(4),EPSI1(4),EPSI2(4),SIG1(4),SIG2(4),AK(4,2),
     1C(4)
      COMMON A,SIGY
      READ INPUT TAPE 2,5,SLNESS,ALPHA,ECC,BETA,A,SIGY,DELT
    5 FORMAT(7E10.3)
   10 T=0.0
      DISPLA=0.0
      VELA=0.0
      DEFLA=0.0
      STRN1B=0.0
      STRN2B=0.0
      STRS1B=0.0
      STRS2B=0.0
      PMAX=0.0
      STRS1M=0.0
      STRS2M=0.0
      STRS2E=0.0
      WORK=0.0
      C(1)=0.0
```

```
      C(2)=C.5
      C(3)=0.5
      C(4)=1.0
      KENERG=1
      KTENS=1
      KONTACT=1
      M=0
40 DO 70 J=1,4
      TC=T+C(J)*DELT
      VC=DEFLA+C(J)*AK(J-1,1)
      IF(0.5*BETA*TC-3.141593)50,55,55
50 X(J)=ALPHA*SINF(0.5*BETA*TC)
      GO TO 60
55 X(J)=C.C
600EPSI1(J)=12.1761/( SLNESS**2 )*(X(J)-0.5*(ECC**2)*VC**2+
     1ECC*VC*(1.0-ECC))
      IF(J-1)62,62,63
62 CALL STRESS(EPSI1(J),STRN1B,STRS1B,SIG1(J))
      STRN1A=EPSI1(1)
      STRS1A=SIG1(1)
      GO TO 64
63 CALL STRESS(EPSI1(J),STRN1A,STRS1A,SIG1(J))
640EPSI2(J)=12.1761/( SLNESS**2 )*(X(J)-0.5*(ECC**2)*VC**2-
     1ECC*VC*(1.0+ECC))
      IF(J-1)65,65,66
```

```
 65 CALL STRESS(EPSI2(J),STRN2B,STRS2B,SIG2(J))
    STRN2A=EPSI2(1)
    STRS2A=SIG2(1)
    GO TO 661
 66 CALL STRESS(EPSI2(J),STRN2A,STRS2A,SIG2(J))
661 IF(KTENS-1)67,665,665
665 IF(KONTACT-1)67,694,694
 67 IF(M-1)675,68,685
675 X1=X(J)
    P1=SIG1(J)+SIG2(J)
    X(J)=CISPLB
    M=M+1
    GO TO 60
 68 X2=X(J)
    P2=SIG1(J)+SIG2(J)
    X(J)=X2-(P2/(P2-P1))*(X2-X1)
    M=M+1
    GO TO 60
685 P=SIG1(J)+SIG2(J)
    IF(P)686,688,688
686 IF(10.0**(-8.0)-ABSF(P))687,693,693
687 X1=X(J)
    P1=P
    X(J)=X2-(P2/(P2-P1))*(X2-X1)
    GO TO 60
```

```
 688 IF(10.0**(-8.0)-ABSF(P))689,693,693
 689 X2=X(J)
     P2=P
     X(J)=X2-(P2/(P2-P1))*(X2-X1)
     GO TO 60
 693 M=0
     KTENS=1
     GO TO 698
 694 IF(SIG1(J)+SIG2(J))695,698,698
 695 IF(0.5*BETA*TC-3.141593)6955,696,696
6955 KTENS=0
     GO TO 675
 696 KONTACT=C
     GO TO 675
6980DDV(J)=0.0410639*( SLNESS**2 )*((SIG1(J)+SIG2(J))*(VC+1.C)-
    1(SIG1(J)-SIG2(J))/ECC)
     AK(J,1)=CELT*(VELA+C(J)*DELT*DDV(J))
  70 AK(J,2)=DELT*DDV(J)
     IF(0.5*BETA*T-3.141593)702,704,704
7020WORK=WORK+0.5*((STRS1A+STRS2A)+(STRS1B+STRS2B))*
    1(ALPHA*(SINF(0.5*BETA*T)-SINF(0.5*BETA*(T-DELT))))
 704 IF(PMAX-C.0410639*( SLNESS**2 )*(STRS1A+STRS2A))71,72,72
  71 PMAX=C.C410639*( SLNESS**2 )*(STRS1A+STRS2A)
     T1=T
  72 IF(STRS1M-STRS1A)73,74,74
```

```
 73 STRS1M=STRS1A
    STRS1E=STRS1M
    T2=T
 74 IF(ABSF(STRS2M)-ABSF(STRS2A))75,751,751
 75 STRS2M=STRS2A
    T3=T
751 IF(STRS2E-STRS2A)752,755,755
752 STRS2E=STRS2A
755 IF(KENERG-1)756,76,76
756 IF(VELB)758,759,757
757 IF(VELA)759,759,81
758 IF(VELA)81,759,759
759 B=3.0/(7.0*(SIGY**(A-1.0)))
    ENERG1= (A*B/(A+1.0))*STRS1E**(A+1.0)+0.5*STRS1B**2
    ENERG2= (A*B/(A+1.0))*STRS2E**(A+1.0)+0.5*STRS2B**2
    ENERGT=0.0821278*( SLNESS**2 )*(ENERG1+ENERG2)
    GO TO 84
 76 IF(KONTACT-1)77,81,81
 77 BENDM1=STRS1B-STRS2B
    BENDM2=STRS1A-STRS2A
    IF(STRS1B)78,78,79
 78 IF(STRS1A)81,80,80
 79 IF(STRS1A)80,80,81
 80 DEFLP=(DEFLA -BENDM2/(BENDM2-BENDM1)*(DEFLA-DEFLB))*ECC
    T4=T
```

```
      KENERG=0
   81 T=T+DELT
      DISPLB=DISPLA
      DISPLA=X(1)
      VELB=VELA
      VELA=VELB+(AK(1,2)+2.0*AK(2,2)+2.0*AK(3,2)+AK(4,2))/6.0
      DEFLB=DEFLA
      DEFLA  =  DEFLB  +(AK(1,1)+2.0*AK(2,1)+2.0*AK(3,1)+AK(4,1))/6.C
      STRN1B=STRN1A
      STRN2B=STRN2A
      STRS1B=STRS1A
      STRS2B=STRS2A
      GO TO 40
   84 WRITE OUTPUT TAPE 4,85,SLNESS, ECC ,BETA,A,SIGY,DELT
  850FORMAT(///14H OUTPUT DATA  //12HSLENDERNESS=F5.0,2X6H  ECC=F5.2,
     12X5HBETA=F4.2,2X2HA=F5.1,2X5HSIGY=F6.3,2X5HDELT=F5.3//)
      WRITE OUTPUT TAPE 4,86
  860FORMAT(6X5HALPHA,7X11HDEFORMATION,3X9HMAX FORCE,5X12HMAX STRESS 1,
     12X12HMAX STRESS 2//)
   87 WRITE OUTPUT TAPE 4,88,ALPHA,DEFLP,PMAX,STRS1M,STRS2M
   88 FORMAT(5E14.4)
      WRITE OUTPUT TAPE 4,885,T4,T1,T2,T3
  885 FORMAT(20X1H(F6.2,1H),6X1H(F6.2,1H),6X1H(F6.2,1H),6X1H(F6.2,1H))
      WRITE OUTPUT TAPE 4,887,WORK,ENERGT
  887 FORMAT(25X5HWORK=E12.4,10X7HENERGY=E12.4//)
```

```
      STOP
      END
      SUBROUTINE STRESS(EPSI,EPSIA,SIGA,SIG)
      COMMON A,SIGY
      IF(EPSI)20,20,21
   20 SIG=SIGA+(EPSI-EPSIA)
      GO TO 33
   21 IF(EPSI-EPSIA)22,22,23
   22 SIG=SIGA+(EPSI-EPSIA)
      GO TO 33
   23 SIGB=SIGA+(EPSI-EPSIA)
      B=3.0/(7.0*(SIGY**(A-1.0)))
      SIG1=EPSI
   24 SIG2=SIG1-(SIG1+B*(SIG1**A)-EPSI)/(A*B*(SIG1**(A-1.0))+1.0)
      IF(ABSF(SIG2*(10.0**(-8.0)))-ABSF(SIG2-SIG1))29,30,30
   29 SIG1=SIG2
      GO TO 24
   30 IF(SIG2-SIGB)31,31,32
   31 SIG=SIG2
      GO TO 33
   32 SIG=SIGB
   33 RETURN
      END
      END
```

APPENDIX V

Maximum Force, Residual Deflection and Maximum Stress Data

Tabulated on the following pages are the maximum force, residual deflection, and maximum stress data for the three slenderness ratios and two eccentricity ratios for all values of α and β which were investigated for pulse loading. The values of maximum lateral deflection that were available are also included in the tabulation. These values were only available from the solutions to computer Program COL 1 used to obtain graphical results. Thus, only a limited number of these values are included in the tabulation.

The dimensionless time increments ΔT used for the numerical integration were the same for a given value of β in all the solutions for both computer programs. These values are as follows:

β	ΔT
0.01	0.10
0.05	0.10
0.10	0.08
0.20	0.04
0.50	0.02
1.00	0.01

The values of ΔT are more than adequate to maintain the accuracy of the numerical scheme. The minimum number of increments for a natural period of first mode lateral vibration of the column in the numerical process is 62. The values of ΔT were selected to display the complete history of the dynamic response to the pulse loading for the graphs shown in App. III using the maximum 900 points permitted in Sub-

routine GRAPH.

The values of maximum stress tabulated on the following pages are maximum compressive stresses if there is no sign before the number, or maximum tensile stresses if there is a negative sign before the number. In either case they are the maximum absolute values of stress that occurred in Spring 1 or Spring 2 of the column model.

APPENDIX V

Maximum Force, Residual Deflection and Maximum Stress Data

$\alpha = 2$ $\quad L/\rho = 100$ $\quad e/\rho = 0.05$

β	Maximum Force (P_m/P_E)	Residual Deflection (y_r/ρ)	Maximum Deflection (y_m/ρ)	Stress 1 Maximum (S_{1max})	Stress 2 Maximum (S_{2max})
0.01	0.953	2.12×10^{-2}	---	0.00282	0.00074
0.05	1.001	2.24×10^{-2}	---	0.00283	0.00078
0.10	1.121	2.50×10^{-2}	---	0.00287	0.00100
0.20	1.319	2.77×10^{-2}	---	0.00289	-0.00129
0.50	1.658	2.40×10^{-2}	---	0.00286	-0.00233
1.00	1.935	1.69×10^{-2}	---	0.00278	0.00213

$\alpha = 2.5$ $\quad L/\rho = 100$ $\quad e/\rho = 0.05$

β	Maximum Force (P_m/P_E)	Residual Deflection (y_r/ρ)	Maximum Deflection (y_m/ρ)	Stress 1 Maximum (S_{1max})	Stress 2 Maximum (S_{2max})
0.01	0.953	5.89×10^{-2}	---	0.00312	0.00084
0.05	1.029	6.45×10^{-2}	---	0.00315	-0.00099
0.10	1.189	7.66×10^{-2}	---	0.00320	-0.00132
0.20	1.470	9.41×10^{-2}	---	0.00327	-0.00188
0.50	1.958	8.88×10^{-2}	---	0.00325	-0.00275
1.00	2.331	9.00×10^{-2}	---	0.00329	-0.00263

APPENDIX V

Maximum Force, Residual Deflection and Maximum Stress Data

$\alpha = 3$ $L/\rho = 100$ $e/\rho = 0.05$

β	Maximum Force (P_m/P_E)	Residual Deflection (y_r/ρ)	Maximum Deflection (y_m/ρ)	Stress 1 Maximum (S_{1max})	Stress 2 Maximum (S_{2max})
0.01	0.954	1.14×10^{-1}	---	0.00334	-0.00110
0.05	1.069	1.28×10^{-1}	---	0.00337	-0.00130
0.10	1.252	1.54×10^{-1}	---	0.00344	-0.00167
0.20	1.602	1.98×10^{-1}	---	0.00352	-0.00236
0.50	2.237	2.20×10^{-1}	---	0.00356	-0.00310
1.00	2.633	2.05×10^{-1}	---	0.00360	-0.00313

$\alpha = 3.5$ $L/\rho = 100$ $e/\rho = 0.05$

β	Maximum Force (P_m/P_E)	Residual Deflection (y_r/ρ)	Maximum Deflection (y_m/ρ)	Stress 1 Maximum (S_{1max})	Stress 2 Maximum (S_{2max})
0.01	0.955	1.81×10^{-1}	---	0.00349	-0.00131
0.05	1.110	2.05×10^{-1}	---	0.00354	-0.00155
0.10	1.314	2.47×10^{-1}	---	0.00360	-0.00195
0.20	1.724	3.25×10^{-1}	---	0.00370	-0.00268
0.50	2.447	3.83×10^{-1}	---	0.00377	-0.00340
1.00	2.851	2.57×10^{-1}	---	0.00380	-0.00352

APPENDIX V

Maximum Force, Residual Deflection and Maximum Stress Data

$\alpha = 4$ $L/\rho = 100$ $e/\rho = 0.05$

β	Maximum Force (P_m/P_E)	Residual Deflection (y_r/ρ)	Maximum Deflection (y_m/ρ)	Stress 1 Maximum (S_{1max})	Stress 2 Maximum (S_{2max})
0.01	0.956	2.54×10^{-1}	---	0.00361	-0.00149
0.05	1.147	2.89×10^{-1}	---	0.00366	-0.00175
0.10	1.382	3.49×10^{-1}	---	0.00373	-0.00219
0.20	1.836	4.56×10^{-1}	---	0.00383	-0.00281
0.50	2.617	5.57×10^{-1}	---	0.00392	-0.00367
1.00	3.011	2.93×10^{-1}	---	0.00394	-0.00381

$\alpha = 1$ $L/\rho = 70$ $e/\rho = 0.05$

β	Maximum Force (P_m/P_E)	Residual Deflection (y_r/ρ)	Maximum Deflection (y_m/ρ)	Stress 1 Maximum (S_{1max})	Stress 2 Maximum (S_{2max})
0.01	0.841	3.17×10^{-2}	---	0.00315	0.00149
0.05	0.840	3.19×10^{-2}	---	0.00315	0.00150
0.10	0.847	3.13×10^{-2}	---	0.00315	0.00153
0.20	0.868	4.13×10^{-2}	---	0.00324	0.00163
0.50	0.934	2.83×10^{-2}	---	0.00312	0.00190
1.00	0.982	6.24×10^{-3}	---	0.00272	0.00224

APPENDIX V

Maximum Force, Residual Deflection and Maximum Stress Data

$\alpha = 1.5$ $L/\rho = 70$ $e/\rho = 0.05$

β	Maximum Force (P_m/P_E)	Residual Deflection (y_r/ρ)	Maximum Deflection (y_m/ρ)	Stress 1 Maximum (S_{1max})	Stress 2 Maximum (S_{2max})
0.01	0.841	2.10×10^{-1}	---	0.00381	0.00149
0.05	0.854	2.09×10^{-1}	---	0.00381	0.00153
0.10	0.898	2.10×10^{-1}	---	0.00381	0.00164
0.20	0.987	2.10×10^{-1}	---	0.00381	0.00184
0.50	1.206	2.04×10^{-1}	---	0.00381	-0.00260
1.00	1.337	1.03×10^{-1}	---	0.00364	0.00314

$\alpha = 2$ $L/\rho = 70$ $e/\rho = 0.05$

β	Maximum Force (P_m/P_E)	Residual Deflection (y_r/ρ)	Maximum Deflection (y_m/ρ)	Stress 1 Maximum (S_{1max})	Stress 2 Maximum (S_{2max})
0.01	0.841	3.79×10^{-1}	---	0.00404	0.00149
0.05	0.878	3.86×10^{-1}	---	0.00405	0.00158
0.10	0.954	3.98×10^{-1}	---	0.00406	0.00176
0.20	1.080	4.05×10^{-1}	---	0.00407	-0.00228
0.50	1.377	3.43×10^{-1}	---	0.00403	-0.00368
1.00	1.516	2.22×10^{-1}	---	0.00402	0.00364

APPENDIX V

Maximum Force, Residual Deflection and Maximum Stress Data

α = 2.5 L/ρ = 70 e/ρ = 0.05

β	Maximum Force (P_m/P_E)	Residual Deflection (y_r/ρ)	Maximum Deflection (y_m/ρ)	Stress 1 Maximum (S_{1max})	Stress 2 Maximum (S_{2max})
0.01	0.841	5.36×10^{-1}	---	0.00418	0.00149
0.05	0.897	5.52×10^{-1}	---	0.00419	0.00161
0.10	0.995	5.77×10^{-1}	---	0.00421	-0.00202
0.20	1.167	5.99×10^{-1}	1.87	0.00423	-0.00308
0.50	1.489	5.03×10^{-1}	---	0.00422	-0.00413
1.00	1.619	3.06×10^{-1}	---	0.00422	0.00393

α = 1 L/ρ = 50 e/ρ = 0.05

β	Maximum Force (P_m/P_E)	Residual Deflection (y_r/ρ)	Maximum Deflection (y_m/ρ)	Stress 1 Maximum (S_{1max})	Stress 2 Maximum (S_{2max})
0.01	0.585	2.67×10^{-1}	---	0.00417	0.00234
0.05	0.592	2.69×10^{-1}	---	0.00418	0.00240
0.10	0.614	2.70×10^{-1}	---	0.00419	0.00251
0.20	0.655	2.63×10^{-1}	---	0.00417	0.00275
0.50	0.731	2.52×10^{-1}	---	0.00419	0.00329
1.00	0.774	8.80×10^{-2}	---	0.00396	0.00366

APPENDIX V

Maximum Force, Residual Deflection and Maximum Stress Data

α = 1.5 L/ρ = 50 e/ρ = 0.05

β	Maximum Force (P_m/P_E)	Residual Deflection (y_r/ρ)	Maximum Deflection (y_m/ρ)	Stress 1 Maximum (S_{1max})	Stress 2 Maximum (S_{2max})
0.01	0.585	5.17×10^{-1}	---	0.00446	0.00234
0.05	0.612	5.16×10^{-1}	---	0.00446	0.00251
0.10	0.654	5.13×10^{-1}	---	0.00446	0.00275
0.20	0.708	5.05×10^{-1}	---	0.00446	0.00307
0.50	0.822	4.03×10^{-1}	---	0.00445	0.00383
1.00	0.864	1.60×10^{-1}	---	0.00435	0.00413

α = 2 L/ρ = 50 e/ρ = 0.05

β	Maximum Force (P_m/P_E)	Residual Deflection (y_r/ρ)	Maximum Deflection (y_m/ρ)	Stress 1 Maximum (S_{1max})	Stress 2 Maximum (S_{2max})
0.01	0.585	7.27×10^{-1}	---	0.00461	0.00235
0.05	0.626	7.34×10^{-1}	---	0.00462	0.00257
0.10	0.679	7.37×10^{-1}	---	0.00462	0.00287
0.20	0.756	7.18×10^{-1}	---	0.00462	0.00338
0.50	0.873	4.93×10^{-1}	---	0.00461	-0.00454
1.00	0.913	2.07×10^{-1}	---	0.00456	0.00439

APPENDIX V

Maximum Force, Residual Deflection and Maximum Stress Data

$\alpha = 2.5$ $L/\rho = 50$ $e/\rho = 0.05$

β	Maximum Force (P_m/P_E)	Residual Deflection (y_r/ρ)	Maximum Deflection (y_m/ρ)	Stress 1 Maximum (S_{1max})	Stress 2 Maximum (S_{2max})
0.01	0.586	9.14×10^{-1}	---	0.00472	0.00236
0.05	0.645	9.30×10^{-1}	---	0.00473	0.00269
0.10	0.700	9.40×10^{-1}	---	0.00473	0.00300
0.20	0.794	8.98×10^{-1}	---	0.00474	-0.00413
0.50	0.909	6.17×10^{-1}	---	0.00475	-0.00475
1.00	0.948	2.41×10^{-1}	---	0.00471	0.00456

$\alpha = 2$ $L/\rho = 100$ $e/\rho = 0.01$

β	Maximum Force (P_m/P_E)	Residual Deflection (y_r/ρ)	Maximum Deflection (y_m/ρ)	Stress 1 Maximum (S_{1max})	Stress 2 Maximum (S_{2max})
0.01	1.003	2.56×10^{-2}	---	0.00287	0.00100
0.05	1.192	3.03×10^{-2}	---	0.00292	0.00118
0.10	1.376	3.29×10^{-2}	1.64	0.00295	0.00149
0.20	1.616	3.30×10^{-2}	1.81	0.00295	-0.00180
0.50	1.911	3.07×10^{-2}	1.93	0.00294	-0.00231
1.00	1.988	2.95×10^{-3}	0.69	0.00250	0.00235

APPENDIX V

Maximum Force, Residual Deflection and Maximum Stress Data

$\alpha = 2.5$ $L/\rho = 100$ $e/\rho = 0.01$

β	Maximum Force (P_m/P_E)	Residual Deflection (y_r/ρ)	Maximum Deflection (y_m/ρ)	Stress 1 Maximum (S_{1max})	Stress 2 Maximum (S_{2max})
0.01	1.017	6.93×10^{-2}	---	0.00317	0.00100
0.05	1.258	8.89×10^{-2}	---	0.00325	-0.00139
0.10	1.486	1.04×10^{-1}	---	0.00331	-0.00185
0.20	1.813	1.17×10^{-1}	---	0.00334	-0.00250
0.50	2.264	1.11×10^{-1}	---	0.00335	-0.00286
1.00	2.423	2.29×10^{-2}	---	0.00306	0.00287

$\alpha = 3$ $L/\rho = 100$ $e/\rho = 0.01$

β	Maximum Force (P_m/P_E)	Residual Deflection (y_r/ρ)	Maximum Deflection (y_m/ρ)	Stress 1 Maximum (S_{1max})	Stress 2 Maximum (S_{2max})
0.01	1.032	1.30×10^{-1}	---	0.00338	-0.00115
0.05	1.320	1.72×10^{-1}	---	0.00348	-0.00173
0.10	1.578	2.07×10^{-1}	---	0.00354	-0.00224
0.20	1.971	2.47×10^{-1}	---	0.00360	-0.00274
0.50	2.535	2.11×10^{-1}	---	0.00359	-0.00326
1.00	2.744	7.27×10^{-2}	---	0.00346	0.00327

APPENDIX V

Maximum Force, Residual Deflection and Maximum Stress Data

$\alpha = 3.5$ $L/\rho = 100$ $e/\rho = 0.01$

β	Maximum Force (P_m/P_E)	Residual Deflection (y_r/ρ)	Maximum Deflection (y_m/ρ)	Stress 1 Maximum (S_{1max})	Stress 2 Maximum (S_{2max})
0.01	1.048	2.00×10^{-1}	---	0.00353	-0.00135
0.05	1.380	2.69×10^{-1}	---	0.00363	-0.00199
0.10	1.666	3.26×10^{-1}	---	0.00370	-0.00255
0.20	2.108	3.86×10^{-1}	---	0.00377	-0.00292
0.50	2.739	3.00×10^{-1}	---	0.00376	-0.00358
1.00	2.961	1.35×10^{-1}	---	0.00372	0.00354

$\alpha = 4$ $L/\rho = 100$ $e/\rho = 0.01$

β	Maximum Force (P_m/P_E)	Residual Deflection (y_r/ρ)	Maximum Deflection (y_m/ρ)	Stress 1 Maximum (S_{1max})	Stress 2 Maximum (S_{2max})
0.01	1.062	2.74×10^{-1}	---	0.00364	-0.00151
0.05	1.433	3.70×10^{-1}	---	0.00375	-0.00220
0.10	1.751	4.52×10^{-1}	2.67	0.00383	-0.00273
0.20	2.230	5.49×10^{-1}	2.97	0.00390	-0.00308
0.50	2.894	3.94×10^{-1}	3.54	0.00388	-0.00383
1.00	3.114	1.93×10^{-1}	2.70	0.00390	0.00374

APPENDIX V

Maximum Force, Residual Deflection and Maximum Stress Data

α = 1 L/ρ = 70 e/ρ = 0.01

β	Maximum Force (P_m/P_E)	Residual Deflection (y_r/ρ)	Maximum Deflection (y_m/ρ)	Stress 1 Maximum (S_{1max})	Stress 2 Maximum (S_{2max})
0.01	0.916	2.54×10^{-2}	---	0.00309	0.00197
0.05	0.927	2.89×10^{-2}	---	0.00313	0.00201
0.10	0.947	3.63×10^{-2}	0.49	0.00320	0.00206
0.20	0.973	2.28×10^{-2}	0.45	0.00306	0.00217
0.50	0.991	3.94×10^{-3}	0.20	0.00264	0.00232
1.00	0.994	1.13×10^{-3}	0.08	0.00252	0.00242

α = 1.5 L/ρ = 70 e/ρ = 0.01

β	Maximum Force (P_m/P_E)	Residual Deflection (y_r/ρ)	Maximum Deflection (y_m/ρ)	Stress 1 Maximum (S_{1max})	Stress 2 Maximum (S_{2max})
0.01	0.922	2.24×10^{-1}	---	0.00383	0.00199
0.05	0.994	2.24×10^{-1}	---	0.00383	0.00212
0.10	1.072	2.22×10^{-1}	---	0.00383	0.00230
0.20	1.181	2.17×10^{-1}	---	0.00383	0.00261
0.50	1.333	1.60×10^{-1}	---	0.00377	0.00315
1.00	1.364	2.11×10^{-2}	---	0.00345	0.00334

APPENDIX V

Maximum Force, Residual Deflection and Maximum Stress Data

α = 2 L/ρ = 70 e/ρ = 0.01

β	Maximum Force (P_m/P_E)	Residual Deflection (y_r/ρ)	Maximum Deflection (y_m/ρ)	Stress 1 Maximum (S_{1max})	Stress 2 Maximum (S_{2max})
0.01	0.930	4.01×10^{-1}	---	0.00406	0.00200
0.05	1.041	4.17×10^{-1}	---	0.00408	0.00222
0.10	1.151	4.17×10^{-1}	---	0.00408	0.00250
0.20	1.296	4.02×10^{-1}	---	0.00408	-0.00309
0.50	1.497	3.04×10^{-1}	---	0.00408	0.00359
1.00	1.542	5.20×10^{-2}	---	0.00388	0.00380

α = 2.5 L/ρ = 70 e/ρ = 0.01

β	Maximum Force (P_m/P_E)	Residual Deflection (y_r/ρ)	Maximum Deflection (y_m/ρ)	Stress 1 Maximum (S_{1max})	Stress 2 Maximum (S_{2max})
0.01	0.939	5.62×10^{-1}	---	0.00420	0.00201
0.05	1.079	6.02×10^{-1}	---	0.00423	0.00231
0.10	1.210	6.17×10^{-1}	1.85	0.00424	-0.00292
0.20	1.382	6.03×10^{-1}	1.95	0.00425	-0.00364
0.50	1.594	3.95×10^{-1}	1.99	0.00425	-0.00396
1.00	1.642	7.93×10^{-2}	0.72	0.00413	0.00405

APPENDIX V

Maximum Force, Residual Deflection and Maximum Stress Data

α = 1 L/ρ = 50 e/ρ = 0.01

β	Maximum Force (P_m/P_E)	Residual Deflection (y_r/ρ)	Maximum Deflection (y_m/ρ)	Stress 1 Maximum (S_{1max})	Stress 2 Maximum (S_{2max})
0.01	0.633	2.71×10^{-1}	---	0.00419	0.00284
0.05	0.658	2.74×10^{-1}	---	0.00420	0.00297
0.10	0.689	2.75×10^{-1}	0.67	0.00421	0.00313
0.20	0.730	2.65×10^{-1}	0.75	0.00421	0.00337
0.50	0.775	1.15×10^{-1}	0.48	0.00403	0.00367
1.00	0.782	1.78×10^{-2}	0.10	0.00384	0.00378

α = 1.5 L/ρ = 50 e/ρ = 0.01

β	Maximum Force (P_m/P_E)	Residual Deflection (y_r/ρ)	Maximum Deflection (y_m/ρ)	Stress 1 Maximum (S_{1max})	Stress 2 Maximum (S_{2max})
0.01	0.636	5.30×10^{-1}	---	0.00447	0.00286
0.05	0.687	5.22×10^{-1}	---	0.00447	0.00311
0.10	0.735	5.02×10^{-1}	1.12	0.00447	0.00338
0.20	0.791	4.57×10^{-1}	1.10	0.00447	0.00369
0.50	0.859	2.62×10^{-1}	0.90	0.00443	0.00411
1.00	0.870	3.66×10^{-2}	0.16	0.00426	0.00422

APPENDIX V

Maximum Force, Residual Deflection and Maximum Stress Data

$\alpha = 1$ $\quad L/\rho = 50$ $\quad e/\rho = 0.01$

β	Maximum Force (P_m/P_E)	Residual Deflection (y_r/ρ)	Maximum Deflection (y_m/ρ)	Stress 1 Maximum (S_{1max})	Stress 2 Maximum (S_{2max})
0.01	0.633	2.71×10^{-1}	---	0.00419	0.00284
0.05	0.658	2.74×10^{-1}	---	0.00420	0.00297
0.10	0.689	2.75×10^{-1}	0.67	0.00421	0.00313
0.20	0.730	2.65×10^{-1}	0.75	0.00421	0.00337
0.50	0.775	1.15×10^{-1}	0.48	0.00403	0.00367
1.00	0.782	1.78×10^{-2}	0.10	0.00384	0.00378

$\alpha = 1.5$ $\quad L/\rho = 50$ $\quad e/\rho = 0.01$

β	Maximum Force (P_m/P_E)	Residual Deflection (y_r/ρ)	Maximum Deflection (y_m/ρ)	Stress 1 Maximum (S_{1max})	Stress 2 Maximum (S_{2max})
0.01	0.636	5.30×10^{-1}	---	0.00447	0.00286
0.05	0.687	5.22×10^{-1}	---	0.00447	0.00311
0.10	0.735	5.02×10^{-1}	1.12	0.00447	0.00338
0.20	0.791	4.57×10^{-1}	1.10	0.00447	0.00369
0.50	0.859	2.62×10^{-1}	0.90	0.00443	0.00411
1.00	0.870	3.66×10^{-2}	0.16	0.00426	0.00422

APPENDIX V

Maximum Force, Residual Deflection and Maximum Stress Data

$\alpha = 2$ $L/\rho = 50$ $e/\rho = 0.01$

β	Maximum Force (P_m/P_E)	Residual Deflection (y_r/ρ)	Maximum Deflection (y_m/ρ)	Stress 1 Maximum (S_{1max})	Stress 2 Maximum (S_{2max})
0.01	0.641	7.44×10^{-1}	---	0.00463	0.00289
0.05	0.709	7.44×10^{-1}	---	0.00463	0.00323
0.10	0.766	7.17×10^{-1}	---	0.00464	0.00354
0.20	0.832	6.27×10^{-1}	---	0.00463	0.00391
0.50	0.907	3.44×10^{-1}	---	0.00463	0.00435
1.00	0.919	4.44×10^{-2}	---	0.00449	0.00446

$\alpha = 2.5$ $L/\rho = 50$ $e/\rho = 0.01$

β	Maximum Force (P_m/P_E)	Residual Deflection (y_r/ρ)	Maximum Deflection (y_m/ρ)	Stress 1 Maximum (S_{1max})	Stress 2 Maximum (S_{2max})
0.01	0.646	9.35×10^{-1}	---	0.00473	0.00291
0.05	0.729	9.45×10^{-1}	---	0.00475	0.00334
0.10	0.789	9.19×10^{-1}	1.65	0.00476	0.00367
0.20	0.863	7.94×10^{-1}	1.60	0.00476	-0.00427
0.50	0.941	4.03×10^{-1}	1.26	0.00476	0.00452
1.00	0.952	5.25×10^{-2}	0.22	0.00465	0.00462

APPENDIX VI

Evaluation of the Approximations and of the Accuracy of the Numerical Scheme

From a consideration of the maximum lateral deflections encountered in the solutions the approximations made in developing the equations for the column model may be evaluated. The maximum value of θ for all solutions was less than 0.08 radian. Based on a maximum θ = 0.08 radian the errors are as follows:

(a) 0.01 per cent error in $(L/2 - e \tan\theta)$ as a result of neglecting $e \tan\theta$

(b) 0.2 per cent error in $\left[\frac{L}{2}\sin\theta - e(1-\cos\theta)\right]$ by considering $\sin\theta = \theta$ and neglecting $e(1-\cos\theta)$

(c) 0.25 per cent error in $\tan\theta$ and 0.11 per cent error in $\sin\theta$ as a result of considering $\tan\theta = \sin\theta = \theta$

(d) less than 0.06 per cent error in $(1-\cos\theta)$ as a result of considering $1-\cos\theta = \frac{1}{2}\theta^2$

From this the approximations which have been made in deriving the equations for the column model are reasonable and produce insignificant error in the results.

As an additional check for cumulative error a comparison of the ram work done on the column model with the net energy input to each of the springs (a combination of strain energy of plastic deformation and the existing elastic strain energy) is made in all computer solutions for the results shown in Figs. 10 thru 14. These agree within 1 per cent thus verifying the compatibility of the equations and check-

ing the accuracy of the numerical scheme for the time increments chosen. Work-energy considerations are not included in the computer program for obtaining graphical results but the dimensionless time increment ΔT used for the numerical integration in both programs for a given value of β was the same.